UNIVERSITY OF SOUTHAMPTON

FACULTY OF NATURAL AND ENVIRONMENTAL SCIENCES

School of Chemistry

Surface Functionalisation of Encoded SU-8 Microparticles and Their Uses in Multiplexed Suspension Biological Assays

by

King Shing Joseph She

Thesis for the degree of Doctor of Philosophy

October 2011

UNIVERSITY OF SOUTHAMPTON

ABSTRACT

FACULTY OF NATURAL AND ENVIRONMENTAL SCIENCES

SCHOOL OF CHEMISTRY

Doctor of Philosophy

SURFACE FUNCTIONALISATION OF ENCODED SU-8 MICROPARTICLES AND THEIR USES IN MULTIPLEXED SUSPENSION BIOLOGICAL ASSAYS

By King Shing Joseph She

Recently, a novel diffractive-based encoded system has been developed for various multiplexed suspension biological assays. These microparticles, which are manufactured using photolithography of a commercial epoxy-based negative photoresist (SU-8), contain micrometre-sized diffractive elements and can encode millions of unique codes. In this thesis, the preparation and surface modification of different diffractive microparticles; the attachment of a range of biological molecules (*e.g.* proteins and peptides) onto the functionalised surfaces; and different on-bead analytical techniques for surface characterisation are described. From a thermodynamic study of a multiplexed immunoassay for immunoglobulins (Ig, MW ~150 kDa), the immobilised probe molecules exhibit high affinity ($K_d = 9 \pm 3$ nM) and excellent specificity (S/N >36:1) for the target analytes. The suspension assay resembles solution-like reaction kinetics allowing detection of multiple target proteins in <20 min. The encoded microparticles can also be used for quantifying small proteins, such as cytokines (MW ~20 kDa). In a particle-based sandwich suspension immunoassay, human tumour necrosis factor-alpha (TNF-α) and interleukin 6 (IL-6) are detected and compared with conventional enzyme-linked immunosorbent assays (ELISA). Correlation coefficients (R^2) for the two cytokines are found to be >0.96. Intra-assay variability (%CV) is determined to be <25%. The sensitivity of the multiplexed immunoassay, expressed as Lowest Detection Limit (LDL), is found to be 379 fM and 1.47 pM for TNF-α and IL-6 respectively, and are comparable to the corresponding ELISAs as demonstrated by the suppliers.

List of Contents

List of Figures

List of Tables

DECLARATION OF AUTHORSHIP

I, **King Shing Joseph She**, declare that the thesis entitled "**Surface Functionalisation of Encoded SU-8 Microparticles and Their Uses in Multiplexed Suspension Biological Assays"** and the work presented in the thesis are both my own, and have been generated by me as the result of my own original research. I confirm that:

- this work was done wholly or mainly while in candidature for a research degree at this University;
- where any part of this thesis has previously been submitted for a degree or any other qualification at this University or any other institution, this has been clearly stated;
- where I have consulted the published work of others, this is always clearly attributed;
- where I have quoted from the work of others, the source is always given. With the exception of such quotations, this thesis is entirely my own work;
- I have acknowledged all main sources of help;
- where the thesis is based on work done by myself jointly with others, I have made clear exactly what was done by others and what I have contributed myself;
- parts of this work have been published as:
  - Broder, G. R.; Ranasinghe, R. T.; She , J. K.; Banu, S.; Birtwell, S. W.; Cavalli, G.; Galitonov, G. S.; Holmes, D.; Martins, H. F.; Macdonald, K. F.; Neylon, C.; Zheludev, N.; Roach, P. L.; Morgan, H. *Analytical Chemistry* **2008**, *80*, 1902.
  - Holmes, D.; She, J. K.; Roach, P. L.; Morgan, H. *Lab on a Chip* **2007**, *7*, 1048.

Signed: ……..

Date:……

Acknowledgements

During the last year of my undergraduate study, I had to spend 6 months in a research lab to complete my undergraduate in-house research project. Initially, I was asked to join the Frey group and participate in an IT-related project, something I was always good at. Just before the new term began, I had an opportunity to work with Dr. Peter Roach in a small summer project. After 6 weeks of "intensive" training, I decided to change my research topic in the area of molecular biology. It was a very risky decision since I had no experience in this field whatsoever, but I am glad I took up the challenge. At the same time, Dr. Roach was trying to obtain some funding for me to continue my research in his group. It was not an easy task and I knew he was being "abused" by some colleagues of his. After a few months on the road, he managed to convince Prof. Hywel Morgan and other academia from the 4G Basic Technology Project to fund my PhD study. Without Peter's effort, none of this would have been possible. I am very grateful to him.

I have had a lot of help with my work from many knowledgeable individuals: Dr. Cameron Neylon, Dr. Gabrial Cavalli, Dr. Rohan Ranasinghe, Dr. Rob Wood, Dr. Marco Kriek, Dr. Sam Birtwell, Dr. David Holmes, Graham Broder and other people from the Roach group and the Morgan group. I would like to thank Dr. Peter Roach, Dr. Rohan Ranasinghe and Dr. Gabriel Cavalli for proof-reading my manuscripts; Alfred Kwok, my best man, for printing and binding my thesis copies, and posting them to the School before the deadline.

I would also like to thank my parents, Teresa and Wingching, my brother, Raphael, my sister, Cecilia, and my brother-in-law, Jack, for their unlimited supports throughout all these years. Finally, I would like to thank my wife, Lilyan, for her unconditional love. Thank you for supporting me throughout my Ph.D. and getting me out of trouble.

Abbreviations

2-D	two-dimensional
3-D	three-dimensional
A.U.	arbitrary unit
Ab	antibody
Ag	antigen
AIBN	2,2'-azobisisobutyronitrile
AP	alkaline phosphatase
APS	ammonium persulfate
APTES	(3-aminopropyl)triethoxylsilane
aq.	aqueous
BCA	bicinchoninic acid
BCR	B-cell receptors
B_{max}	maximum binding
BODIPY-FL	boron-dipyrromethene-based fluorophore. ex_{max} ~ 500 nm. em_{max} ~ 506 nm
cat.	catalytic
CCD	charge-coupled device
cDNA	complementary DNA
CPG	controlled-pore glass
CV	coefficient of variation
Cy3	cyanine-based fluorophore. ex_{max} ~ 550 nm. em_{max} ~ 570 nm
Cy5	cyanine-based fluorophore. ex_{max} ~ 649 nm. em_{max} ~ 670 nm
DCM	dichloromethane
Dde	1-(4,4-dimethyl-2,6-dioxacyclohexylidene)ethyl

DIC	*N,N'*-diisopropylcarbodiimide
DIPEA	*N,N*-diisopropylethylamine
DMAP	4-dimethylaminopyridine
DMF	*N,N*-dimethylformamide
DMT	4,4'-dimethoxytrityl
DNA	deoxyribonucleic acid
dNTP	deoxyribonucleotide triphosphate
E. coli	*Escherichia coli*
EDC	*N*-(3-Dimethylaminopropyl)-*N'*-ethylcarbodiimide
ELISA	enzyme-linked immunosorbent assay
em_{max}	emission maximum
eq.	equivalents
ex_{max}	excitation maximum
F_{ab}	fragment antigen-binding
FACS	fluorescence-activated cell sorter
F_c	fragment crystallisable
FDT	fluorescein diphosphate tetraammonium salt
Fmoc	9-fluorenylmethoxycarbonyl
FSC	forward scattering
GMA	glycidyl methacrylate
GOX	glucose oxidase
HABA	4'-hydroxyazobenzene-2-carboxylic acid
HEG	hexa(ethylene glycol)
HIV	human immunodeficiency virus
HOBt	1-hydroxybenzotriazole
HPV	human papillomavirus
IFN	interferon
Ig	immunoglobulin

IL	interleukin
IVD	*in vitro* diagnosis
JAK	Janus kinase
K_d	equilibrium dissociation constants
LDL	lowest detection limit
m/z	mass to charge ratio
MALDI-TOF	Matrix-assisted laser desorption/ionization Time-of-flight
MHC	major histocompatibility complex
mRNA	messenger RNA
MS	mass spectrometry
MW	molecular weight
NA	nucleic acid
NHS	*N*-hydroxysuccinimide
NIH	National Institutes of Health
NMP	*N*-Methyl-2-pyrrolidone
NMR	nuclear magnetic resonance
NTA	nitrilotriacetic acid
pAPC	professional antigen-presenting cell
PBS	phosphate buffered saline
PBST	phosphate buffered saline with Tween-20
PC	personal computer
PCR	polymerase chain reaction
PEG	poly(ethylene glycol)
PEGA	poly(ethylene glycol)-acrylamide
PNA	peptide nucleic acid
POC	point-of-care
POD	peroxidase

QD	quantum dot
qPCR	quantitative polymerase chain reaction
qRT-PCR	quantitative reverse transcriptase-PCR
r.t.	room temperature
R^2	correlation coefficient
RIA	radioimmunoassay
RNA	ribonucleic acid
S. aureus	*Staphylococcus aureus*
S/N	signal to noise ratios
SD	standard deviation
SE	standard error
sPEG	star-shaped poly(ethylene glycol)
ss	single-stranded
SSC	side scattering
STAT	signal transducer and activator of transcription
SU-8	EPON® Resin SU-8
sulfo-NHS	*N*-hydroxysulfosuccinimide sodium salt
t-Boc	*N*-tertiary butoxycarbonyl
TBTU	*N,N,N',N'*-tetramethyl-*O*-(benzotriazol-1-yl)uronium tetrafluoroborate
TCA	trichloroacetic acid
TCR	T-cell receptors
TEA	triethylamine
Tf	trifyl
T_h	helper T cells
THF	tetrahydrofuran
TLC	thin-layer chromatography
TNF	tumour necrosis factors
Ts	tosyl

UV	ultra-violet
v/v	volume/volume percentage
Vis	visible light
w/v	weight/volume percentage
XPS	X-ray photoelectron spectroscopy
ε	molar extinction coefficient (M^{-1} cm^{-1})

Chapter 1 Encoding technologies for multiplexed biological assays

1.1 Introduction

"Biological assays" is a generic term that describes a variety of tests for the detection and quantification of specific molecules in biological samples. These molecules include antibodies,[1] antigens,[2] proteins,[3] peptides,[4] nucleic acids (NA),[5] metabolites,[6] carbohydrates[7] and synthetic molecules.[7] These assays are carried out routinely in the fields of molecular diagnostics,[8] drug discovery[9] and environmental monitoring.[10] Many of these assays are based on the detection of specific molecular interactions, including NA-NA;[11] protein-protein;[12] protein-NA;[13] ligand-receptor,[14] antibody-antigen[15] and enzyme-substrate.[16] Conventional assays are typically carried out in microtiter plates (Figure 1.1), in which numerous manual liquid manipulation steps are often required.[17] Assay throughput and labour are often the limiting factors in traditional microtiter plate-based assays. However, with the aid of robotic arms and automated liquid handling systems, assay throughput is enhanced and labour force is greatly reduced.[18]

In diagnostics and therapeutics, there is an increasing need to diagnose diseases at an early stage, so that personalised targeted treatments can be provided to patients.[19] In the future, high risk diseases may be predicted based on individual's genetic profiles.[20,21] These advanced treatments are accompanied by better diagnostic information which provides an accurate overview on the complex biological network in the body. Conventional assay platforms are often expensive to operate and increasingly incapable of fulfilling the demand.[22] Hence there is a need to develop alternative technologies which can provide

high-density information in a cost effective manner. One set of promising solutions are the multiplexed assay technology, which permit the monitoring of multiple analytes in a single sample.[23,24]

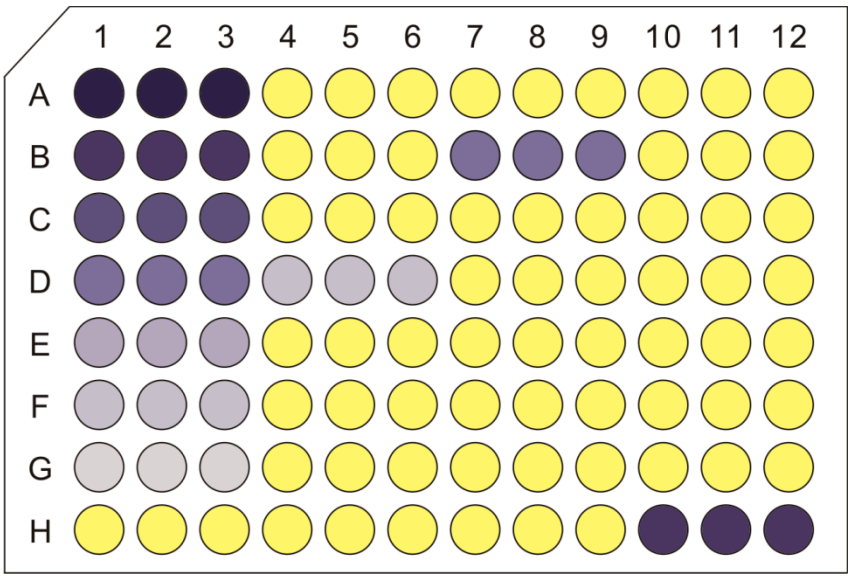

Figure 1.1. A graphical illustration of a typical colourimetric-based biological assay on a 96-well plate.

1.2 Solution-phase multiplexed assays

1.2.1 Fluorescence encoding

Conventional solution-phase biological assays can be multiplexed by using fluorescent markers. One example is the multiplexed quantitative PCR (qPCR), in which multiple target gene sequences are quantified simultaneously in one single sample. This concept was first demonstrated by Higuchi *et al.* in 1992[25] and was later adapted by other groups.[26,27] Figure 1.2 illustrates the principle of a conventional and multiplexed qPCR. A short single-stranded (ss) DNA, called the reporter probe, is used to detect the target gene. This probe is labelled with a fluorophore-quencher pair and produces an increase of fluorescence signal once it is activated during the PCR process (see legend to Figure 1.2). In order to

detect multiple sequences in a single sample, a series of reporter probes, each labelled with a different fluorescence-quencher pair, have to be employed. In practice, the design of different primers and reporter probes with similar hybridisation efficiency, and the selection of fluorophore-quencher pairs with minimal spectral overlapping are proving to be challenging.[28] These limitations confine the use of this technology for low-multiplex (typically <5-plex) applications.[29]

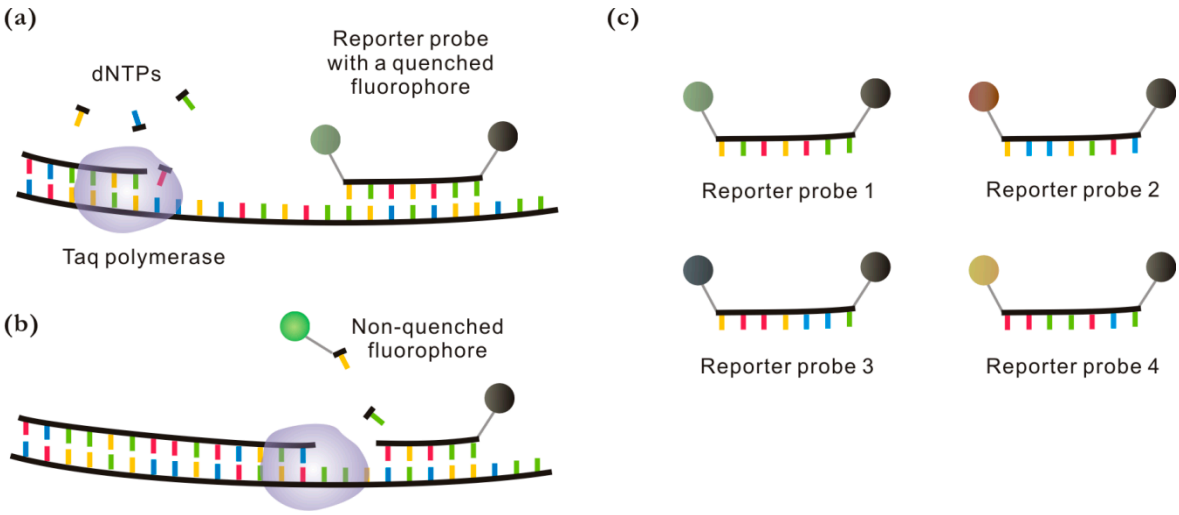

Figure 1.2. Schematic diagram of conventional and multiplexed qPCR. (a) During amplification, the forward and reverse primers hybridise to the sense and antisense strands of the target sequence respectively. As the primers are extended by the polymerase, incorporating the complementary dNTPs to the 3' end, the enzyme moves along the target gene and eventually reaches the pre-occupied detection region by the reporter probe. (b) The polymerase then exhibits exonuclease activity and degrades the probe and then continues with the extension. The degradation causes an increase of fluorescence of the reaction mixture since the fluorophore and quencher are no longer in close proximity. As the amount of the target sequence increases exponentially after each amplification cycle, more reporter probes are degraded and the rate of the increase of fluorescence can be used to quantify the original target concentration. (c) In multiplexed qPCR, a series of reporter probes, each labelled with a different fluorescence-quencher pair, are used to detect multiple gene sequences.

1.3 Planar arrays

1.3.1 DNA microarrays

The use of different fluorescent labels as reporters in multiplexed solution-phase assays is not suitable for large-scale studies, especially in genome- or proteome-wide analysis, in which a high-density of information on many molecular interactions is acquired.[30] For such applications, a heterogeneous planar array, or microarray, system may be suitable. The first DNA array was demonstrated by Maskos *et al.* in 1992, in which a short oligonucleotide was synthesised from a microscope slide and showed the ability to hybridise to the ^{32}P-labelled complementary sequence.[31] This methodology was iterated into the modern DNA microarray technologies (Figure 1.3).[32,33] In these examples, a large number of spatially resolved ssDNA capturing probes are either synthesised from or attached to a solid support, typically a glass slide. Each unique sequence can be identified by its x and y coordinates on the 2-dimentional grid of the solid support. To capture the target sequence, the solid support is immersed into the sample, in which the fluorescently-labelled target sequences (e.g. prepared by PCR) diffuse from the bulk solution to the surface and hybridise to the corresponding immobilised capture probes. After washing away the excess targets, a fluorescence micrograph of the solid support is acquired. The fluorescence intensity at each defined position is used to estimate the amount of target probes captured on the surface. With a modern high-end microarrayer, tens of nanolitres of biomolecules can be spotted onto a glass slide with a spot diameter of tens of micrometres and probe density of $>10^3/cm^2$.[34,35]

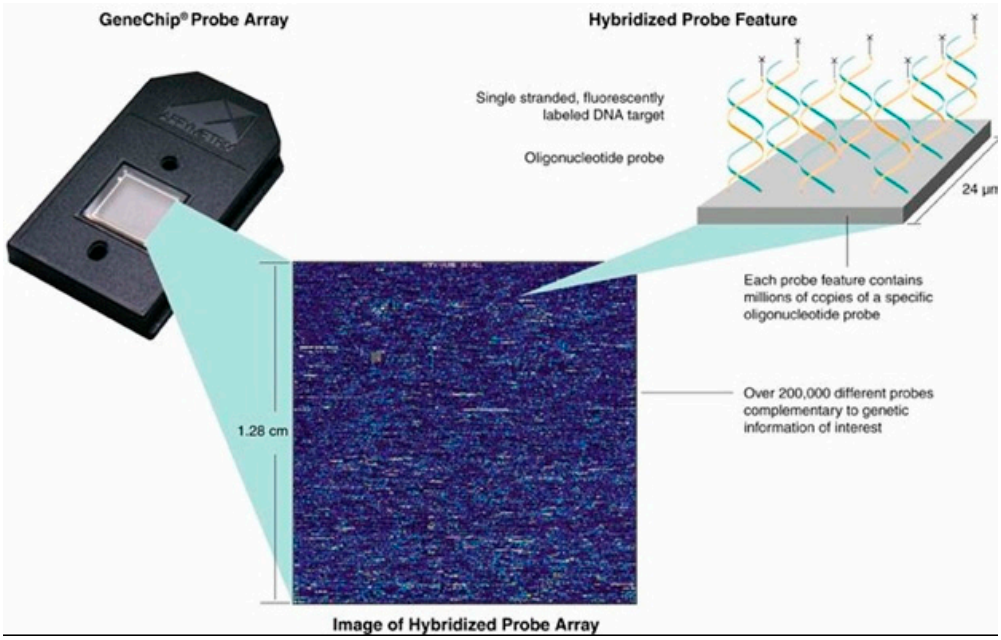

Figure 1.3. A commercially available DNA microarray chip (GeneChip, Affymetrix, CA, USA). This diagram was obtained from reference 36.

1.3.2 Protein Microarrays

Microarray technologies are also being applied to proteomic studies.[37,38] The concept was first demonstrated by G. MacBeath and S. L. Schreiber in 2000 (Figure 1.4).[39] In this example, protein G, p50 and GST-FRB were immobilised onto a microscope glass slide using a commercially available DNA microarrayer. Each spot had a diameter between 150 and 200 μm with a probe density of 1600 spots/cm^2. The solid support was then immersed in a solution containing the fluorescently-labelled target proteins. This experiment showed that the immobilised capturing proteins retained their functional properties on the solid support and were able to bind to their targets with high specificity. These studies also showed the potential of microarray technologies in studying thousands of protein-protein interactions in a highly parallel format.

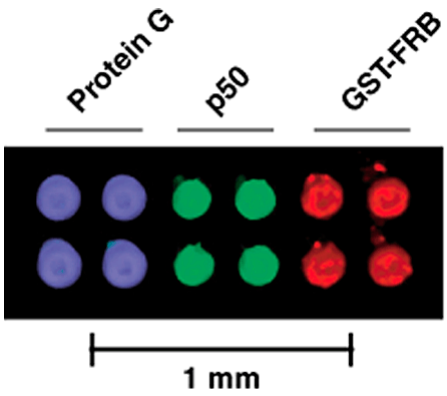

Figure 1.4. An example of a multi-colour protein microarray. This diagram was adapted from reference 39.

1.3.3 PNA encoding

Microarrays have certain disadvantages, including relatively slow reaction kinetics due to the diffusion of target molecules to their binding sites (a distance of several millimetres). Harris and Winssinger demonstrated an encoding technology that combined the fast reaction kinetics in solution-phase reactions with the high multiplex capacity in microarrays.[40] In this study, a library of kinase substrates, each conjugated to a unique single-stranded peptide nucleic acid (PNA) sequence, was assayed with a kinase in solution (Figure 1.5). After phosphorylation, the PNA-encoded substrates were immobilised onto a microarray by direct hybridisation to the tethered complementary sequences. The incorporated phosphate group on the target tyrosine residue was then probed with a fluorescently labelled anti-phosphotyrosine antibody for accessing the kinase activity. This method has also been applied to other studies, including protease profiling.[41]

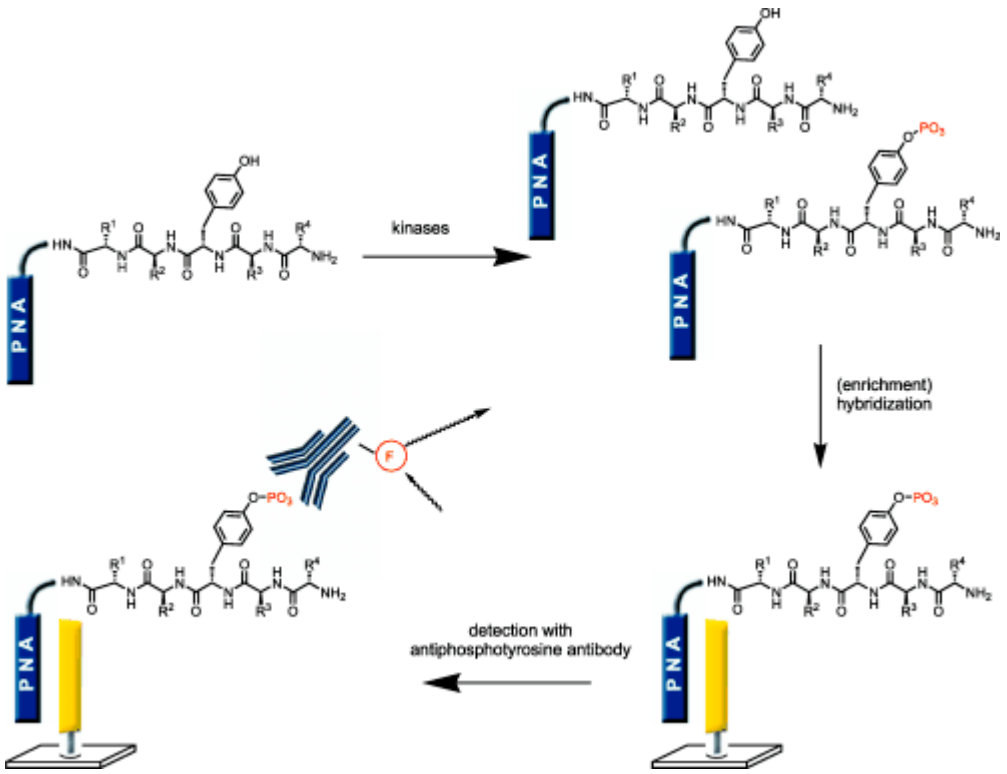

Figure 1.5. PNA-DNA encoded solution-microarray hybrid assay. This material was adapted from reference 40.

1.4 Microparticle-based suspension arrays

Microarray technologies have revolutionised the field of genomics and proteomics. The ability to study tens of thousands of molecular interactions in a highly parallel format provides a very powerful method for high-throughput analysis. However, microarrays have certain disadvantages, such as slow reaction kinetics due to the diffusion-limited rate determining binding step.[42] The need for using specialised instruments for the construction of the arrays also limits the flexibility on probe combinations.[43] Another approach to allow multiplexed biomolecular assays has emerged and makes use of microparticles.[23,44,45] This technique offers a flexible approach for monitoring large numbers of simultaneous reactions in a single sample. In general the technique uses a mixture of micrometre-sized particles (microparticles), each of which carries a unique code which identifies the capturing biomolecule on the surface, is suspended in a solution containing the target analytes, and the

binding of the analyte to the immobilised capturing biomolecules is detected by the signal development on the surface (Figure 1.6). This has advantages over other static heterogeneous planar assays, including faster reaction kinetics and flexibility on the development of an assay panel.

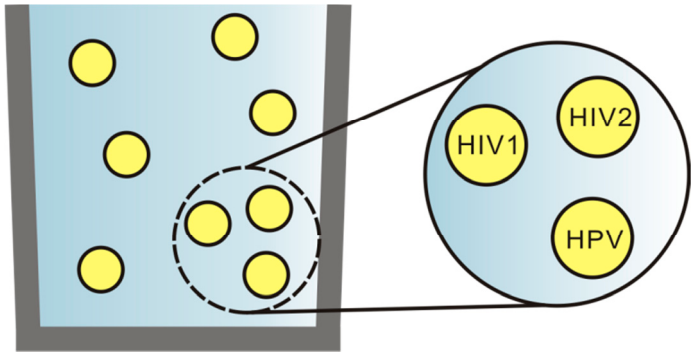

Figure 1.6. The principle of microparticle-based multiplexed suspension arrays. Each microparticle contains a code which is used to identify the capturing biomolecules on the surface. A mixture of these microparticles is suspended in the sample and captures the target analytes simultaneously.

1.4.1 Fluorescence encoding

There are a number of methods for encoding microparticles. One of the most widely used techniques is based on fluorescence encoding.[23,44-46] Figure 1.7 illustrates the principle of multiplexed fluorescence encoding based on the use of multiple fluorophores and intensities.[47] The use of 10 defined intensity levels of one fluorophore gives 10 unique codes. With 2 fluorophores and 10 intensity levels, the encoding capacity increases to 100. In general, n^m of codes can be generated with m fluorophores and n intensity levels.[47]

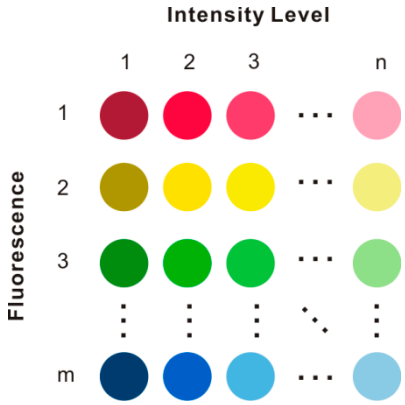

Figure 1.7. The principle of multi-colour/multi-intensity encoding system.

One of the most widely used fluorescence-based encoding systems is the *x*MAP technology developed by Luminex Corporation (Figure 1.8).[48,49] In this example, the 5 μm polystyrene beads were internally dyed with a red and infra-red fluorophore mixture. Code reading was accomplished by illuminating the beads with a 633 nm beam, for which the intensity levels of the red and infra-red fluorescence were used to identify the bead population. This platform is accompanied with a flow cytometer for code detection and assay readout. An additional 488 nm beam is used for illuminating the labelled biological complex on the beads' surface. This *x*MAP technology offers 100 sets of unique beads based on the two-colour/ten-intensity system ($n^m = 10^2$). Recently, this platform expanded the encoding capacity to 500 by incorporating a third fluorescent dye with 5 intensity levels (FlexMap 3D).[50] This technology has been applied for the detection and quantification of specific DNA sequences,[51] antibodies[52], proteins[53], and synthetic molecules[54] in a multiplexed manner.

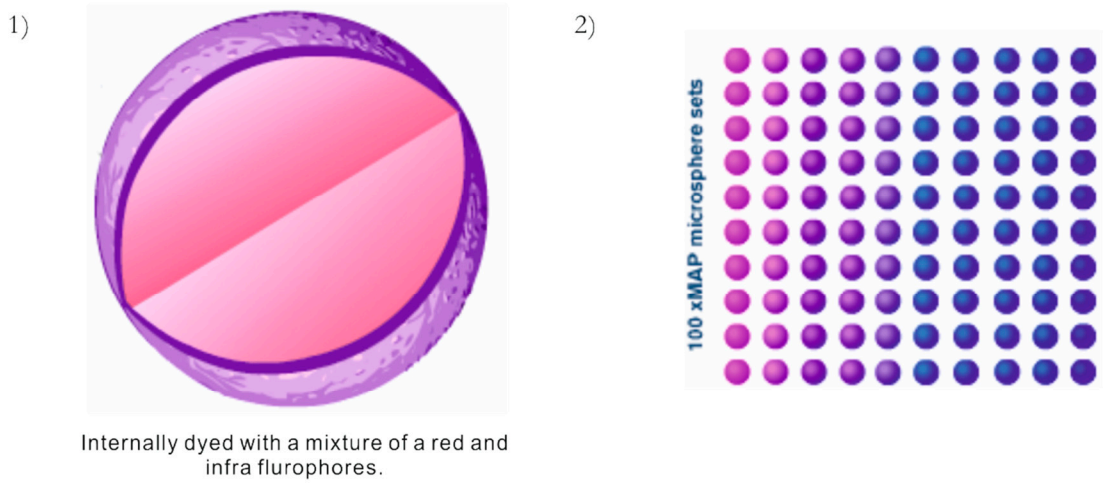

Figure 1.8. The principle of the 2-colour/10-intensity encoding system used in the *x*MAP technology. 1) Each bead contained a mixture of a red and infra fluorophores at specific concentrations. 2) By varying the concentration of each dye, 100 unique sets of beads can be generated using the two-colour/ten-intensity system. The images were adapted and modified from reference 49.

Another system that uses multiple fluorophores for encoding is the BeadArray technology from Illumina Inc.[55] The encoding methodology is similar to the *x*MAP technology developed by Luminex, in which the beads were internally dyed with different fluorophores. However, BeadArray employs a different assay readout strategy. After capturing the targets in a suspension array, the beads are trapped in pre-defined microwells on an optical fibre. Each microwell is equally distributed on the surface and is designed to accommodate one single bead. Code reading and assay readout are accomplished by measuring the fluorescence intensity of the beads through the optical fibre.

The use of organic fluorophores for encoding has certain limitations,[56] including poor photostability and instability in aqueous buffers. In addition, the encoding capacity is limited due to broad excitation/emission spectra and spectral overlapping of the fluorophores.[57] Quantum dots (QDs) offer an alternative solution for fluorescence encoding. These are semi-conductor nanocrystals which show excellent optical properties and narrow excitation/emission profiles.[58,59] Han and co-workers demonstrated the use of

QDs embedded polystyrene beads for quadruplex-DNA hybridisation assays (Figure 1.9).[47] In this example, the beads were encoded by different ratios of blue, green and red QDs. In general, the fluorescence emission profile of the embedded QDs was found to be narrower than organic fluorophores and free QDs.

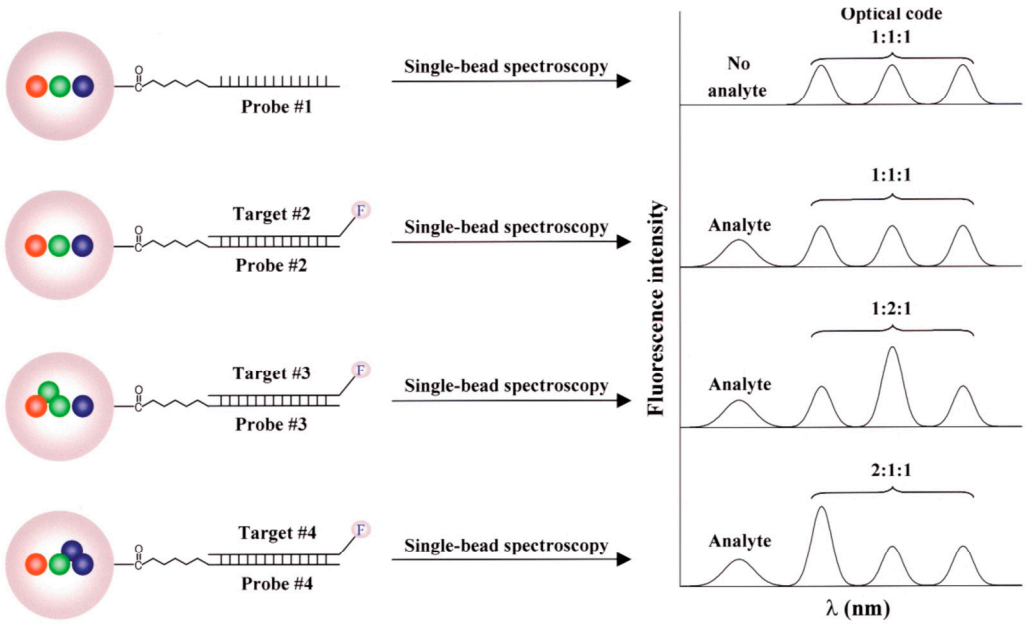

Figure 1.9 An example of the use of QDs-encoded microparticles in a multiplexed DNA hybridisation assay. The microparticles were identified by the fluorescence intensity levels of the red, green and blue QDs. This diagram was adapted from reference 47.

K. Braeckmans *et al.* demonstrated an alternative fluorescence-based encoding technology, termed spatial selective photobleaching (Figure 1.10).[60] Using this method, polystyrene microspheres (45 μm mean diameter) were internally dyed with a green fluorophore (*N*-(7-nitrobenz-2-oxa-1,3,diazol-4-ul)diethyl amine) which showed fast photobleaching. By using a modified confocal microscope equipped with a 30 mW 488 nm laser, a code was "written" into the microsphere by selective photobleaching. To read the code, the encoded microsphere was illuminated with a lower power laser beam (30 μW), in which the non-photobleached region showed higher fluorescence intensity than then the

photobleached code regions. The encoding process was time consuming and required complex and precise optical systems. The decoding was found to be practically difficult because each individual bead had to be perfectly aligned to the detector so that the code could be read in the correct orientation.[61]

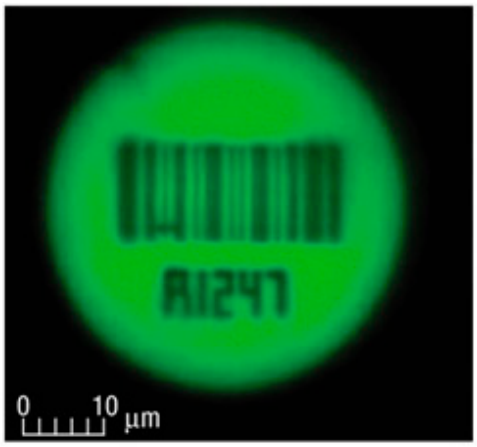

Figure 1.10. Fluorescence micrographs of the microparticles encoded by spatial selective photobleaching. This diagram was adapted from reference 60.

1.4.2 Reflectance encoding

Other optical encoding technologies have also been investigated. One example was the metallic barcodes developed by Nicewarner-Pena and co-workers (Figure 1.11).[62] In this example, the multi-metal microrods with alternating sections of different metals were prepared by sequential electroplating metal layers inside an alumina template. The length of each metallic section can be controlled by the amount of current used in each electroplating step. The barcodes were generated by illuminating the metallic microrods with an incident beam with a fixed wavelength. The microrods produced a series of bright and dark sections according to the reflectivity of the metal layers and code detection was accomplished by analysing these reflectance patterns.

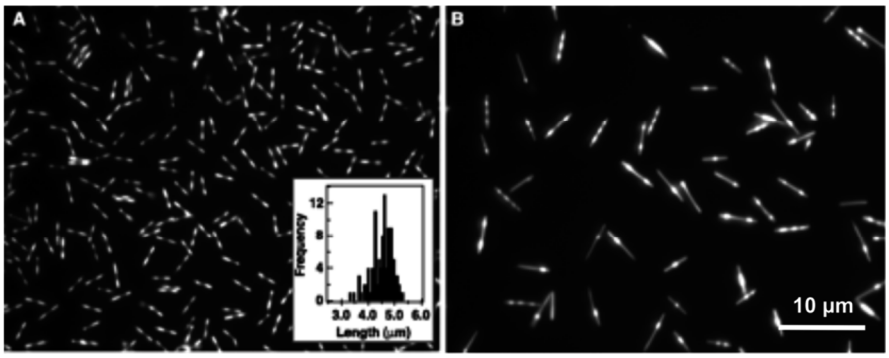

Figure 1.11. An optical micrograph of the 4 μm Ag/Au microrods under 405 nm illumination with varying reflectance patterns. This diagram was adapted from reference 62.

1.4.3 Digital encoding

Another popular technology for multiplexed biological assays is based on digital encoding. The principle of this technology is analogous to a punch card system where the solid support contains digital information of the code (e.g. binary) represented by the presence or absence of holes at defined positions. One of the earliest examples is ImageCode developed by 3D Molecular Sciences Ltd.[63] Figure 1.12 shows a micrograph of the microparticle. The microfabrication and encoding of these particles were accomplished by a one-step photolithography of a negative epoxy-based photoresist, SU-8. Code reading was achieved by analysing the optical micrographs of the microparticles, in which the holes along the top and right edges were used to define the position and orientation of the code.

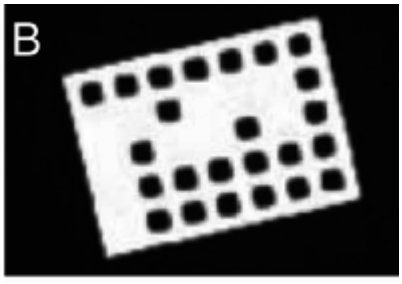

Figure 1.12. A fluorescence micrograph of an ImageCode. This image was adapted and modified from reference 63.

A similar technology called UltraPlex was developed by SmartBead Technologies (Figure 1.13).[64] In this example, a series of holes in an aluminium rod were used to define the binary code. To fabricate the metallic rods, a layer of aluminium was deposited onto a silicon substrate. A solution of a photoresist was spin-coated onto the aluminium layer. The photoresist was cross-linked by UV exposure through a photomask. Excess non-polymerised photoresist was washed away, leaving the structured polymer on top of the aluminium layer. The unprotected aluminium was dry-etched which defined the shape of the metallic rods and the holes. After dissolving the photoresist, the structured aluminium microrods were released from the substrate and collected. The resulting free metallic rods had a dimension of 100 × 10 × 1 μm.

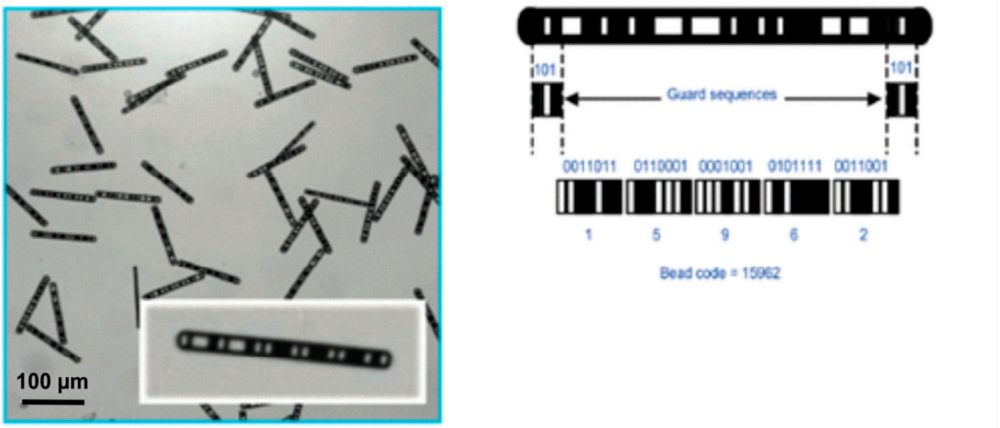

Figure 1.13. An optical micrograph showing the UltraPlex aluminium rod. Images were adapted from reference 64.

Recently, Pregibon and co-workers demonstrated a microfluidic system with the ability to fabricate digitally encoded particles and conjugate capture probe molecules in one single step (Figure 1.14).[65] In this system, two streams of polymerisable monomers were flowed into the microfluidic channel in parallel. Due to the laminar flow characteristic, the two monomers remained separated from each other. One of the monomers contained a

fluorescent dye and the other contained an acrylamide-modified ssDNA. The monomers were polymerised into the shape of the desired microparticles by a short illumination of UV light. The polymerised particles were then collected from the outlet of the system.

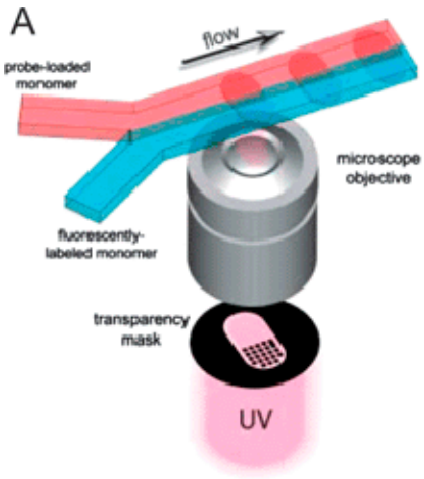

Figure 1.14. A schematic diagram of the microfabrication of the probe-loaded PEG microparticles by continuous-flow lithography inside a microfluidic channel. This diagram was adapted and modified from reference 65.

1.4.4 Shape and size encoding

Microparticles can be encoded by their physical properties. Lee and co-workers demonstrated an encoding system based on the size and shape of the microparticles (Figure 1.15).[66] In this example, different hydrogel microparticles (~100-250 μm in size) were prepared by UV-initiated radical polymerisation of poly(ethylene)glycol (PEG) diacrylate monomers. The shape and size of the particles were determined by the photomask used during the UV cross-linking. Biomolecules were encapsulated within the polymeric matrix by mixing with the monomers for polymerisation. To demonstrate the use of these particles in a multiplex enzyme activity assay, alkaline phosphatase (AP) and glucose oxidase/peroxidase (GOX/POD) mixture were entrapped into two sets of hydrogel

particles respectively. A mixture of these particles was suspended in a solution containing the quenched fluorogenic substrates (AP: fluorescein diphosphate tetraammonium salt; GOX/POD: Amplex Red/glucose). The enzyme activity was studied by monitoring the increase of fluorescence in these microparticles.

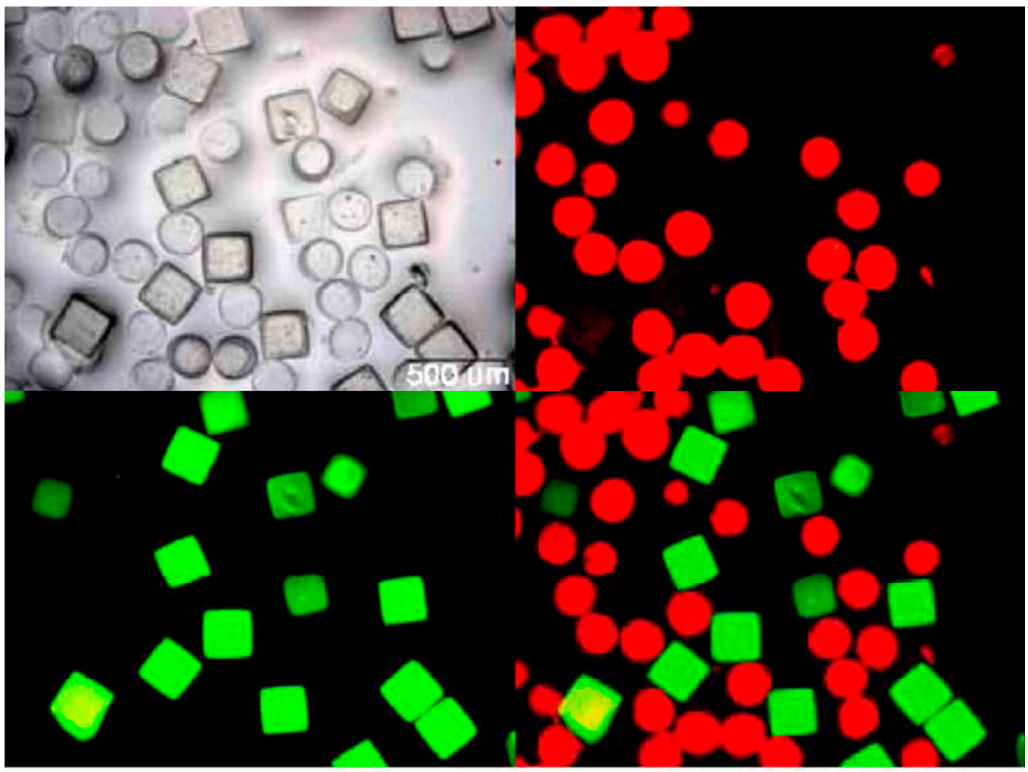

Figure 1.15. The use of shape-encoded hydrogel microparticles in a multiplex enzyme activity study. The round shape hydrogel particle contained GOX/POD and the square shape hydrogel particle contained AP. After the multiplexed reaction, the fluorescence of the hydrogel particles was measured at 515 nm for FDT and 580 nm for Amplex Red. Images were adapted from reference 66.

1.4.5 Diffractive encoding

Illumina Inc. developed a hologram-based diffractive encoding system known as the VeraCode technology (Figure 1.16).[67,68] A nanometre-scale holographic image was inscribed inside a 240 × 28 µm glass rod. Once illuminated by an incident laser beam, the

holographic component diffracted the beam and produced a diffraction pattern. By analysing the optical patterns the code of the glass rod could be identified.

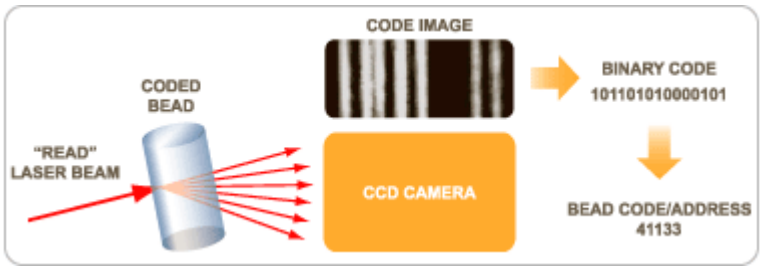

Figure 1.16. A schematic diagram of the VeraCode technology. A laser beam is used to illuminate the micrometre-scaled glass rod. The resulting diffraction image is analysed and the extracted code information is used to identify the microparticle population. This diagram was adapted from reference 67.

Galitonov and co-workers have demonstrated another diffraction-based encoding technology (Figure 1.17).[69] In this method, a microdiffraction grating was patterned onto a small microparticle, either during photolithography or by nano-imprinting. The pitch of the grating, a, contained the information on the identity of the code. When a particle was illuminated with a laser beam at wavelength λ, a number of diffracted beams at angles $m \times \theta$ were produced, where m is the order of the diffraction pattern (0, 1, 2...). By measuring the distance between the first-order patterns, and the distance between the particle and the projected image, θ can be determined. Theoretically, the encoding capacity can be greatly increased by superimposing a number of grating pitches on a single microparticle. By superimposing 5 gratings, approximately 10^5 unique codes can be generated on a 20-μm wide microparticle.[70]

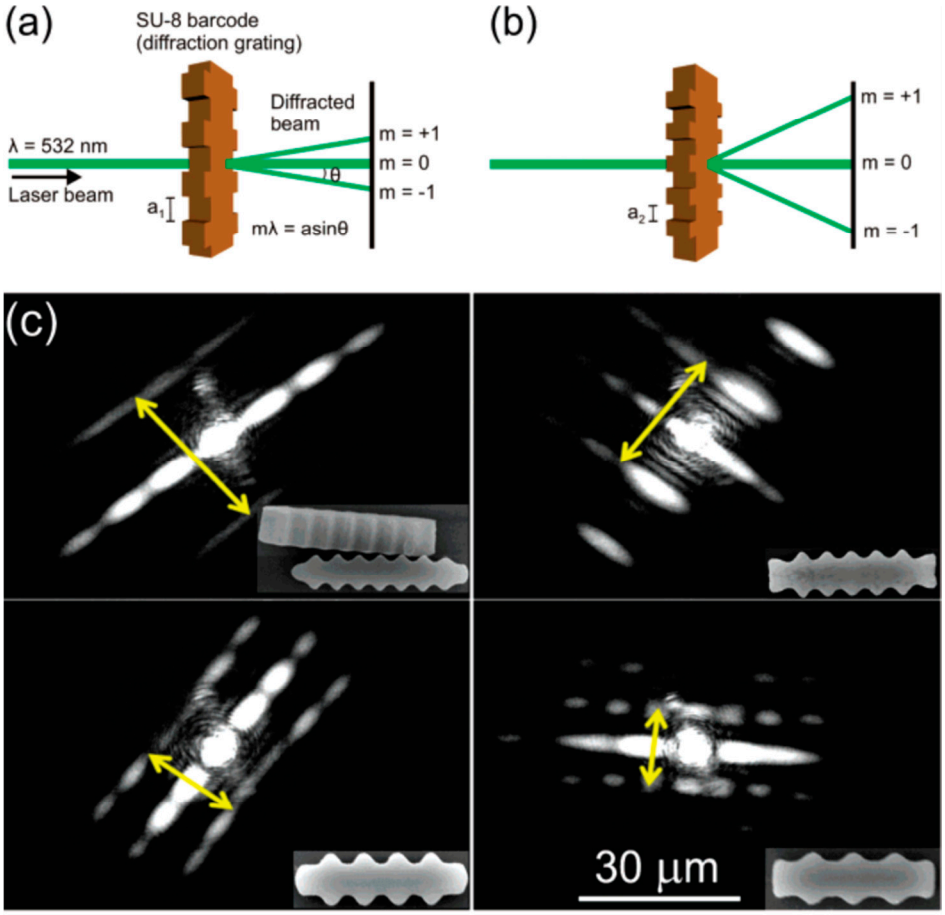

Figure 1.17. A graphical illustration showing the principle of the diffraction-based encoding technology. (a) A diffractive particle with pitch a_1 produces first-order diffraction beams ($m = \pm 1$). (b) Another diffractive particle with pitch a_2, where $a_1 > a_2$, produces a different diffraction pattern. (c) Four different SU-8 microparticles with their corresponding diffraction patterns. This diagram was adapted and modified from reference 71.

1.5 Aims of this thesis

The primary objective of this thesis was to demonstrate the use of encoded SU-8 microparticles in multiplexed suspension biological assays. In order to do so, the surface of the polymeric microparticles had to be modified, so that different molecular handles could be incorporated for the attachment of different biological and synthetic molecules. Once a biomolecule was attached to the surface, the functionality of the immobilised biomolecule could be measured. Subsequently, the use of the functionalised SU-8 microparticles in multiplexed immunoassays was investigated. The kinetics and thermodynamics of

microparticle-based antibody-antigen interactions were studied. Finally, the polymeric SU-8 particles were used in a suspension sandwich immunoassay for the quantification of small proteins. The assay sensitivity, selectivity, reproducibility and other parameters were measured and compared with conventional immunoassays.

Chapter 2 Methods for functionalising polymeric SU-8 particles

Encoded polymeric SU-8 particles are attractive alternatives to other solid supports for multiplexed microparticle-based suspension arrays. To enable their use in such applications, it was necessary to develop robust synthetic methods for attaching probe molecules (e.g. peptides, proteins and nucleic acids) to the particles' surfaces. In this chapter, several methods for chemically modifying the polymer surface for attaching different biological molecules, as well as the analytical techniques used for monitoring the reactions are described.

2.1 Introduction

Many conventional *in vitro* biological assays are carried out in a heterogeneous environment. In general, a molecular probe molecule (e.g. single-stranded DNA or antibody) that recognises a specific target is immobilised onto the surface of a solid-support. Once a sample containing the target is added, the immobilised probe captures the target molecule by affinity binding. A classic heterogeneous *in vitro* assay is the enzyme-linked immunosorbent assay (ELISA),[15] in which the target molecule (antigen) from a biological sample is detected by its antibody immobilised onto the surface of a microtiter plate. Another example is the use of DNA microarrays for genotyping,[72] in which a ssDNA probe is immobilised onto a glass surface before capturing the amplified target sequence by hybridisation.

2.1.1 Immobilisation strategies for heterogeneous *in vitro* assays

The technique used for attaching probe molecules to the surface plays a crucial rôle in the sensitivity and selectivity of the assay platform. There are three major immobilisation methods: 1) adsorption; 2) covalent coupling; and 3) affinity binding. Each of these will be briefly discussed below.

2.1.1a Adsorption

The first protein immobilisation was demonstrated in 1916 in which an enzyme, invertase, was immobilised onto charcoal by adsorption.[73] Since then, many proteins and other biological molecules have been attached to a wide range of surfaces by this method.

Biological molecules can be adsorbed onto surfaces *via* intermolecular forces, including electrostatic, hydrophobic and hydrophilic interactions.[74] The resulting layer of biomolecules is normally non-uniform and the molecules are randomly orientated. This can lead to reduced activity of the immobilised biomolecules.[75] Nevertheless, passive adsorption is still being widely used for attaching proteins and DNA molecules to static 2-D substrates.[76]

2.1.1b Covalent binding

Although immobilising biological molecules by passive adsorption is very straightforward, the process is often time consuming (e.g. 4 °C, 12-24 h). In addition, the immobilised biological molecules are in equilibrium with the solution phase. The molecules are constantly being adsorbed and desorbed from the surface, resulting in a non-permanent linkage. In case of protein attachment, the immobilised proteins may be denatured and this can reduce their activity.[77,78] To overcome these problems, chemistry for covalent attachment of different biological molecules to a wide range of surfaces has been

developed.[79-82] During the recent advances in DNA[83] and protein microarray[39] technologies, proteins and oligonucleotides are routinely coupled to chemically functionalised surfaces.

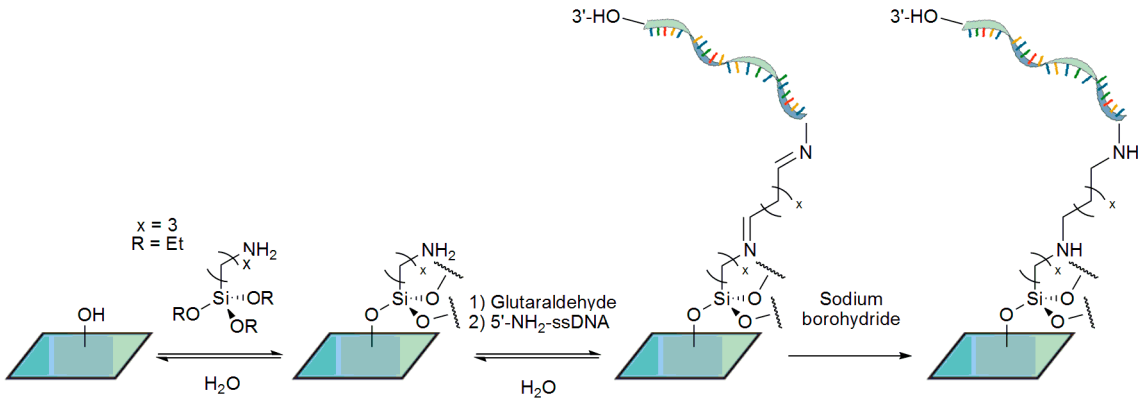

Figure 2.1. Schematic diagram of the functionalisation of a glass surface with a single-stranded DNA probe. The surface silanol group reacts with an amino-organosilane (e.g. (3-aminopropyl)triethoxylsilane, APTES) to introduce a primary amine to the surface. Glutaraldehyde serves as a cross-linker and bridges between the glass surface and the 5'-NH2-ssDNA molecule. A final treatment with sodium borohydride reduces the hydrolysable imines to more stable secondary amines.

Glass surfaces are routinely used for the preparation of DNA or protein microarrays.[84,85] Before the capture molecules can be covalently attached to the solid-support, the glass surface must be chemically modified to introduce reactive functional groups for the coupling. In general, the silanol groups on the glass surface react with a functionalised organosilane (e.g. amino-, mercapto-, or epoxy-).[39,86-89] Depending on the terminal group functionality, biological molecules can be attached to the surface by a number of different ways. For instance, glutaraldehyde is often employed as a cross-linker between the amino-functionalised surface and 5'-NH_2-oligonucleotides (Figure 2.1).[90] Other examples use the direct coupling of biomolecules to an epoxy-[89] or isothiocyanate-functionalised surface (Figure 2.2).[91]

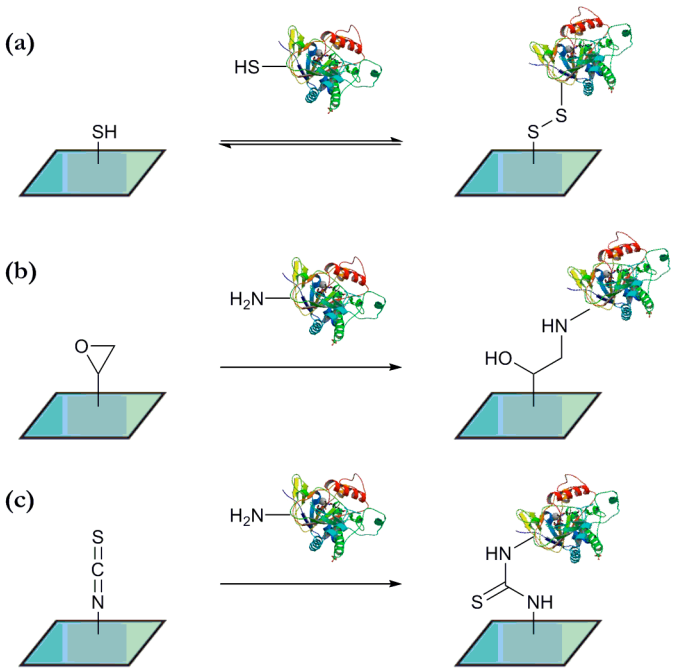

Figure 2.2. Examples of different functional groups and their attachment chemistry for biological molecules; (a) a thiolated surface forming a disulfide bridge with the Cys-residue of a protein; (b) a surface epoxide is ring-opened by a primary amine (e.g. from Lys-residue); (c) an isothiocyanate is attacked by a primary amine and forms a stable thiourea.

2.1.1c Affinity binding

Another very popular method for immobilising biological molecules to the surface is by affinity binding. One of the widely used methods is the nickel-NTA metal-chelate affinity system.[92] In this method, the solid supports for immobilising the target protein are functionalised with nitrilotriacetic acid (NTA), a tetradentate ligand that binds a Ni^{2+} cation. As shown in Figure 2.3, a protein molecule conjugated with a polyhistidine tag can be immobilised onto the surface by forming a complex with the metal ion *via* the histidine side chains. This method is mainly used in affinity chromatography for protein purification, however it has also been shown to immobilise proteins onto glass slides for protein microarrays.[75] Since the polyhistidine tag is normally conjugated at either the N- or C-terminus, the orientation of the immobilised protein can be partly controlled and this way potentially result in a higher protein activity.[75,93,94] In addition, many recombinant proteins

are expressed with polyhistidine tag so that extra manipulation is not needed. This attractive property is very useful for applications where the orientation of the protein is important, for example in sandwich immunoassays and protein microarrays.

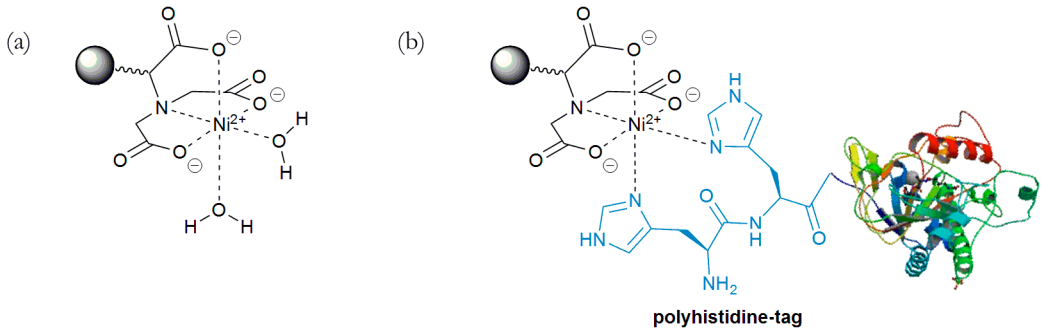

Figure 2.3. (a) Resins used in the nickel-NTA affinity purification system are functionalised with NTA molecules which are capable of binding to Ni(II) cations. (b) A polyhistidine-tagged protein uses two of the histidine side chains to bind to the immobilised Ni(II) cation on the solid support.

Another commonly used affinity binding system is the (strept)avidin-biotin system. Streptavidin[95] (from *Streptomyces avidinii*) and avidin[96] (from avian egg white) are tetrameric proteins that bind biotin (vitamin H) with an equilibrium dissociation constant (K_d) of 10^{-13} M[97] and 10^{-15} M[98] respectively (Figure 2.4). They are considered as the strongest non-covalent interactions in biology as the bindings are almost irreversible under physiological conditions. An example of its use is in DNA microarrays in which a piece of glass slide is coated with a layer of NeutrAvidin[99] (genetically engineered version of non-glycosylated avidin with low non-specific binding to DNA) for capturing biotinylated ssDNA probe molecules.[100]

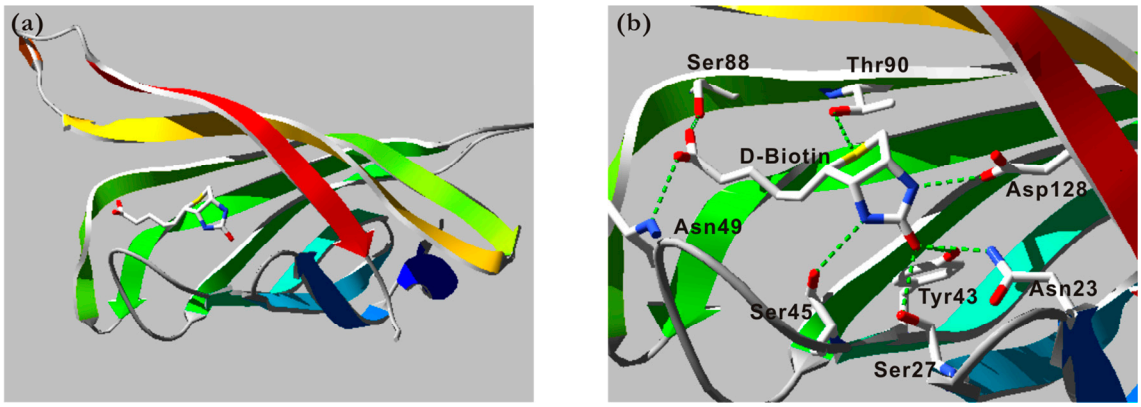

Figure 2.4. (a) A crystal structure of a monomeric streptavidin complexed with a biotin molecule (PBD ID: 1STP[101]). (b) A close-up image of the crystal structure showing the biotin molecule is hydrogen-bonded (green dotted lines) to a number of side-chains in the binding pocket.

2.1.2 Polymerised SU-8 particles

In the development of microparticle-based suspension arrays, one of the requirements is to use a suitable solid-support. If chemical modification of the surface is needed, then the solid support must be stable in all organic solvents that are used for the required reactions, which may include DMF, toluene, MeCN, alcohols and other common chlorinated solvents used for the manipulations. It also has to be biologically inert so that it does not interfere with the biological system of interest. The solid-support also has to be mechanically robust to withstand agitation and centrifugation. For multiplexed assays, the solid support has to be encodable so that each particle can be identified after a biological reaction.

EPON® Resin SU-8 (SU-8) can potentially fulfil the above requirements. SU-8 is an epoxy negative photoresist developed by IBM in 1989 for use in cationic polymerisation.[102,103] This material is excellent for making high aspect ratio structures and has been applied to fabricate micro-scale metallic parts and other structures.[102,104] Due to its robustness in different chemical and biological environments, SU-8 has also been used as structural material in micro- and nanotechnologies.[105]

2.1.2a Preparation of SU-8 macromonomer

SU-8 macromonomer can be synthesised from phenol through a series of condensation reactions (Figure 2.5).[106] First, two phenol molecules are condensed at the *para* position with acetone forming *bis*-phenol A. This molecule further reacts with formaldehyde, bridging multiple *bis*-phenol A molecules at the *ortho* position to form the macromonomer backbone. Finally the phenolic groups are reacted with epichlorohydrin yielding the glycidyl ether product.

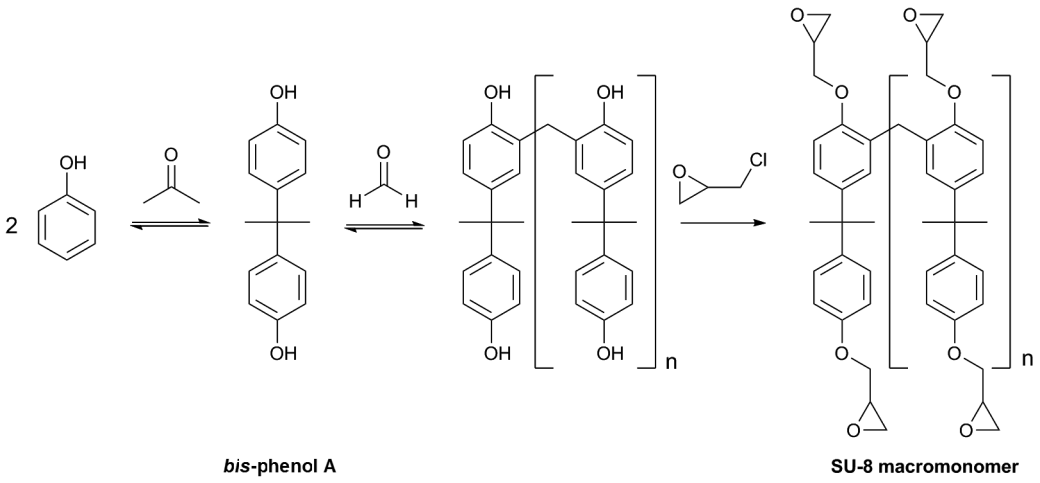

Figure 2.5. The preparation of SU-8 macromonomer.

2.1.2b Polymerisation of SU-8 by conventional photolithography

Commercially available SU-8 monomer solutions normally contain a photoacid (e.g. Ph_3SSbF_6), which upon exposure to UV light (λ = 365 nm) protonates the epoxy groups on the SU-8 monomer and catalyses the cationic polymerisation reaction (Figure 2.6).[107]

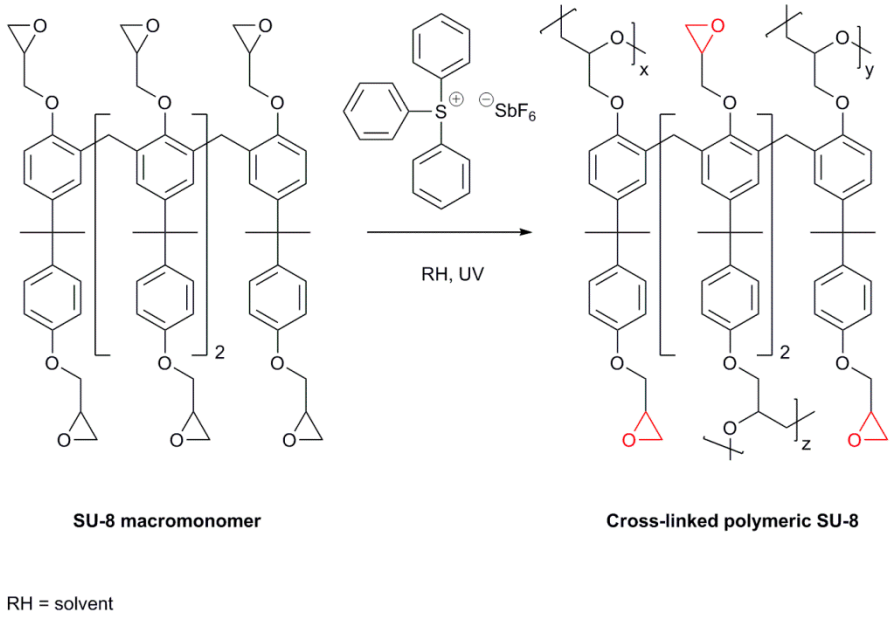

Figure 2.6. Photoacid activation of cationic SU-8 polymerisation. The unmodified epoxides (coloured in red) can be used as an initial point of attachment for further chemistry.

2.1.2c Microfabrication of polymeric SU-8 particles

Banu and co-workers demonstrated the microfabrication of SU-8 particles by photolithography (Figure 2.7).[108,109] First, a thin layer of aluminium (~100 nm) was deposited onto a silicon wafer by evaporation. On top of this was spin coated a solution of SU-8 monomer with ~10 μm thickness. Excess solvent was removed by soft-baking the wafer. Next, the SU-8 layer was exposed to UV light through a photolithographic mask so that the particles were structured on the wafer by polymerisation. Shaded areas were protected from the UV exposure and therefore contained the unpolymerised SU-8 monomer. This could be easily washed away by rinsing the wafer in water after the cross-linking step. Unlike conventional protocols for fabricating SU-8 microstructures, the polymeric particles did not undergo post-baking for further cross-linking. This was to preserve as many epoxy groups as possible for further chemical modifications at the later stage. Finally, to release the particles from the wafer, the aluminium layer (sacrificial layer) was wet etched using a solution containing tetramethylammonium hydroxide. The free particles could then be collected by filtration or centrifugation for further manipulations.

Figure 2.8 shows the micrographs of various SU-8 microparticles that were microfabricated by the method described above.

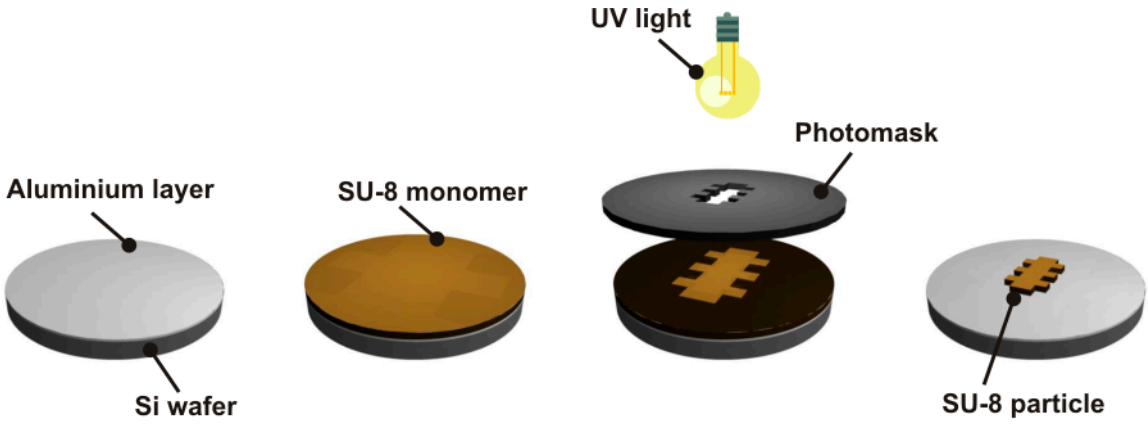

Figure 2.7 Schematic diagram of the microfabrication of SU-8 particles by photolithography.

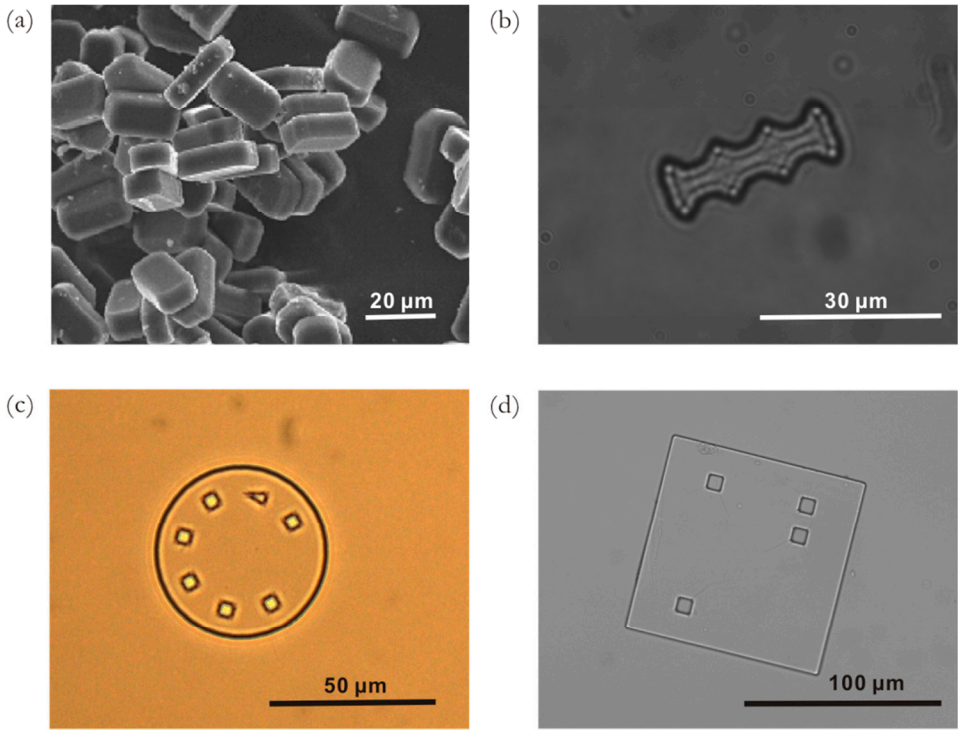

Figure 2.8. Different type of encoded SU-8 particles microfabricated by photolithography; (a) "Caterpillar"; (b) encoded bar; (c) disc[110]; and (d) square film.

2.1.2d Multistep synthesis on polymeric SU-8 particles

Cavalli *et al.* demonstrated the use of the polymeric SU-8 solid supports for step-wise solid-phase synthesis of peptides and oligonucleotides.[109] In solid-phase peptide synthesis, the residual epoxy groups on the particle surface provided an initial point of attachment for the first protected amino acid. The peptide chain was extended by standard Fmoc chemistry and the resultant product was found to be comparable with the one synthesised from commercially available Wang resin. Similarly, the SU-8 solid support was used for oligonucleotide synthesis through the standard phosphoramidite methodology.[111] Although the purity of the oligonucleotide product was lower than expected, the work of Cavalli *et al.* showed the potential of encoded SU-8 particles for pre-programmed mix-and-split combinatorial synthesis.

2.1.2e Attaching biological molecules to polymeric SU-8 surfaces

There are only a few examples in the literature of attaching biological molecules to the polymerised SU-8 surface.[112] One example for attaching DNA probes was by spotting amino- or unmodified oligonucleotides to the polymerised SU-8 film.[113] The precise chemistry underlying this immobilisation method was not characterised and hence the probe orientation and density was not determined. Another example was to react the surface hydroxyl group with organosilanes, for which may be further functionalised with proteins or oligonucleotides.[114,115]

2.1.3 The aims of this section

After the inception of this project, we envisaged using the encoded SU-8 particles in suspension arrays for different biological applications. To this end, the solid support needs to be chemically modified so that different types of biological molecules can be attached in a controlled manner. The aim of this part of the project is to develop methods for attaching

proteins, peptides and other biological molecules to the SU-8 particles, and to develop analytical tests for monitoring the chemical reactions at different stages.

2.2 Results and Discussion

2.2.1 Development of analytical tests for quantification of functional groups on the surface

Monitoring chemical reactions on solid supports using conventional analytical techniques, such as mass spectrometry, NMR, chromatography and infra-red spectroscopy are very challenging because the products are covalently attached to an insoluble support.[116] Although this can be overcome by releasing the product from the surface through a cleavable linker, the relatively large amount of material needed for analysis makes this method impracticable for routine reaction monitoring, especially for pico- to nanomole scale synthesis.[117-119] Rapid, straightforward and preferably quantitative methods for monitoring reactions on solid support are therefore needed. In this section, a number of techniques for on-bead reaction monitoring of SU-8 particles are described.

2.2.1a Quantification of free amino groups on surfaces by Kaiser test

Amino groups are one of the most important functional groups for solid-phase synthesis. There are many colourimetric tests for detecting this functional group.[120] Among these Kaiser test provides a straightforward and sensitive method for detecting primary amines. The use of ninhydrin to detect free primary amines in solution was first demonstrated by E. Kaiser *et al.* in 1970.[121] This involves reaction of free amino group with ninhydrin to form a chromophore, Ruhemanns Purple, which absorbs light at ~570 nm. The method was later adopted and modified by V Sarin *et al.* for quantification of $-NH_2$ groups during solid-phase peptide synthesis (Figure 2.9).[122]

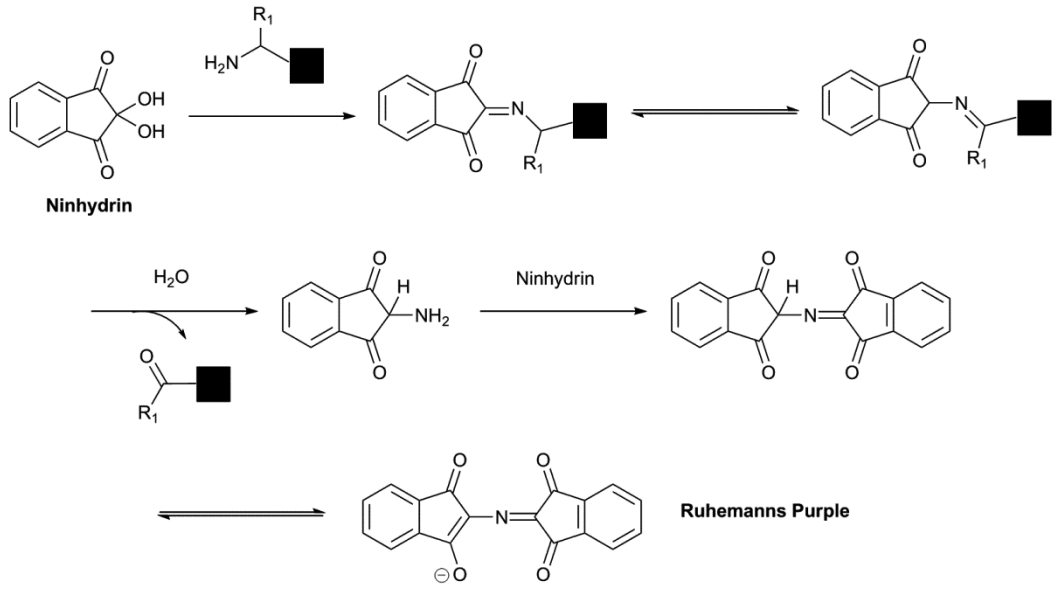

Figure 2.9. The principle of an on-bead Kaiser test. Ninhydrin reacts with primary amines to yield an amino-functionalised intermediate which further reacts with another ninhydrin molecule forming Ruhemanns Purple.

Table 2.1. Typical loading level of solid-supports as determined by quantitative Kaiser test.

Particle type	Dimension (μm)	Expected loading level (μmol/g)	Kaiser test measurement (μmol/g)
H_2N-Gly-Wang	N/A	500	530 ± 5
H_2N-GMA (sphere)	5	5.6	6 ± 2
H_2N-SU-8 (encoded bar)	30 × 10 × 5	15-25*	25 ± 3

*Literature value[109]

To demonstrate detection of primary amines on SU-8 particles, a modified method from V Sarin was used. The particles (encoded bar, Figure 2.8b) were functionalised by the general method of Cavalli *et al.*[109] The loading level was calculated from a mathematical formula (Equation 2.3) derived from the Beer-Lambert law (Equation 2.1) and molarity (Equation 2.2).

$$A = c \times \varepsilon \times l \qquad \text{Equation 2.1}$$

$$c = \frac{n}{v} \qquad \text{Equation 2.2}$$

$$LL = \frac{A \times v}{\varepsilon \times l \times w} \qquad \text{Equation 2.3}$$

where A is the absorbance of the Ruhemanns Purple chromophore at 570 nm; c is the concentration of the chromophore (M); ε is the molar extinction coefficient of the chromophore at 570 nm (15000 M^{-1} cm^{-1}); l is the path length (cm); n is the quantity of chromophore (moles); v is the volume of the Kaiser test (L); LL is the loading level of the solid support (mol g^{-1}); and w is the mass of the solid support (g).

Initially the Kaiser test procedure was assessed on commercially available solid supports, including Wang resin (loaded with glycine) and amino-functionalised glycidylmethacrylate beads (GMA beads, Bangs Laboratories, IN, USA), and on the amino-functionalised SU-8 particles. The results are summarised in Table 2.1. In general, the loading levels estimated by Kaiser test were comparable to the claimed values. For the SU-8 particles, the measured loading level was found to be close to the previously reported literature value.[109]

From the scheme shown in Figure 2.9, the soluble purple chromophore resulting from the reaction of ninhydrin and primary amines should not be attached to the surface. The chromophore results from the deamination of primary amino groups and the cleaved nitrogen atom is incorporated in Ruhemanns Purple. In general, the coloured product is expected to be completely released from the solid into the solution and the absorbance of this molecule can be measured quantitatively. However, it was found that the chromophore was only partially released from the large SU-8 particles (e.g. square film, dimension 150 × 150 × 10 μm, Figure 2.8d). Despite numerous attempts to wash the particle, a proportion of the coloured chromophore remained strongly adsorbed or covalently linked to the surface. This

observation suggests that Kaiser test might not be suitable for measuring amino groups on relatively large SU-8 particles.

2.2.1b Fmoc quantification

Another approach for quantifying the amount of amino groups is by quantitative Fmoc test (Figure 2.10). This method is based on the quantitative UV analysis of the Fmoc deprotection product, dibenzofulvene-piperidine adduct.

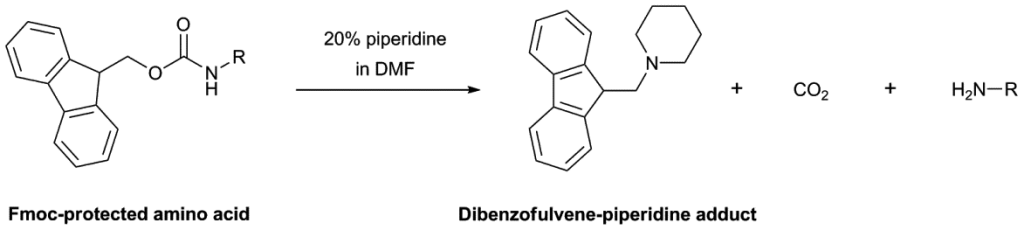

Figure 2.10. Fmoc deprotection using 20% piperidine in DMF. The amount of the dibenzofulvene-piperidine adduct released can be quantified by UV analysis.

Fmoc-protected species (e.g. Fmoc-Gly-OH) were covalently coupled to the amino functionalised GMA or SU-8 particles (encoded bar, Figure 2.8b) using the TBTU/HOBt procedures described by Cavalli *et al.*[109] The Fmoc group was then removed using 20% piperidine in DMF. The amount of the released dibenzofulvene-piperidine adduct was measured by UV/Vis spectroscopy at 290 nm (ε = 7800 M^{-1} cm^{-1}).

Table 2.2. Measurements of loading level on solid-supports by quantitative Fmoc test.

Particle type	Dimension (μm)	Initial loading level (μmol/g)	Fmoc test measurement (μmol/g)
H_2N-Gly-Wang	N/A	530 ± 5	528 ± 3
H_2N-GMA (sphere)	5	6 ± 2	6 ± 2
H_2N-SU-8 (encoded bar)	30 × 10 × 5	25 ± 3	27 ± 2

Table 2.2 summarises the loading levels of different solid supports estimated by Fmoc test. As anticipated, the measured loading levels were very comparable to the result obtained from the previous Kaiser test. This also indicated that the coupling of Fmoc-Gly-OH and the removal of Fmoc group were high yielding on all three types of solid supports. This method could potentially provide an additional confirmation on the loading level measurements.

2.2.1c Surface hydroxyl groups quantification by DMT absorption measurement

Currently there are only a few methods for quantifying surface hydroxyl groups. These methods normally require sophisticated instruments, including ellipsometry[123] and X-ray photoelectron spectroscopy (XPS).[124] The use of these instruments is generally time consuming and not suitable for routine reaction monitoring. To this end, we aimed to develop a quantitative colorimetric test for routine hydroxyl group measurements.

Similar to the Fmoc test described above, the method being developed was based on the quantitative absorbance analysis of the 4,4'-dimethoxytrityl (DMT) deprotection product. A known amount of epoxy SU-8 particles (~5×10^4 particles) was subject to hydrolysis under acidic or basic conditions at room temperature for 24 h to ring open the epoxide. The resulting hydroxyl-functionalised particles were reacted with a DMT-protected nucleoside phosphoramidite as described by McBride.[111] After that, the DMT group was removed using 3% (v/v) trichloroacetic acid (TCA) in DCM. The resulting bright orange DMT deprotection product was quantified by absorbance at 498 nm (Figure 2.11).

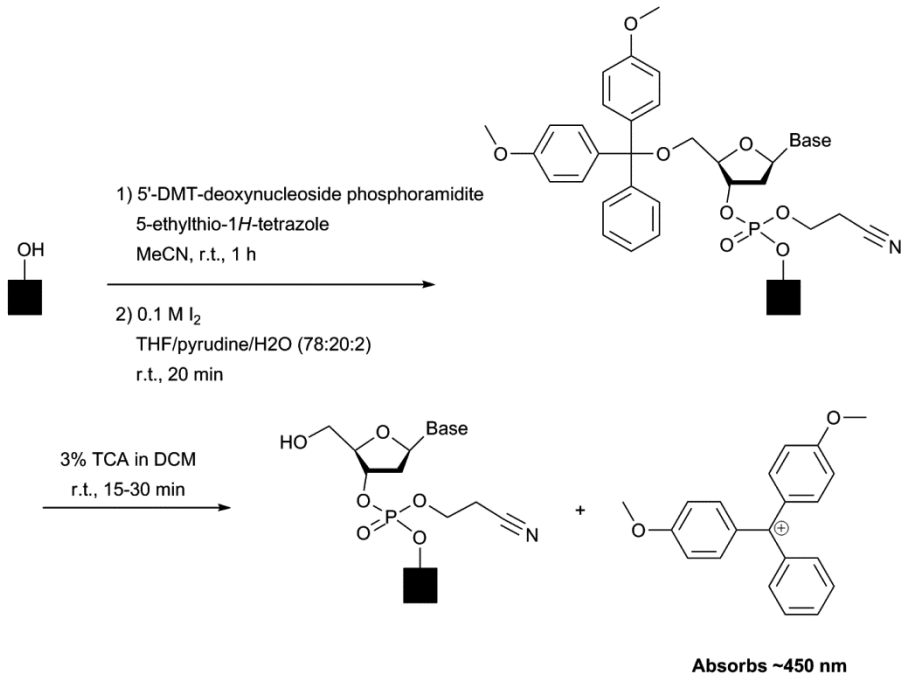

Figure 2.11. During DMT deprotection the bright orange DMT cation liberated can be quantified by measuring the absorbance.

The loading level of hydroxyl groups on SU-8 particles estimated by DMT test was found to be 370 ± 120 μmol/g. Non-DMT protected hydroxyl-SU-8 particles were used as negative controls and produced no significant measurements. The coefficient of variation (CV) of this measurement after 5 repeated measurements was found to be ~30%, which is larger than other established quantification methods on SU-8 microparticles (i.e. Kaiser test and Fmoc test ~10%). The relatively large variation might be due to the instability of the DMT cation, which could react with water and form the spectroscopically inactive DMT-OH. Nevertheless, this experiment demonstrated that the DMT test provided a quick and easy way to monitor hydroxyl group-based reactions as well as estimating the loading level of surface hydroxyl groups.

2.2.1d BCA protein assay

Apart from monitoring specific functional groups on the surface, it was also necessary in this work to monitor the attachment of biological molecules, especially proteins and peptides.

The generic quantitative tests described above could not be used to measure protein density on the surface because the amino acid side chain's functional groups could potentially interfere with the specific chemical reactions.

One attractive alternative is the bicinchoninic acid (BCA) protein assay (Figure 2.12).[125] This assay detects the formation of cuprous cation (Cu^{+}) as a result of a reduction reaction of cupric cation (Cu^{2+}) by protein molecules in an alkaline environment (Biuret reaction). The resultant Cu^{+} cations bind to a ligand, BCA, and exhibit a linear absorption at 562 nm with increasing protein concentration.

Unlike other colorimetric tests, the BCA protein assay is not an end-point assay. The amount of the purple product produced in the reaction depends on the protein to be tested and the time and temperature of the reaction. For this reason, calibration curves based on measurements of standard protein samples with known concentrations were plotted every time the assay was used (Figure 2.13).

To demonstrate the quantification of protein on SU-8 particles (encoded bar, Figure 2.8b), a known number of SU-8 particles (~5 × 10^4 particles) coated with recombinant *Staphylococcus aureus* protein A (protein A – see section 2.2.2c for details on protein immobilisation) was incubated in commercially available BCA protein assay solution (a mixture of BCA and Cu^{2+} in NaOH solution) at 60 °C for 15 min. The purple supernatant was separated from the suspension before the absorbance was measured at 562 nm. To estimate the protein concentration, a correlation factor was determined from the standard curve (Figure 2.13), and then used to convert the measured absorbance value into concentration.

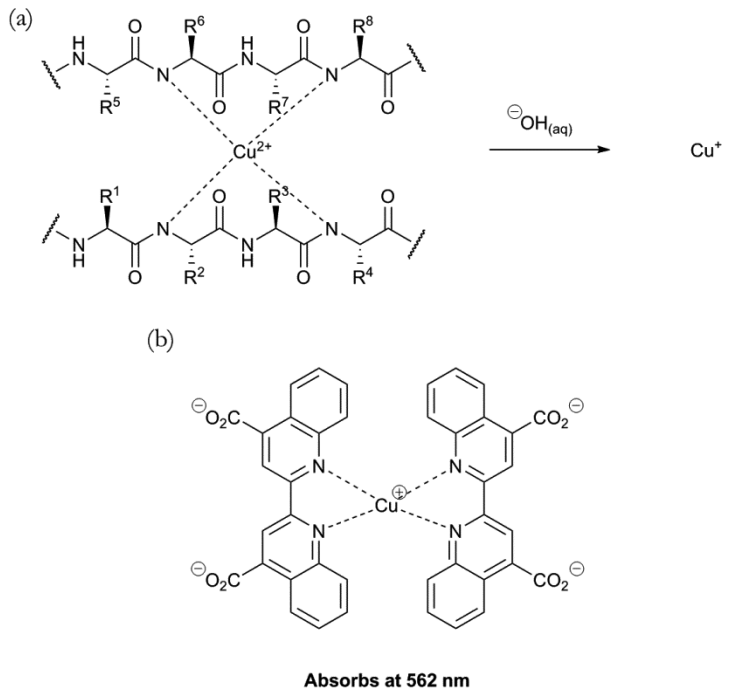

Figure 2.12. (a) Amide bonds within the polypeptide chain chelate with Cu^{2+} ions and act as a reductant, producing Cu^{+} ions under alkaline conditions. (b) Cu^{+} ions form purple coloured complex with BCA which absorbs at 562 nm.

The BCA protein assay was found to be very sensitive and could measure as little as 100 nM of protein in aqueous buffer. The method was very useful for determining the amount of immobilised proteins or peptides without using a large quantity of functionalised SU-8 particles. As shown in Table 2.3, a very low noise signal was generated from the carboxyl-functionalised SU-8 particles, whereas the protein A-functionalised SU-8 particles could be detected and quantified.

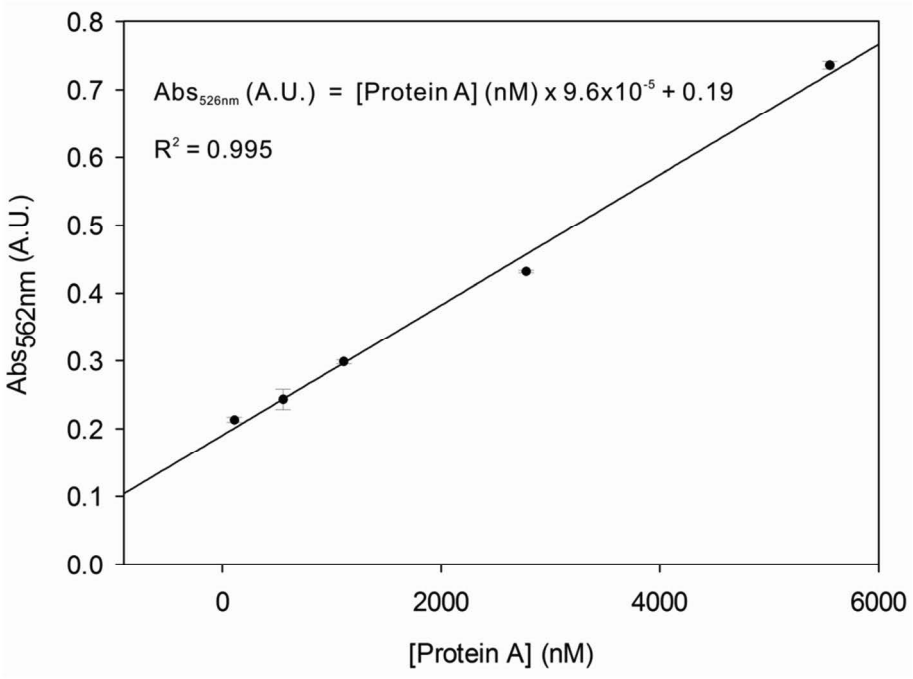

Figure 2.13. An example of a BCA calibration curve of protein A from *S. aureus*. Each data point represents the mean of three repeated measurements. The standard deviation of these measurements is shown as error bars on the graph.

Table 2.3. Loading level of protein A on SU-8 particle.

Particle Type	Loading level (nmol/g)
Carboxyl-SU-8	0 ± 1
Protein A-SU-8	243 ± 6*
*Based on three repeated measurements of one set of SU-8 microparticles.	

2.2.2 Chemistry on SU-8 microparticles

Having developed a number of useful analytical techniques for measuring functional groups on surfaces, attention turned to functionalising the SU-8 microparticles with biological molecules.

2.2.2a Releasing SU-8 microparticles from aluminium-coated silicon wafer

The SU-8 microparticles (Figure 2.8a,b and d), except the "disc-shaped" microparticles (Figure 2.8c), were microfabricated by S. Banu and K Chamberlain (School of Chemistry and School of Electronics and Computer Science, University of Southampton) according to the published method.[108] "Disc-shaped" SU-8 microparticles were provided by Biocartis S.A. (Lausanne, Switzerland). These particles, dimension between 20 μm and 150 μm, were prepared by conventional photolithography as described in section 2.1.2c. To lift off SU-8 microparticles from the silicon wafer, the aluminium sacrificial layer was wet etched using an aqueous solution of tetramethylammonium hydroxide (2.2% w/v) containing 1% (w/v) surfactant (Microposit MF-319 developer, Rohm and Haas, MA, US). With the aid of sonication, the microparticles were released into the etch solution in 0.5-3 h, depending on the size of the particles. Subsequently the particles were harvested by centrifugation (3100 *g*, 5 min) and then washed sequentially with Tween-solution (0.1% Tween-20 in water), MeOH and DMF (or MeCN).

Table 2.4. The recovery yield of SU-8 particles from silicon wafer after wet etching the aluminium sacrificial layer.

Particle Type	Dimension (μm)	Estimated Recovery Yield (%)
"Caterpillars"	20 × 10 × 5	~95
Encoded bars	30 × 10 × 5	~95
Discs[110]	50 × 50 × 10	~85
Square films	100 × 100 × 10	~70

Long sonication was avoided as it heated the water in the tank as well as the etch solution. The elevated temperature could potentially further cross-link the SU-8 particles and hence reduce the amount of residual epoxy groups on the surface. An alternative method to release the particles was by repeated pipetting the etch solution on to the wafer.

Using this method the SU-8 particles (30 × 20 × 10 μm) were released within 5 min at room temperature.

The amount of particles recovered from the lift off process was estimated using a haemocytometer and the results are shown in Table 2.4. For relatively small particles, such as the "Caterpillars" and encoded bars, the recovery yield was found to be sufficiently high (~95%). However, for larger particles, such as the square film, 30% of the particles were lost during the lift off process. These particles were found to adhere to the glass container, probably due to their relative large surface area. This may be overcome by adding more detergent to the lift off solution and employing sonication during the recovery process.

2.2.2b Methods for protein immobilisation

To use the SU-8 microparticles for microparticle-based suspension arrays, the surface must be functionalised with biologically interesting molecules. A good example is provided by the adsorption of immunoglobulin G (IgG) or oligonucleotides[113] (unmodified or 5'-NH_2-modified) onto unmodified SU-8-coated glass slides. Although this method provides a straightforward route for coating proteins or DNA onto the surface, the attachment mechanism behind this method was not well understood, leading to a risk of unpredictable loading and heterogeneity of binding modes. In order to gain control of these parameters, we sought to develop alternative methods for covalently conjugating different biological molecules to the surface in a control manner.

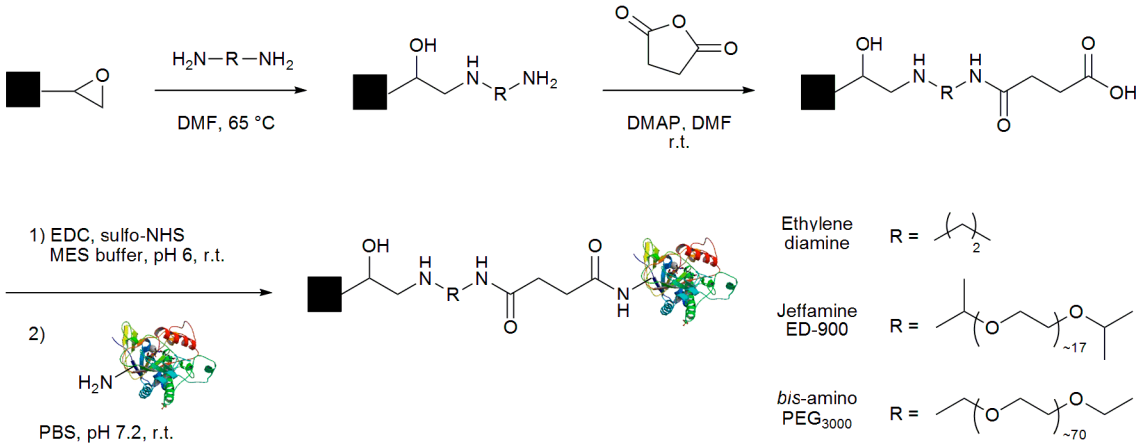

Figure 2.14. Schematic diagram of protein immobilisation onto SU-8 particles *via* surface residual epoxy groups.

SU-8-NH$_2$ One of our approaches to functionalise the SU-8 particles was *via* the residual epoxy groups on the surface. In this method, the free epoxy groups on the encoded bars were ring opened by reaction with a *bis*-amine (ethylene diamine, Jeffamine ED-900 or H_2N-PEG_{3000}-NH_2) to yield free –NH_2 groups on the surface (Figure 2.14).

The loading level of –NH_2 on the surface was quantified by Kaiser test (section 2.2.1a) and the results are shown in Table 2.5. The use of ethylene diamine resulted in a loading level of 116 ± 8 μmol/g, whereas Jeffamine ED-900 and H_2N-PEG_{3000}-NH_2 gave a loading level of 25 ± 3μmol/g and 11 ± 6 μmol/g respectively.

Table 2.5. The loading levels of primary amines on SU-8 particles after functionalised with different *bis*-amines

Spacer	MW	Loading Level (μmol/g)
H_2N-$(CH_2)_2$-NH_2	60.1	116 ± 8
Jeffamine ED-900	~900	25 ± 3
H_2N-PEG_{3000}-NH_2	~3000	11 ± 6

The lower loading levels observed with the longer *bis*-amines (i.e. Jeffamine ED-900 and H_2N-PEG_{3000}-NH_2) may be due to their bulky structures which reduce their access to the free epoxy groups on the surface, and severely restrict access to any epoxides within the pores.

On the other hand, ethylene diamine may be small enough to enter these pore structures and react with the shielded epoxy groups within the polymeric matrix as well as the more accessible reactive groups at the particle surface.

SU-8-COOH Many existing methods for protein immobilisation onto surfaces employ glutaraldehyde as a cross linker, bridging the amino groups on the surface with the lysine residues on the protein surface. This method is widely used because of its simplicity and relatively short reaction time (~1 h). However, the resulting Schiff base can potentially be hydrolysed under physiological conditions, resulting in a non-permanent covalent linkage. One method to overcome this problem is to reduce the imine with a reducing agent, such as sodium borohydride, to give a more stable secondary amine. The stability of the linkage is greatly improved, however the use of reducing agents might damage the attached biological molecules (e.g. by reducing disulfide bonds, which are of particular importance in the structure of antibodies).

An alternative method is to couple amines of the protein molecules to carboxyl-functionalised surface with the aid of coupling reagents. The resulting amide bond is highly robust and is virtually irreversible under physiological conditions. To this end, a method for producing carboxyl-functionalised SU-8 particles was developed.

As shown in Figure 2.14, amino-functionalised SU-8 particles were reacted with succinic anhydride and DMAP in DMF at room temperature to yield free carboxyl groups. The reaction was monitored by Kaiser test and considered to be completed when a negative Kaiser test was observed. The yield of the reaction was found to be >90% after 2 rounds of reaction.

2.2.2c Immobilisation of proteins onto carboxyl-functionalised SU-8 particles

To demonstrate protein immobilisation, polyclonal human IgG was coupled to the carboxyl-functionalised SU-8 particles using EDC/sulfo-NHS-mediated coupling chemistry (Figure 2.15). Two strategies were tested: 1) a one-pot reaction where the particles were agitated in a mixture of EDC, sulfo-NHS and the protein of interest; and 2) a two-step coupling method where the carboxyl-functionalised particles were first reacted with EDC and sulfo-NHS to form an active ester intermediate before the addition of the protein. After the coupling reactions, SU-8 microparticles prepared by the two methods were subjected to BCA protein assay to estimate the protein loading level.

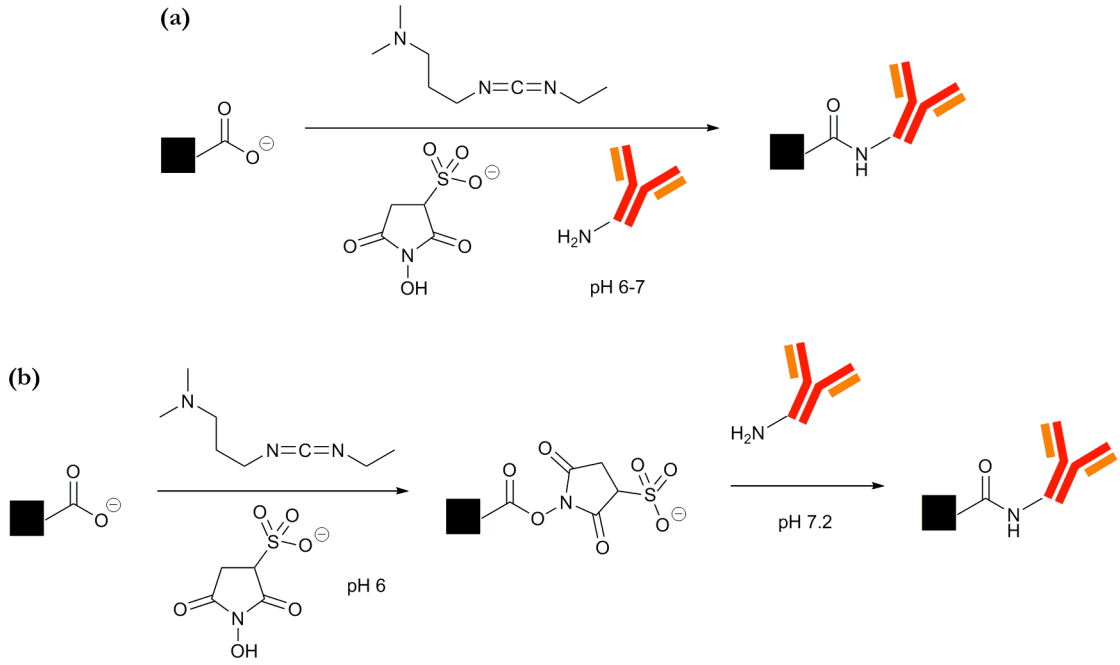

Figure 2.15. Protein immobilisation onto carboxyl-functionalised SU-8 particles *via* the (a) one-step or (b) two-step method.

Table 2.6. The amount of human IgG immobilised onto carboxyl-SU-8 particles using one-pot or two-step methods.

	Loading Level (nmol/g)	
	One-pot method	Two-step method
Human IgG-SU-8	103 ± 11	23 ± 8

The loading level of IgG on SU-8 using the one-pot method was found to be 103 ± 11 nmol/g (~9 layers) whereas the two-step method gave a loading level of 23 ± 8 nmol/g (~2 layers). Using the one-pot protocol, the amount of protein immobilised was roughly four times higher than the two-step method. This was probably due to undesired side-reactions that cross-linked the protein molecules together *via* coupling between amines and carboxylic acids at the protein termini, or on amino acid side chains. In the two-step method, the cross-linking of IgG is expected to be reduced because most of the residual EDC was removed during the intermediate washing step.

The use of these protein-coated SU-8 particles in multiplexed immunoassays will be discussed in detail in Chapters 3 and 4.

2.2.2d Surface functionalisation *via* hydroxyl groups

Functionalisation of SU-8 particles *via* residue epoxy groups provides a step-wise and controllable method for attaching a range of biomolecules to the surface. This route is particular useful for immobilising relatively large biomolecules (e.g. proteins) because the amount of functional groups on the surface is sufficient for immobilising a monolayer of such biomolecules. However, when coupling a small peptide or a short oligonucleotide, the epoxy routes may not be optimal. The amount of functional groups available for the attachment is relatively low and may vary hugely from one batch of particles to another, as a result of hydrolysis of epoxides during storage or polymerisation of SU-8 macromonomer, or processing of microfabricated particles. For instance, small variations in the preparation of

the particles, such as the age of the SU-8 monomer, slight variation in photolithography, sonication time in etch solution and temperature, can have a profound effect on the amount of free epoxy groups available for functionalisation, even though the mechanical properties of the polymerised materials may appear identical. It was therefore necessary to develop an alternative method to enhance the amount of functional groups on the surface for a more controllable loading level. To this end, a hydroxyl group based surface chemistry strategy was exploited.

Residual epoxy groups on the particles' surfaces were fully hydrolysed by incubation in 1 M HCl (aq.) at room temperature for 24 h. The resulting hydroxyl groups, as well as other hydroxyl groups produced from the etching/release process, were available for further functionalisation as reactive alcohols. To demonstrate this, the hydroxyl-SU-8 particles were reacted with a spacer, DMT-HEG-phosphoramidite, in the presence of a tetrazole derivative coupling agent in anhydrous MeCN at room temperature. Subsequently the particles were treated with an oxidising agent containing 0.1 M I_2 at room temperature for 20 min to generate a stable phosphate triester and then washed extensively with MeCN (Figure 2.16).

To quantify the hydroxyl group loading level, the DMT-HEG spacer was deprotected using 3% TCA in DCM as described in section 2.1.1c (Figure 2.11). The loading level was found to be 370 ± 120 μmol/g. When compare with amino-functionalised SU-8 particles (highest loading level: 116 ± 8 μmol/g), the amount of –OH groups on the particle was found to be relatively high. This indicated there were more accessible hydroxyl groups on the surface, potentially providing a higher biomolecule density on the surface.

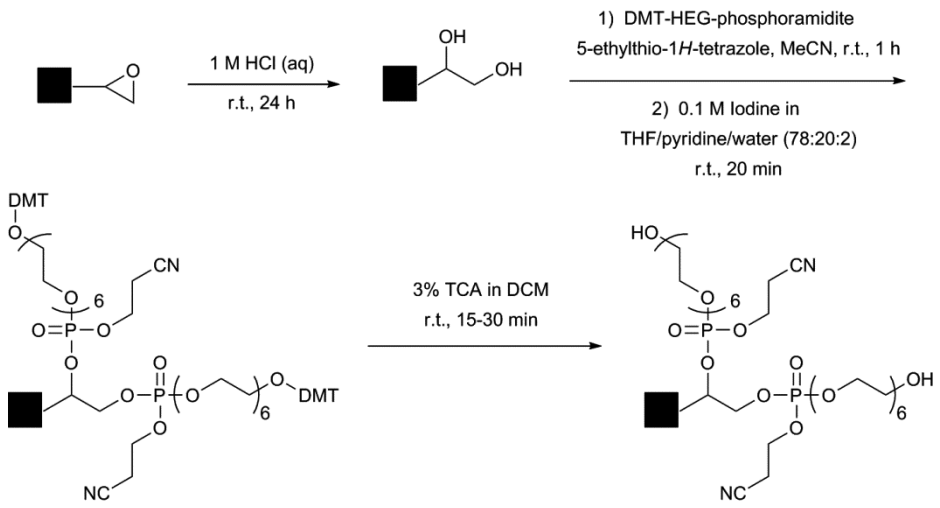

Figure 2.16. Functionalisation of hydroxyl-functionalised SU-8 particles *via* phosphoramidite chemistry.

2.2.2e Preparation of azido-SU-8 microparticles

Organic azides have emerged as an important functional group in synthetic chemistry and bioconjugation. They are frequently used as a masking agent for amines, in Staudinger ligations for conjugating different molecules, and other applications.[126] Moreover, the recent discovery of the Cu(I)-catalysed 1,3-dipolar cycloaddition of azides and terminal alkynes (Click chemistry), which is bio-orthogonal and highly efficient in water, has promoted the interest in the use of azides in biotechnology.[127,128]

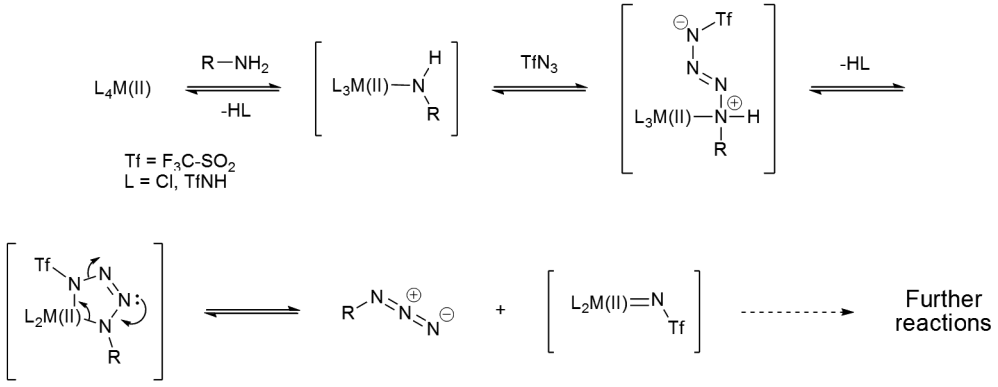

Figure 2.17. Proposed mechanism for the transition metal-catalysed diazotransfer reaction. (M = Cu^{2+} or Zn^{2+})

There are a few methods available for the introduction of azide moieties into a molecule. One method is by an S_N2 reaction in which a leaving group (e.g. –OTs or –Br) is displaced by an azide ion (e.g. from NaN_3).[126] In solution-phase chemistry, this reaction can be followed by common analytical methods, such as mass spectrometry, IR and NMR. However, the preparation of an azide on a solid-support using this method is difficult to monitor. Another approach to prepare organic azides is by transition metal-catalysed diazo-transfer reaction using trifyl azide (TfN_3) as an diazo donor.[129] This reaction has been shown to convert a primary amine into an azide in mild condition with high yield.[129-131] Potentially, this reaction can be monitored by measuring the consumption of primary amine by quantitative Kaiser test.[132] The reaction mechanism was recently proposed by Nyffeler *et al.* (Figure 2.17).[130]

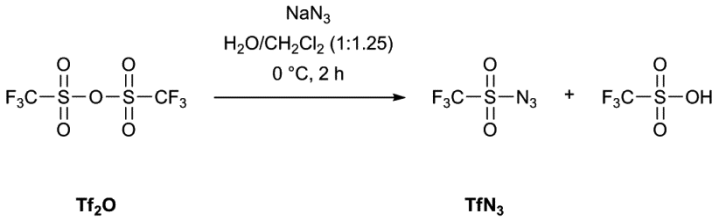

Figure 2.18. Preparation of trifyl azide (TfN_3)

The preparation of TfN_3 was first described by Ruff[133] and later modified by other research groups.[129-131] For this work described herein, TfN_3 was prepared according to the method of Canvender *et al.*[131] (Figure 2.18). In brief, trifluoromethanesulfonic anhydride (Tf_2O) was added dropwise to a biphasic mixture of NaN_3 in water and CH_2Cl_2 at 0 °C. The reaction mixture was stirred at 0 °C for 2 h. After that the organic phase was isolated and the aqueous phase was extracted twice with CH_2Cl_2. Finally, the combined organic phase was extracted with saturated Na_2CO_3 solution and then used directly for the diazo-transfer reaction without further purification.

Although TfN_3 was shown to be a good diazo-transfer reagent, the use of this compound in the reaction is problematic. Dried TfN_3 is reported to be explosive and has to be stored as a solution. In addition, the TfN_3 solution has a poor shelf-life and necessitates its preparation prior to use. To overcome these problems, Goddard-Borger *et al.* proposed a more stable alternative compound, imidazole-1-sulfonyl azide (Figure 2.19), which could potentially replace TfN_3 as a diazo donor in the diazo-transfer reaction.[134]

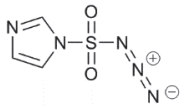

Figure 2.19. Chemical structure of imidazole-1-sulfonyl azide.

The preparation of alkyl azide on amino-functionalised GMA beads and SU-8 microparticles by the transition metal-catalysed diazo-transfer reaction was assessed. The surface primary amine was reacted with 100-fold molar excess of imidazole-1-sulfonyl azide (generously provided by Dr. R. T. Ranasinghe, School of Chemistry, University of Southampton) or freshly prepared TfN_3. Different divalent metal cations, namely Cu(II) and Zn(II), were used as a catalyst.[129-131] The reaction progress was monitored by qualitative Kaiser test as described in section 2.2.1a.

Table 2.7 summarises the results of the diazo-transfer reaction on GMA beads and SU-8 microparticles (encoded bar, Figure 2.8b). In general, the use of TfN_3 as a diazo donor and Cu(II) as a catalyst successfully converted $–NH_2$ to $–N_3$ on GMA beads and SU-8 microparticles. Zn(II) was found to be less efficient as a catalyst. Interestingly, imidazole-1-sulfonyl azide successfully introduced the azide moiety on GMA beads but failed to initiate the reaction on SU-8 microparticles under similar reaction conditions. Oyelere and co-workers reported that the diazotransfer reaction with TfN_3 or its derivatives behave very differently on different surfaces depending on the matrix backbone.[132] For

instance, it was reported that a 90% conversion yield was achieved with TentaGel resin at 25 °C in 4 h, whereas in the same condition amino-functionalised CPG failed to react with TfN_3.

Table 2.7. The conversion yield of amine to azide on different solid supports.

Solid support	Diazo donor	Catalyst	Estimated $\%NH_2$ conversion (%)[a]
NH_2-SU-8	TfN_3	Cu(II)	>95
(encoded bar)		Zn(II)	~50
	Imidazole-1-sulfonyl azide	Cu(II)	<5[b]
		Zn(II)	<5[b]
NH_2-GMA	TfN_3	Cu(II)	>95
		Zn(II)	~50
	Imidazole-1-sulfonyl azide	Cu(II)	>95
		Zn(II)	<5[b]

[a] $\%NH_2$ conversion was calculated from Kaiser test measurements in which the disappearance of $-NH_2$ on the solid-support over the course of the reaction was monitored. [b] Close to the limit of detection of Kaiser test.

2.2.2f Attachment of alkyne-derivitised peptide to azido-functionalised GMA beads

To demonstrate the use of the azido-functionalised solid supports in a Cu(I)-catalysed "Click" reaction, an alkyne-derivitised fluorescently-labelled hexapeptide was incubated with the 1) azido-functionalised GMA beads in the presence or absence of the Cu(I) catalyst; and 2) amino-functionalised GMA beads at room temperature for 20 h (Figure 2.20). After removing the excess labelled peptide, the beads were washed with the reaction buffer (1 mL × 4) and then analysed by fluorescence flow cytometry.

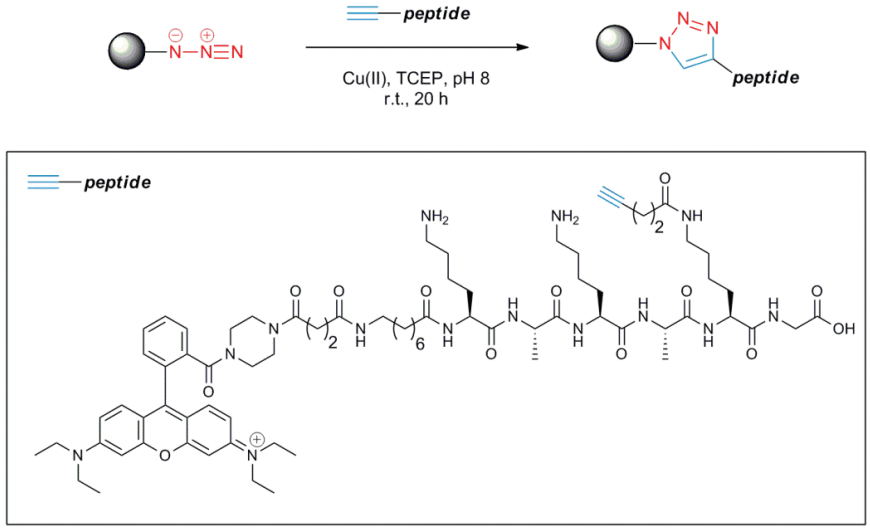

Figure 2.20. Attachment of an alkyne-derivitised peptide to azido-functionalised solid support by the Cu(I)-catalysed "Click" chemistry.

Figure 2.21 summarises the results of the fluorescence measurement. A negative control of amino-functionalised GMA beads which had not been reacted with the peptide indicated the background fluorescence level of the solid supports. The azido-functionalised beads reacted with the alkyne-derivitised peptide in the presence of the Cu(I) catalyst. Under the same reaction conditions, a relatively small amount of the labelled peptide was found to attach to the amino-functionalised GMA beads, presumably due to non-specific binding. Interestingly, in the absence of the Cu(I) catalyst, the labelled peptide was able to react with the azido-functionalised beads, but with less efficiency.

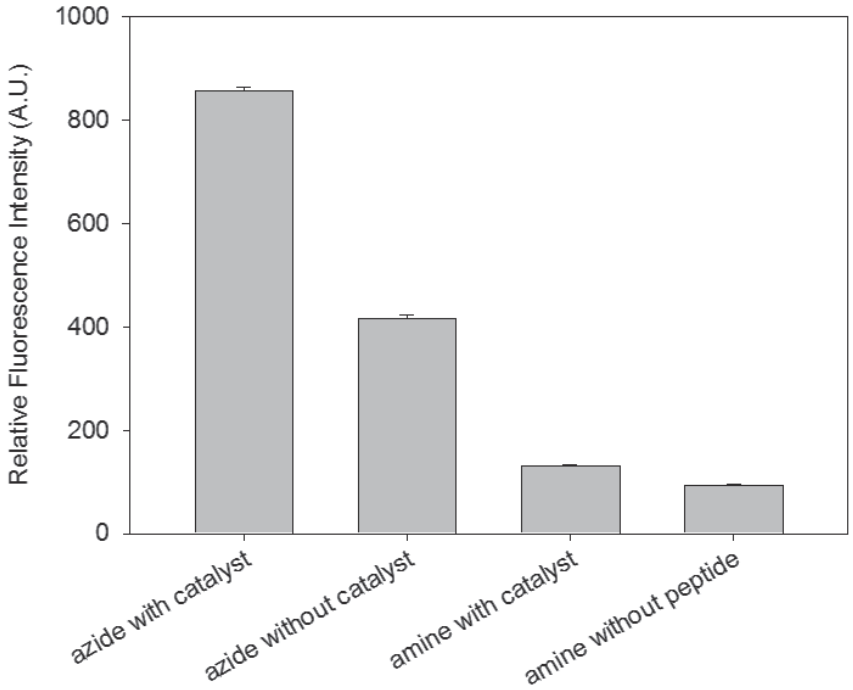

Figure 2.21. Fluorescence histogram of the functionalised GMA beads after incubation with an alkyne-derivitised hexapeptide in the presence or absence of the Cu(I) catalyst.

2.2.3 Reducing non-specific binding of undesired biological molecules

Polymerised SU-8 structures are widely used as microfluidic devices, bio-sensors, biological assay platforms and drug delivery carriers. The material is physically and chemically robust and shown to be biologically inert. However, the highly hydrophobic nature of SU-8 could potentially be a limitation in biological applications. For instance, many proteins, DNA molecules and other molecules are reported to bind to polymeric SU-8 surfaces non-specifically.[113,135] During *in vitro* biological assays, these biofouling effects must be greatly reduced in order to enhance the sensitivity and selectivity. To this end, many efforts have been made to reduce non-specific binding by a number of methods.[115,135,136] A simple method, as commonly employed for other surface-based detection platforms, is to

shield the surface with blocking molecules, such as BSA and casein, by adsorption.[137] This method has a number of disadvantages, such as reducing the target signal intensity; producing a non-uniform surface and, in some cases, increasing the noise level.[138] In addition, since the coating is not permanently attached to the surface, the protein layer might be washed off over the course of the assay.

An alternative method to reduce non-specific binding is to coat the surface with a layer of molecules to increase the non-fouling properties. Poly(ethylene glycol) (PEG) and its derivatives have been widely used to coat silicon-based substrates[139,140] and gold surfaces[141,142] to reduce undesired binding and improve assay specificity. The covalent attachment of PEG on polymeric SU-8 surface was demonstrated by S Tao and co-workers, and the conditioned surfaces showed promising results in a cellular assay.[115]

In the following sections, the covalent attachment of different PEG derivatives on polymeric SU-8 microparticles, and their resulting non-fouling effects are reported. To this end, two routes were tested: 1) "Grafting to" method; and 2) "Grafting from" method.

2.2.3a "Grafting to" method

In the "grafting to" method, a pre-synthesised polymer is conjugated to the target surface by physisorption, chemisorption, or a combination of both. In essence, the attachment of Jeffamine ED-900 and H_2N-PEG_{3000}-NH_2 to the polymeric SU-8 particles described in this chapter, and the attachment of silane-PEG described by S. Tao *et al.* are examples of this grafting technique.

We tested the non-fouling property of the SU-8 particles (square film, Figure 2.8d) grafted with a) ethylene diamine (MW 60.1), b) Jeffamine ED-900 (MW ~900), c) H_2N-PEG_{3000}-NH_2 (MW ~3000) and d) star-shaped PEG_{12000} isocyanate[143,144] (sPEG-NCO; MW 12000; donated by T. Newman, School of Biological Sciences, University of

Southampton). *Bis*-amino spacers were attached to the surface by ring opening the residual epoxy groups on the surface as described above (section 2.2.2b). For sPEG-NCO conjugation, polymeric SU-8 particles were first functionalised with ethylene diamine to yield an amino-functionalised surface. Freshly prepared sPEG-NCO solution in deionised water (10 mg/mL, 1 mL) was then added to the particles and the reaction mixture was agitated at room temperature for 30 min. After thorough sequential washing with deionised water, methanol and DMF, the sPEG-NCO-coated particles were reacted with ethylene diamine to produce amino-functionalised surfaces. The presence of the amino groups was confirmed by Kaiser test.

To test the non-fouling properties of the polymeric SU-8 particles grafted with the different spacers, the particles were agitated in a solution of Cy5-labelled streptavidin (50 μg/mL) in PBS (1 mL) at room temperature for 1 h. After washing with PBS, the particles were isolated and then examined under a fluorescence microscope (Axiovert 200, Zeiss, Germany) equipped with a mercury broadband lamp and Cy5 filter sets. Fluorescence images of the particles were recorded with a cooled-CCD digital camera (Hamamatsu OCAR-ER, 5 s exposure time, gain = 200). The mean fluorescence intensity was analysed using a publically available open software package (ImageJ v1.41o, National Institutes of Health, USA).

Figure 2.22 shows the result of the non-specific binding experiment. Polymeric SU-8 functionalised with ethylene diamine and Jeffamine ED-900 exhibited the most non-specific binding of Cy5-labelled streptavidin. As seen in the fluorescence image (Figure 2.22a), the surface grafted with ethylene diamine showed a uniform fluorescence across the surface. In contrast, Jeffamine ED-900 (Figure 2.22b) produced a relatively inhomogeneous surface. The surface coated with $H_2N\text{-}PEG_{3000}\text{-}NH_2$ (Figure 2.22c) or sPEG (Figure 2.22d) showed better non-fouling property. Interestingly, the edges of the surfaces contained a higher

amount of non-specifically bound proteins, except with the H_2N-PEG_{3000}-NH_2 coated surface in which the entire surface produced a relatively low and uniform fluorescence.

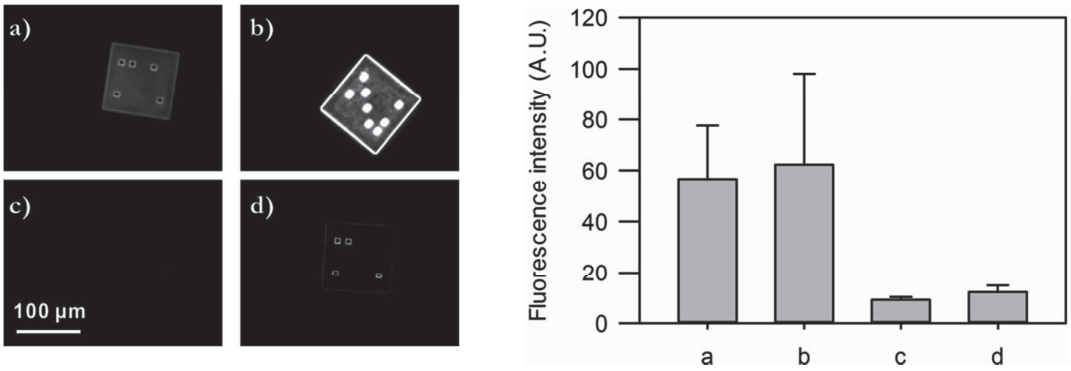

Figure 2.22. Cy5-streptavidin (50 µg/mL) was incubated with SU-8 particles (square film) functionalised with a) ethylene diamine; b) Jeffamine ED-900; c) H_2N-PEG_{3000}-NH_2; and d) amino-sPEG. After washing with PBST the particles were imaged using a fluorescence microscope (Cy5 filter set, 5 s exposure time, gain = 200). The mean fluorescent intensities of five particles from each population are shown in the graph. The standard deviation of the measurements is represented by the error bars.

The above experiment suggested that a long linear PEG chain or sPEG should be used for reducing non-specific protein binding on polymeric SU-8 surfaces. However, sPEG-NCO has a relatively short shelf-life due to its nature of high reactivity and moisture sensitivity, which would limit its practical use. Commercially available sPEGs functionalised with amino- or other stable functional groups might be more suitable for this purpose. The use of H_2N-PEG_{3000}-NH_2-grafted SU-8 particles for multiplexed immunoassays will be discussed in Chapter 4.

2.2.3b "Grafting from" method

Another grafting technique commonly used is the "grafting from" method. Instead of attaching a pre-synthesised polymer onto the target surface, the polymer is grown *in situ* from the surface. This has a number of advantages over the "grafting to" method, such as a higher polymer density leading to better non-fouling property.[145-147] Biologically interesting molecules can also be embedded into the polymer matrix, increasing the loading level and potentially the sensitivity and dynamic range of the assay platform.

Poly(ethylene glycol)-acrylamide (PEGA) is a polymerisable version of PEG. First described by M. Meldal in 1992,[148] the PEGA polymer has found many applications in solid-phase synthesis and biosensors and been shown to exhibit excellent non-fouling property.[149-153]

The following section describes the grafting of PEGA on the SU-8 particles using a radical polymerisation method. In this approach, the PEGA monomer was synthesised and the polymerisation of this monomer was investigated. PEGA monomer was synthesised using a method developed by Won (Figure 2.23),[154] in which acryloyl chloride was reacted with the terminal amino group of Boc-PEG_{3500}-NH_2 in the presence of TEA in anhydrous DCM and produced the desired product in ~70% overall yield.

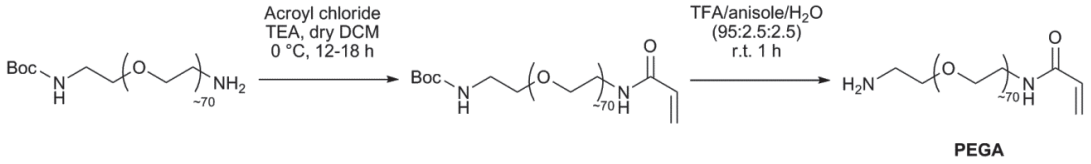

Figure 2.23. Preparation of PEGA monomer

Polymerisation The polymerisation reaction of the PEGA monomer was also studied in solution. A solution of the PEGA monomer was incubated with increasing concentration of the initiator, ammonium persulfate (APS, 0.003-30 mol%) in water. The time needed for

complete polymerisation, as indicated by gel formation, was recorded and the results are shown in Table 2.8. In general, the time needed for complete polymerisation decreased as the amount of APS in the reaction increased. At 30 mol%, the monomer failed to polymerise, probably due to quenching of monomer radicals by excess APS. At 0.003 mol%, the polymerisation reaction could not be sustained with such a low concentration of radical initiator.

Table 2.8. Determining the optimal amount of initiator for radical polymerisation in aqueous environment.

APS (mol%)	Time needed for polymerisation (min)
0.003	Did not polymerise
0.03	60
0.3	30
3	1
30	Did not polymerise

"Grafting from" SU-8 surface Figure 2.24 illustrates the schematic diagram of the proposed "grafting from" reaction. The PEGA monomer was conjugated to the particle surface by ring opening the residual epoxy groups with its primary amine. In an initial experiment, a solution of APS (3 mol% to typical amine loading level) in deionised water was added to the particles to activate the PEGA monomer on the surface. This was followed by the addition of a solution of PEGA monomer (1 mg/mL). After 18 h of reaction, no amino group was detected by Kaiser test. This suggested that either the conjugation of the PEGA monomer to the polymeric SU-8 surface failed to proceed or the polymerisation could not be sustained. A revised method for introducing the PEGA monomer onto the surface was investigated.

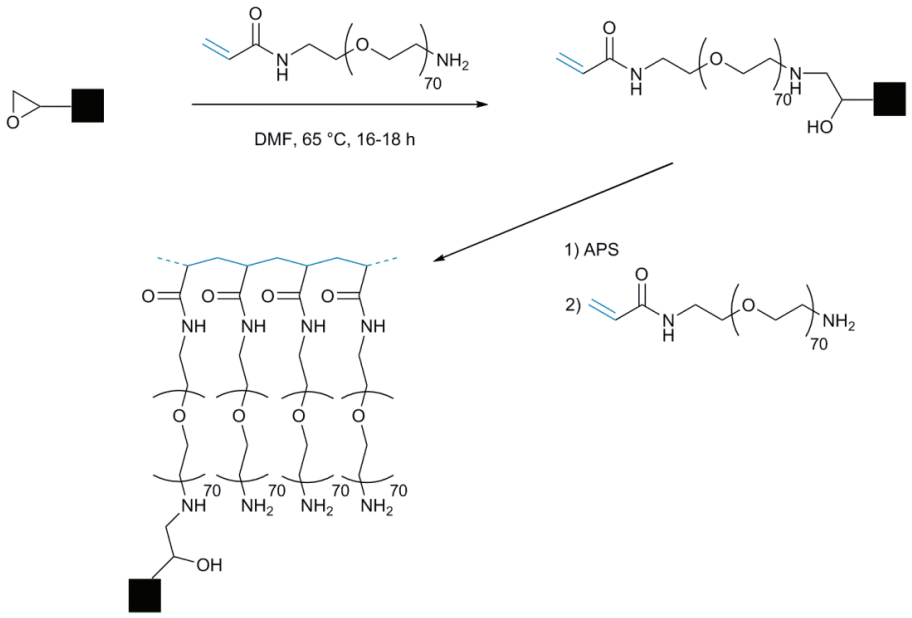

Figure 2.24. A schematic diagram of the proposed "grafting from" reaction by radical polymerisation on SU-8 microparticles.

Instead of conjugating the PEGA monomer onto the particle surface, the polymerisable acrylamide moiety was generated directly on the particle (Figure 2.25). In this method, $H_2N\text{-}PEG_{3000}\text{-}NH_2$ was attached to the particle surface by ring opening the residual epoxy groups as described above (section 2.2.2b). After a positive Kaiser test, the terminal amino groups were reacted with acryloyl chloride in the present of TEA in anhydrous DCM at room temperature for 18 h. A negative Kaiser test indicated the surface primary amines were potentially converted to the acrylamide group. Polymerisation was carried out as described above and the reaction was monitored by the presence of amino groups assayed using the Kaiser test.

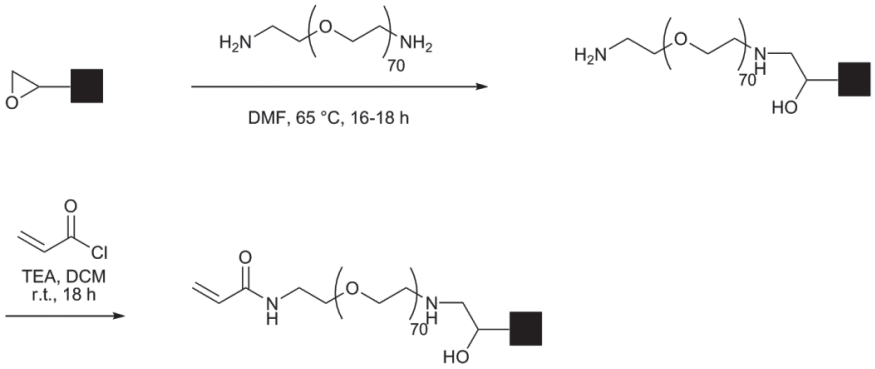

Figure 2.25. Preparation of PEGA monomer on SU-8 microparticles.

Although the PEGA monomer was successfully incorporated onto the particles surface, the polymerisation failed to proceed. It was possible that the monomer (MW ~ 3500) was too bulky and therefore sterically hindering the reactive radicals to polymerise. The use of APS as radical initiator may not be a suitable choice for this type of grafting reaction due to uncontrolled radical formations. As suggested by Barbey *et al.*, it might be more appropriate to attach the radical initiator, which can be activated (e.g. by heat or UV radiation), on the surface.[155] An example of a suitable radical initiator is 2,2'-azobisisobutyronitrile (AIBN). The size of the monomer should also be reduced so that a large amount of polymer could be grafted from the surface forming a highly-dense non-fouling layer. Although these experiments were not successful the polymerisation was ultimately achieved by G. R. Broder.[156]

2.3 Conclusion

In this chapter, the development of different colorimetric-based analytical tests for monitoring different chemical reactions on polymeric SU-8 particles was described. In general, these tests were found to be sensitive and could be used to detect target functional groups or biological molecules on a day-to-day basis. With the aid of these useful analytical techniques, the preparation of polymeric SU-8 particles with different functionalities, namely

amino-, carboxyl, azido- and hydroxyl-, was demonstrated. Immobilisation of different proteins onto the polymeric particles was also tested. For *in vitro* biological assays, it is important to reduce the highly hydrophobic nature of the SU-8 surface. For these studies, different methods for grafting a layer of non-fouling material onto the particles were investigated. Using the "grafting on" method, it was demonstrated that a long linear PEG and a star-shaped PEG could reduce non-specific binding dramatically. The other method for synthesising the non-fouling polymer from the particles surface required further optimisation.

Chapter 3 Development of multiplexed immunoassays on SU-8 particles

Multiplexing of assays is a technique that quantifies multiple analytes simultaneously in a single reaction vessel. This method is economically attractive because it reduces the "cost per data point" by using smaller quantities of expensive reagents and requires less labour time. Technically, multiplexed assays are very challenging to develop. One of the difficulties is to ensure that the different components in the assay react with their targets specifically and do not interfere with the others.[157] To ensure selectivity for each of the individual components, careful optimisation and development of the multiplexed assay platform is required. In this chapter, the use of encoded SU-8 particles for simultaneous detection of multiple targets in a single vessel is described.

3.1 Introduction

Biological tests are commonly used to detect and quantify a wide range of molecules. In hospitals and central laboratories, these tests are used for many purposes including *in vitro* diagnosis (IVD),[158] clinical trial monitoring,[159] transplantation screening (human leukocyte screening),[160] environmental monitoring[161] (e.g. for weaponised microorganisms), food safety assurance[162] (e.g. *E. coli* O157) and drug of abuse testing.[163] In basic research, the same types of test are also used for new biomarker discovery,[164] drug screening[165] and enzyme activity studies.[5]

3.1.1 Immune system[166-170]

"Immunoassay" is a broad term that describes biological tests that detect specific targets (antigens) using antibodies. In nature, vertebrates produce antibodies to aid the elimination of specific pathogens. In the following sections, the production of antibodies and their rôle in the immune response are briefly described (The following materials were adapted from references 167-171).

3.1.1a Innate immunity

In vertebrates, when the host is invaded by disease-causing micro-organisms (also known as pathogens), such as viruses, bacteria, fungi and parasites, the immune system is alerted and uses a number of defence mechanisms to eliminate these invaders. This is known as an immune response and can be classified into innate immunity and adaptive immunity.

Pathogens infect the host for a single purpose: to reproduce. To do so, they must enter the host body, multiply, spread to other parts of the body, and ultimately infect another host. During the course of an infection, the pathogen can cause severe damage to the surrounding tissues and organs and, in extreme circumstances, kill the host. To counteract an infection, vertebrates have developed a number of defence mechanisms to fight against these invaders. One of these is the use of an outer protective layer. This is composed of tightly joined epithelial cells which serve as a barrier to block most pathogens from entering to the body. Those that succeed in passing through this layer are rapidly challenged by immune cells that form part of the innate immune response. Macrophages are one type of immune cell that reside in tissues. When in contact with a pathogen, the macrophage engulfs the pathogen and digests the foreign cell inside a phagocytic vesicle using lysosomal enzymes, a process called phagocytosis. At the same time, the activated

macrophage triggers a series of cellular signals that activate the host defences. One example is the release of mediators from the activated macrophage to induce an inflammatory response. Inflammation changes the properties of local blood vessels so that other cells from the immune systems can be delivered to the infected site. Neutrophils, a type of leukocyte, are recruited in response to these signals to the site of infection. Similarly to macrophages, they can eliminate pathogens by phagocytosis. Many invaders are effectively removed from the host body by the innate immune response. However, some pathogens can overwhelm this defence mechanism and survive in the host body. Without efficient removal from the host body they replicate, colonise and spread to other parts of the body.

3.1.1b Adaptive immunity

During an innate immune response, activated macrophages recruit other immune cells to the site of infection to strengthen the defence response. At the same time, they also activate the adaptive immune response to promote target-specific destruction. This process can be further divided into cell-mediated immunity and humoral immunity. The cell-mediated immunity is governed by T-lymphocytes which induce apoptosis of infected cells and activate macrophages and natural killer cells to destroy the pathogen. In another distinct branch of the adaptive response, the humoral immunity is controlled by B-lymphocytes which produce target-specific antibodies to neutralise pathogens and flag them for phagocytosis.

3.1.1c Production of antibodies

The production of antibody begins when innate immunity is overwhelmed by the invading pathogen, triggering an adaptive immune response. B-cells are responsible for the

antibody production. These cells, along with other professional antigen-presenting cells (pAPCs), such as macrophages and dendritic cells, have the ability to engulf the pathogen and degrade the pathogen's proteins into smaller peptide fragments (Figure 3.1.1). These fragments are then transferred to the surface of the APC and complexed with cell-surface glycoprotein called major histocompatibility complex (MHC) class II proteins. In order to produce antibodies, B-cells require two stimuli. The first comes from antigen binding to the B-cell receptors (BCR). These are antibody-like glycoproteins attached to the cell surface. The second signal comes from the binding of T-cell receptors (TCR) on helper T cells to the antigen:MHC complexes on B-cells, a process called "antigen presentation" (Figure 3.1.2). Upon binding, the activated helper T-cells release cytokines which signal the B-cells to proliferate and differentiate into plasma cells (Figure 3.1.3) and memory cells (Figure 3.1.4).

The activation of this process is governed by three major steps. First, the antigen must bind to the BCRs. The surface proteins have the same antigen binding sites as the product antibodies so only antibodies specific to the target antigen are produced. Second, the processed antigen fragments after degradation must have an epitope that can bind to the MHC class II proteins. Third, the antigen:MHC complexes must be recognisable by the TCRs on helper T cells.

Plasma cells are terminally differentiated and their rôle is to produce antibody molecules. Typically the production of antibodies lasts for approximately 3-4 days upon immunisation. In contrast, memory cells do not produce antibodies but they retain cell-surface receptors for binding to the target antigens. These cells remain in circulation and respond rapidly to subsequent exposure to the same antigens by triggering the adaptive immune response, a process called "secondary immune response".

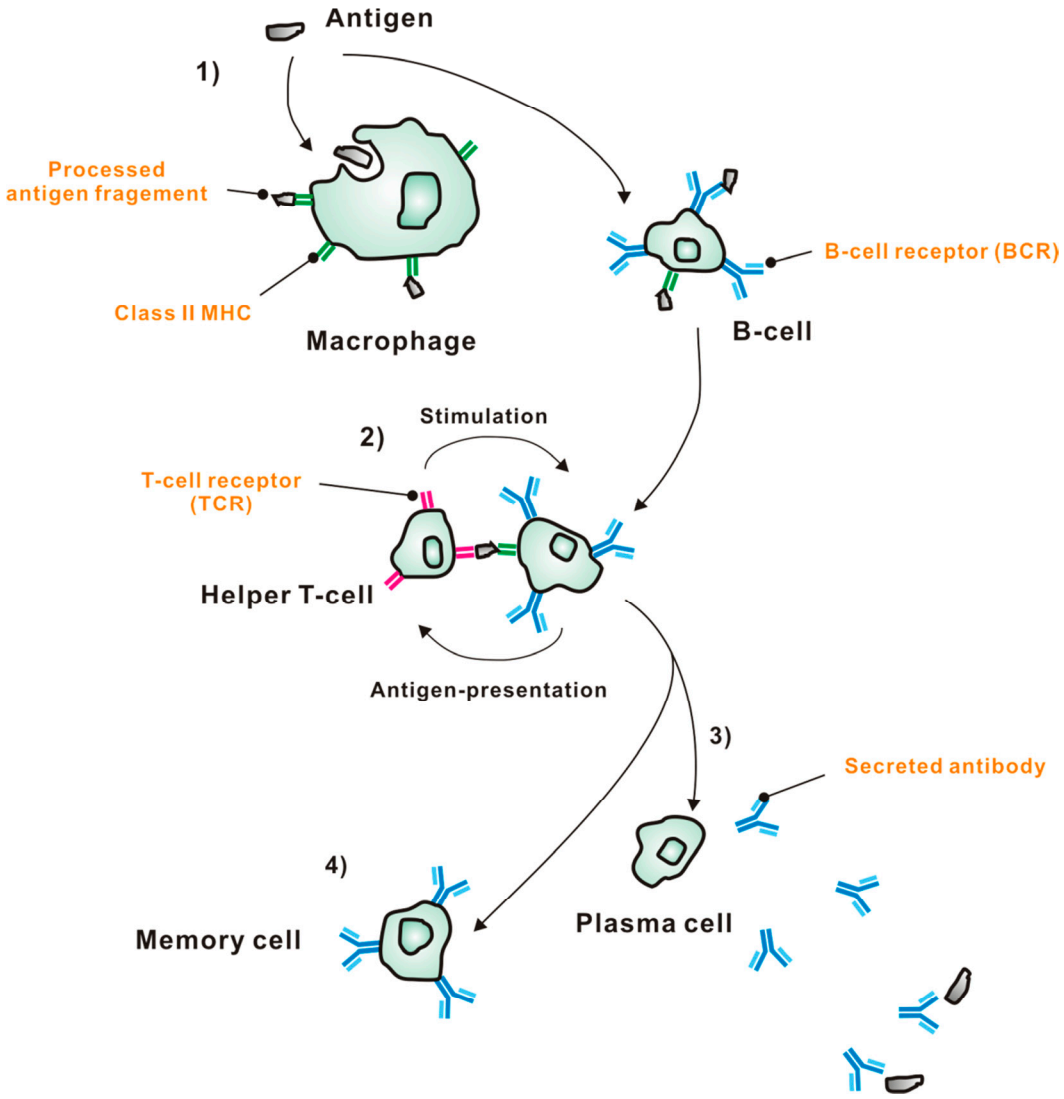

Figure 3.1. Antibody production during the humoral response. 1) An antigen is fragmented by professional antigen-presenting cells, such as macrophages and B-cells. The fragment is transferred to the cell surface and binds to MHC class II proteins. 2) The antigen:MHC complex is recognised by the T-cell receptor on helper T cell which in turn stimulates proliferation and differentiation of B-cells. 3) The B-cell is terminally differentiated into antibody-producing plasma cell. The secreted free antibody binds to the antigen and triggers antigen-specific immune responses. 4) Some B-cells are differentiated into memory cells which trigger antibody production more rapidly in response to repeat exposure to the same antigen.

3.1.1d Antibodies

Antibodies, also called immunoglobulins (Ig), are products of the terminally differentiated plasma cells during the humoral responses. Structurally, they are composed of one or more "Y" shape units, each of which has a molecular weight of about 150,000 Da.

As shown in Figure 3.2, each "Y" monomer contains two identical light (L) polypeptide chains and two identical heavy (H) chains. These are arranged into two sections: fragment antigen-binding (F_{ab}) and fragment crystallisable (F_c). A single L chain contains approximately 220 amino acid residues whereas each H chain is roughly 440 amino acids long. Sequence analysis shows that all antibodies contain one of the two subtypes of L chains, the κ light chain or the γ light chain. In contrast, there are five different subtypes of H chains: α, δ, ε, γ and μ chains. According to the composition of the H chain, antibodies are classified into five isotypes: IgA, IgD, IgE, IgG and IgM (Table 3.1).

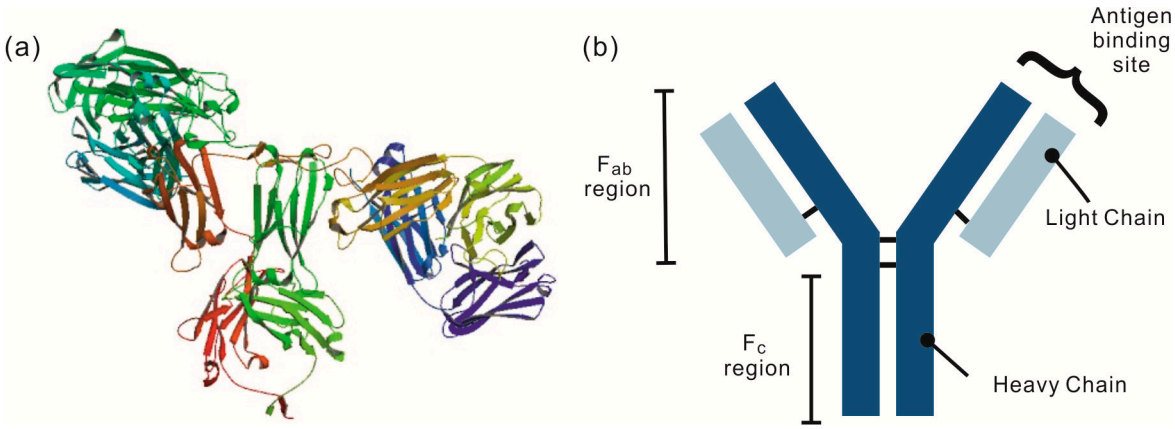

Figure 3.2. (a) A crystal structure of human IgG. The protein exhibits a "Y" shape which is composed of two light chains (yellow and green ribbons) and two heavy chains (red and blue ribbons) – PBD ID: 1IGT.[171] (b) A simplified representation of an antibody used throughout this chapter.

Antibodies are able to bind to a wide range of antigens. This is due to the huge variation in the amino acid sequences in a region of the H and L chains from one antibody to another. These regions are called the variable regions (V_H and V_L) which fold together to make up the antigen-binding sites. The rest of the antibody molecule, called the constant regions (C_H and C_L), is conserved in vertebrates. In the chromosome, the gene that encodes an antibody is divided into different parts, or gene segments. For the heavy chain, these groups of genes are called *variable* (V), *diversity* (D), *joining* (J) and *constant* (C)

segments. Similarly, light chain genes are grouped into V, D and C. Before a mature antibody gene is transcribed into mRNA and then translated into the corresponding polypeptide sequence, it is constructed from these gene segments through a mechanism called somatic recombination, also known as V(D)J recombination. Taking a heavy chain gene as an example, the first step is the recombination of a D gene with a J gene. One segment of each is randomly selected, spliced and then ligated to each other (D-J combination, Figure 3.3a). The newly formed DNA sequence then undergoes a second round of recombination with a randomly chosen V segment (V-DJ recombination, Figure 3.3b). The resulting gene is then transcribed into mRNA (Figure 3.3c) followed by translation to form the heavy chain polypeptide chain (Figure 3.3d). The light chain gene is constructed in a similar fashion (V-J recombination).

Table 3.1. The properties of IgA, IgD, IgE, IgG and IgM.

	IgA	IgD	IgE	IgG	IgM
Heavy chain	α	δ	ε	γ	μ
Light chain			κ or λ		
Structure	Dimer	Monomer	Monomer	Monomer	Pentamer
Valency	4	2	2	2	10

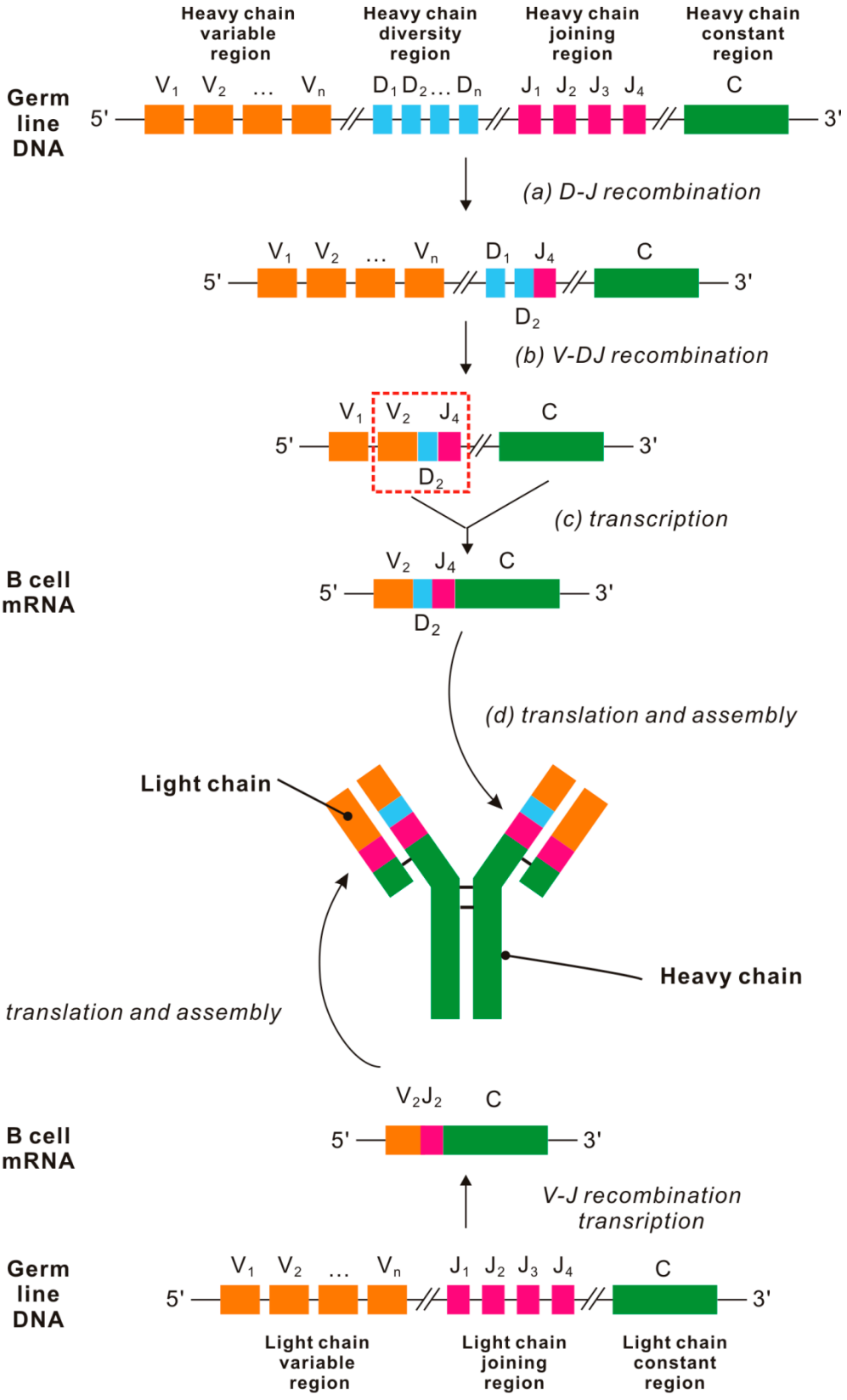

Figure 3.3. A schematic diagram of V(D)J recombination. The functional genes encoding the heavy chain and light chain of Ig are assembled by randomly selecting segments of genes from different regions. This creates the diversity for the antigen-binding sites.

Polyclonal antibodies Antibody molecules produced by the immune system have great diversity in terms of antigen recognition and binding affinity. This is because different B-cells respond to different antigen fragments during the adaptive immune response. In a population of B cells, each cell will have responded to a different epitope from the antigen and subsequently differentiated into a group of plasma cells that produce antibodies selective for different antigens. Purified samples of antibodies that are derived from this mixed population of B cells are termed "polyclonal". Commercially, these antibodies are produced by immunising a host (e.g. mouse, rat, rabbit and horse) with a sample of the target molecule or antigen. The "infected" host then develops an immune response and produce antibodies to the target after a few days. The majority of the antibodies are found in serum and can be readily purified by chromatography.

Monoclonal antibodies Although polyclonal antibodies can be extracted from live animals after immunisation, their binding properties vary significantly from one batch to another as they are produced by a mixed population of plasma cells. A method for producing antibodies with defined specificity and reproducible binding affinity was desirable. Many efforts were made to produce such antibodies continuously *in vitro*. However, since the antibody-producing plasma cells are terminally differentiated they cannot be grown in tissue culture, and therefore cannot be used as a source for antibodies. In 1975, Köhler and Milstein developed a technique that allowed the growth of antibody-producing cells continuously.[172] In this method a plasma cell was isolated from the host and fused with a tumour cell (myeloma cell). These so called hybridomas can be maintained *in vitro* and continue to produce antibodies with defined specificity. Since these antibodies originate from a single B-cell, they result from a single protein sequence and are known as monoclonal antibodies.

In general, immunisation, screening and hybridoma production takes months or even years to complete. However, once an antibody with defined epitope selectivity and specificity is developed, it can be produced *in vitro* continuously and, in theory, indefinitely.

3.1.2 Immunoassays

The sections above described how vertebrates eliminate pathogens by using different immune responses, the rôle of antibodies in the immune system, and the production of antibodies. In the following sections, the use of antibodies for a selection of biological assays is discussed.

3.1.2a Radioimmunoassay

The radioimmunoassay (RIA) was one of the earliest techniques for "determining of virtually any biological substance of interest".[173] The principle of the assay is illustrated in Figure 3.4. In 1956, Berson and Yalow demonstrated a method for measuring the concentration of human insulin from an unknown sample in a competitive radioimmunoassay.[174] The principle of the assay is as follows: anti-insulin antibodies were first saturated with ^{131}I-labelled insulin (Figure 3.4.1). A sample containing an unknown concentration of human insulin was added to compete in the binding to antibody with the radioactively-labelled control (Figure 3.4.2). The radioactivity of the free ^{131}I-insulin molecules, which is displaced into solution, is then measured (Figure 3.4.3 and Figure 3.4.4). Like many other biological assays, the radioactive readout of the immunoassay is calibrated using human insulin solutions with known concentrations and then plotted as a standard curve. When the unknown sample was assayed, the radioactivity was measured and correlated with the standard curves to estimate the original concentration.

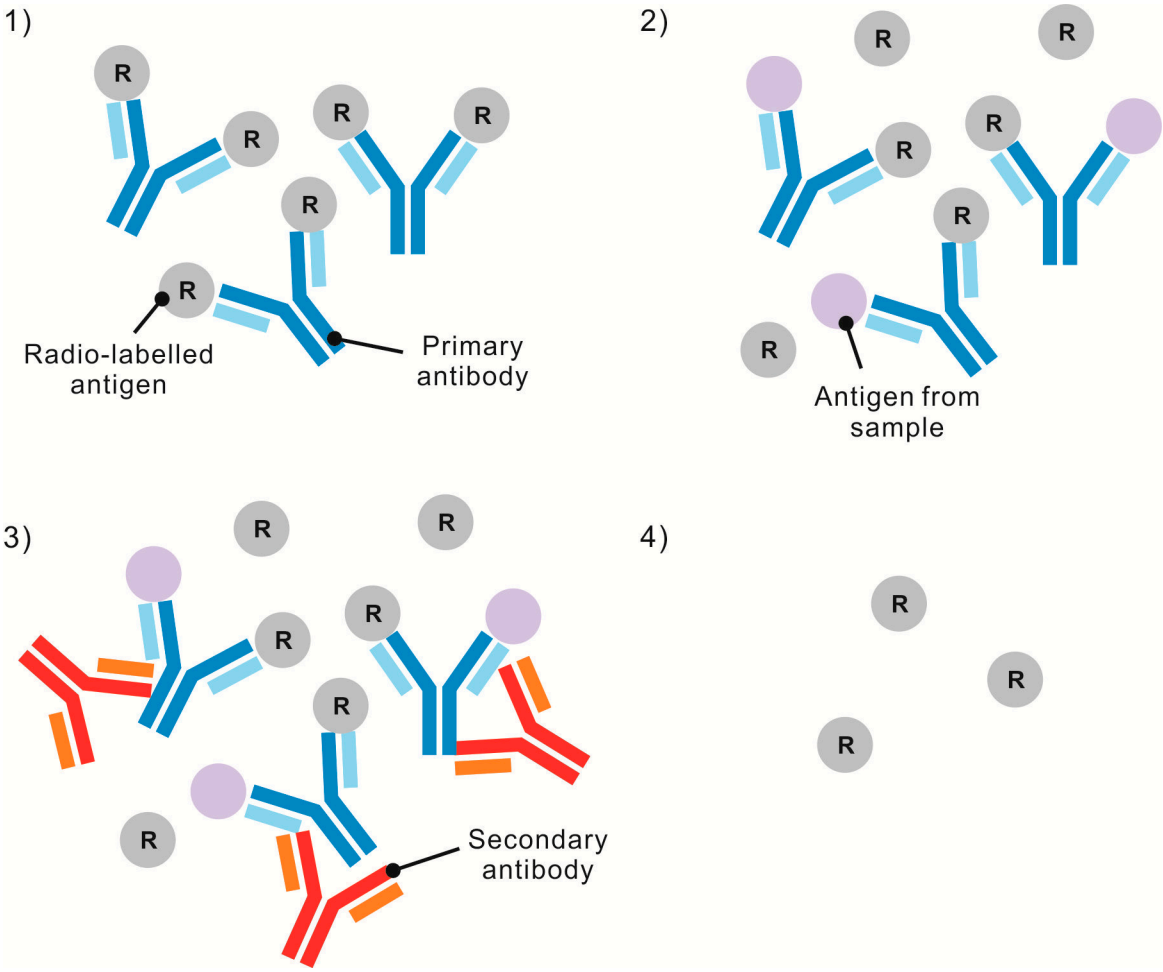

Figure 3.4. The principle of radio-immunoassay (RIA). 1) The primary antibody is first saturated with radio-labelled antigen. 2) The antigen from the sample displaces the bound labelled antigen in a competitive manner. 3) The antigen:antibody complex is removed from the sample by immune-precipitation using a secondary antibody. 4) The radioactivity released into the supernatant is measured.

The main drawback of RIA is the difficulty of handling radioactive substances. Although this technique is very sensitive (as little as 50 fM[173] of antigens is readily detectable), it was eventually replaced by other techniques that use colorimetric and fluorescence labels.[175]

3.1.2b Enzyme-linked Immuno-Sorbent Assay

The term "enzyme-linked immunosorbent assay" (ELISA) was first used by Engvall and Perlmann in 1971 to describe an enzyme-based immunoassay method which is useful for the detection of antigen qualitatively and quantitatively.[15,176,177] Later, Voller *et al.* demonstrated an ELISA using a microtiter plate for the detection of malaria, which ultimately became one of the standard formats for the ELISA of the present day.[178,179] The ELISA is a heterogeneous system, in which the antibody:antigen complex is formed on a surface. Once a target antigen is bound, an enzyme-conjugated detector antibody is used to label the complex and causes a chromogenic substrate to generate a signal (Figure 3.5).

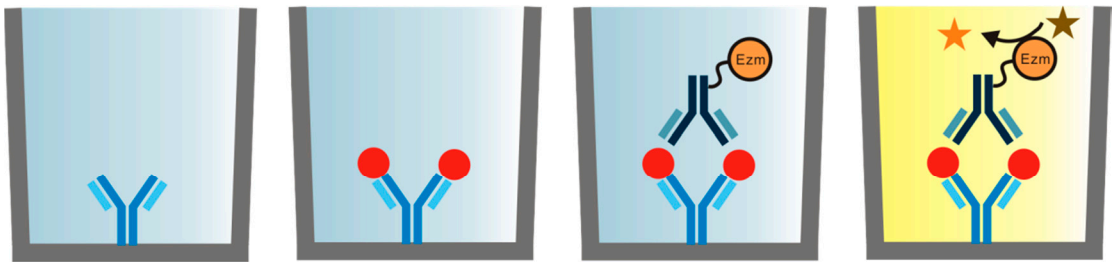

Figure 3.5. The principle of ELISA for the detection of target antigen. A capture antibody is coated at the bottle of the reaction vessel. The target antigen from the sample is bound to the immobilised capture antibody. An enzyme-linked detection antibody is added which recognises the captured antigen and forms a complex. A substrate is added which is converted into a detectable form by the enzyme on the detection antibody.

ELISAs can also be used for the quantification of an antibody (Figure 3.6). In this modified method, a capture antigen is attached to the solid support. After the blood sample preparation step, the isolated serum or plasma sample containing the antibody is incubated with the immobilised antigen. After washing to remove unbound material, an enzyme-conjugated secondary antibody is added. This protein binds to any captured target antibody on the surface. Unreacted material is removed by washing before the substrate is

added. The colour change indicates the amount of immobilised detector antibody, which is proportional to the amount of bound antibody in the sample.

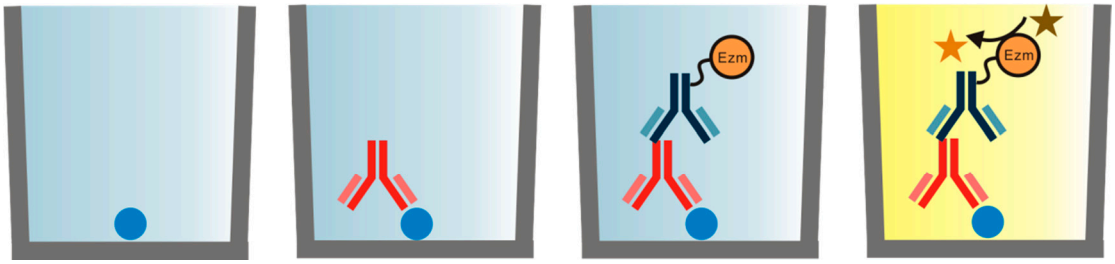

Figure 3.6. The principle of ELISA for the detection of target antibody. The antigen is coated at the bottle of the reaction vessel. A sample containing the target antibody is added which binds to the immobilised antigen. An enzyme-linked secondary antibody is introduced which binds to the captured target antibody. A substrate is added which is converted to a detectable form by the enzyme on the secondary antibody.

3.1.2c Western Blotting

Another popular technique for detecting specific proteins using labelled antibody is Western Blotting (Figure 3.7).[180,181] In this method, a solution of protein mixture extracted from a raw sample (e.g. whole blood, tissue culture or cells) is applied to a polyacrylamide gel and the proteins are separated according to their size by electrophoresis. After this the separated proteins are transferred ("blotted") to a nitrocellulose membrane. Finally, the membrane is incubated in a solution of labelled antibody which binds to the immobilised target protein specifically and generates a signal.

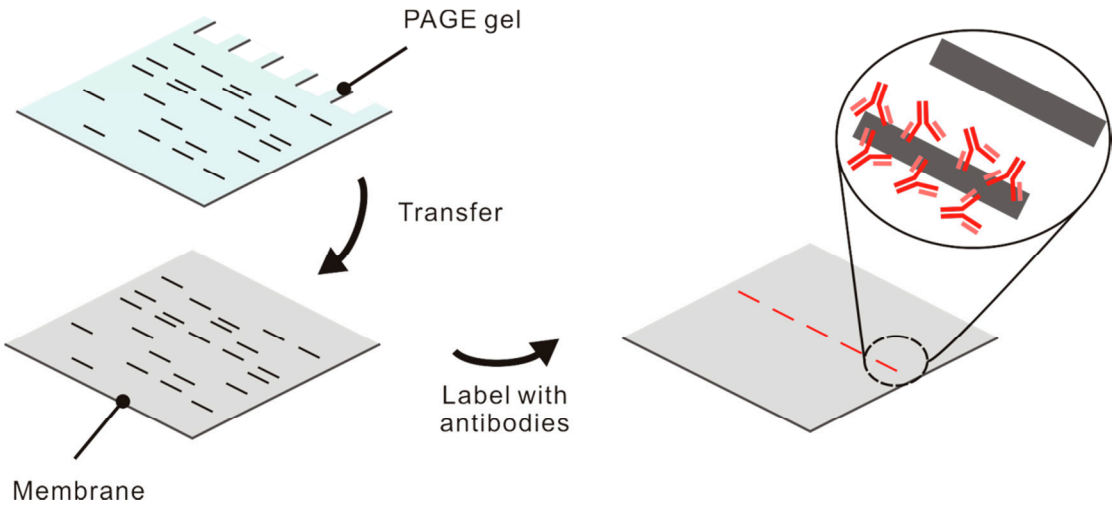

Figure 3.7. The principle of western blot. A solution containing a mixture of proteins is loaded onto a poly-acrylamide gel and then separated by gel electrophoresis. The separated proteins are transferred to a membrane. The membrane is then placed in a solution of labelled antibody (normally fluorescently labelled) which recognises the target protein immobilized onto the membrane.

3.1.2d Suspension immunoassay

Suspension arrays are a newly emerging platform for immunoassays.[23,45] In this method, a micro- or nanoparticle coated with a capture probe molecule on the surface is suspended in a complex biological sample (Figure 1.6). The target molecule in the sample is captured by the immobilised probe on the surface by affinity binding. By using a fluorescently-labelled detection molecule, binding can be visualised using a conventional fluorescence microscope.[182] When using a commercially available fluorescence flow cytometer, a very large number of particles can be analysed rapidly (~5,000 particles s^{-1})[183,184] and therefore greatly improve the assay throughput. Since most commercial flow cytometers can resolve several fluorescent dyes from a single bead simultaneously, suspension arrays have the potential for detecting multiple targets in a multiplexed manner.[185] In an attempt to develop a miniaturised fluorescence flow cytometer for point-of-care (POC) tests, Holmes *et al.* demonstrated a bead-based multiplexed

immunoassay using a microfluidic flow cytometer and showed comparable data quality with a commercially available fluorescence-activated cell sorter (FACS).[186]

3.1.2e Other immunoassays

Apart from using labelled-antibodies for detection, much effort has been put into the development of other detection methods.[187] One example is Magnotech (Figure 3.8) developed by M. W. J Prins and his group from Philips Corporate Technologies.[188] In this setup, magnetic nanoparticles are coated with a capture antibody and binds to the target antigen in a reaction chamber (Figure 3.8a). At the bottom of the chamber is coated with a layer of detection antibody (active layer). When a magnetic force is applied from the bottom of the chamber, the nanoparticles carrying the target antigen are pulled to this surface, in which the target molecule is sandwiched between the detection antibody of the active layer and capture antibody attached to the nanoparticles (Figure 3.8b). Unreacted nanoparticles are also pulled to the active layer by the magnetic force. To remove these particles, a second magnetic force from the top of the reaction chamber is applied (Figure 3.8c). By fine-tuning the magnetic moment, the unreacted nanoparticles are driven to the top layer, leaving the specifically-bound nanoparticles on the active layer. The amount of bound nanoparticles, which correlates to the concentration of antigen in the sample, can then be quantified by optical diffraction (Figure 3.8d).

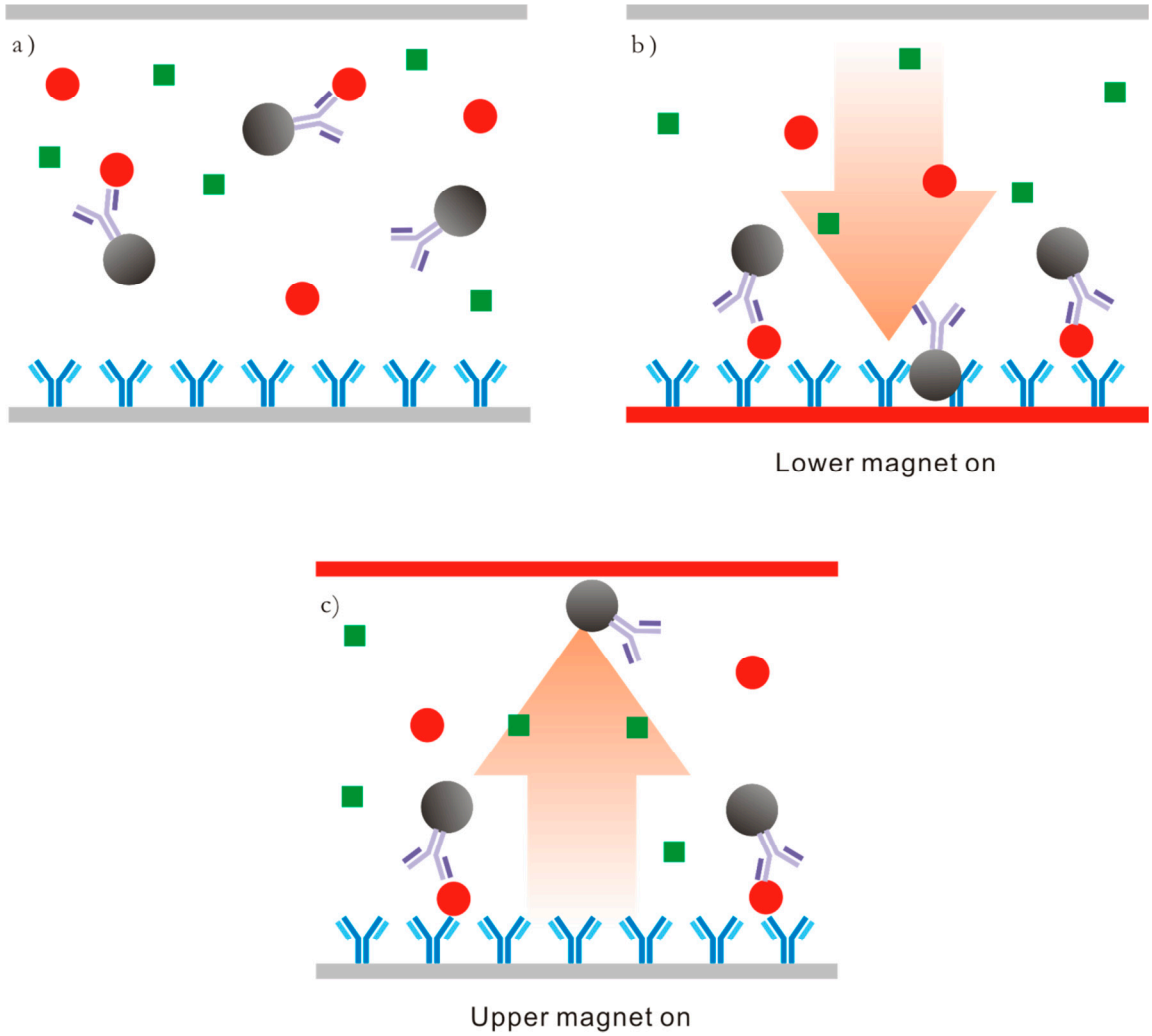

Figure 3.8. A schematic diagram of the Magnotech immunoassay system. (a) A set of magnetic particles coated with a specific antibody is incubated with a biological sample containing the target antigen. (b) A magnetic force is applied at the bottom of the reaction vessel and attracts the magnetic particles to the active layer. (c) The magnetic force from the upper layer is applied and pulls the free magnetic particles away from the active layer. The amount of particles remain on the active layer is then measured.

3.1.3 Aims of this chapter

Multiplexed assays can be used for screening a library of antibodies against a library of antigens simultaneously from a single sample. This has the advantage of greatly reducing the amount of samples and reagents and produces multiple data sets at the same time.[23] One of the greatest challenges in the assays is to identify each reaction in the reaction vial.

One approach to overcome this problem is to encode the microparticles so that the immobilised biomolecules can be identified.[23,45]

The aim of this part of the project was to demonstrate a simple multiplexed immunoassay on the functionalised encoded SU-8 particles. The assay platform would also permit the study of binding kinetics and thermodynamics of such heterogeneous systems.

3.2 Results and Discussions

3.2.1 Principle of the assays

The principle of the multiplexed immunoassays described in this chapter is similar to the suspension immunoassay discussed in the previous section. The detection of various IgGs from different species on the particle surface was investigated. To do so, a set of microparticles coated with the complementary antigen were suspended in a sample. The target antibody in the sample recognised and interacted with the immobilised antigen on the surface. By labelling the antibody:antigen complex on the surface (e.g. by fluorescence or radioactive label) the amount of the captured target antibody on the surface could be quantified by measuring the signal from the particles.

The schematic diagram of the proof-of-principle multiplexed immunoassay on a solid-support is shown in Figure 3.9. Two sets of particles, each coated with a different primary antibody (which served as an antigen in this experiment), were used to detect their target secondary antibodies in one single sample. The targets were directly labelled with a fluorescent dye (Cy3 or Cy5, Figure 3.10) so that additional labelling step was avoided.

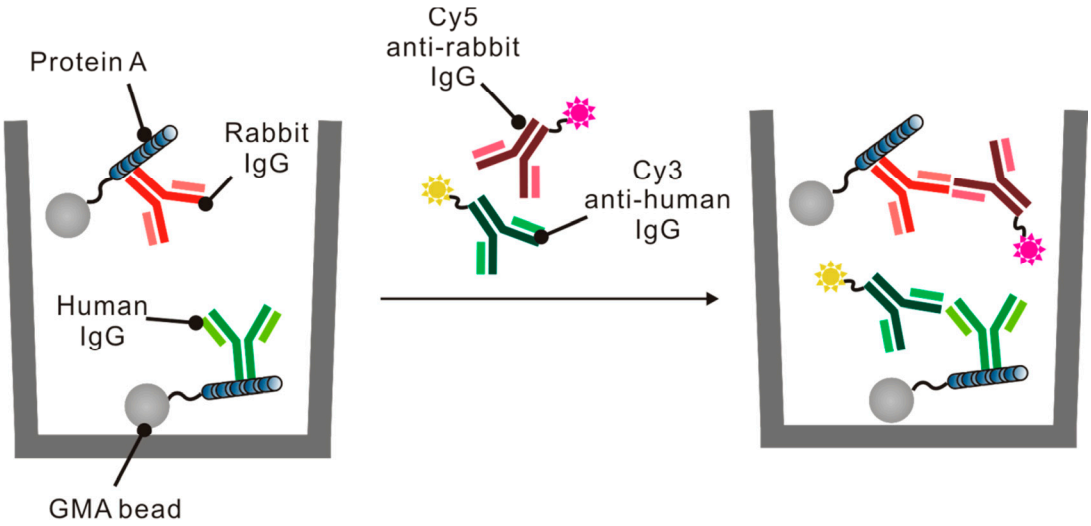

Figure 3.9. A schematic diagram of the designed multiplexed immunoassay.

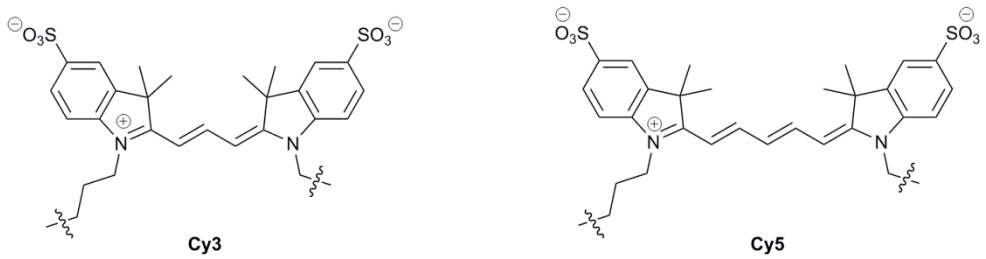

Figure 3.10. Chemical structures of Cy3 and Cy5.

3.2.2 Protein A

As shown in Figure 3.9 above, the particles to be used in a multiplexed immunoassay are coated with the antigen of interest (e.g. human IgG). This can be done by a number of methods, such as affinity binding, covalent coupling and adsorption as described in Chapter 2. For the proof-of-principle experiments, the aim was to develop a simple and generic method for attaching a wide range of IgGs from various species to the surface. In this section, the attachment of IgG by affinity binding based on protein A capture is described.

Protein A from *Staphylococcus aureus* (*S. aureus*) is a cell surface protein that binds to IgG from various species (Table 3.2).[189] Matured protein A has a molecular weight of 42 kDa and exhibits a rod-like shape which is comprised of five repeated domains (E, D, A, B and C).[190] Each domain can bind with high affinity to the F_c portion of IgG. Protein A has found application in antibody purification,[191-193] cell labelling[194] and *in vitro* and *in vivo* immunoassays.[195,196] With its high affinity, specificity and selectivity to IgGs, protein A was chosen as the immunosorbent for attaching IgGs to the solid-supports.

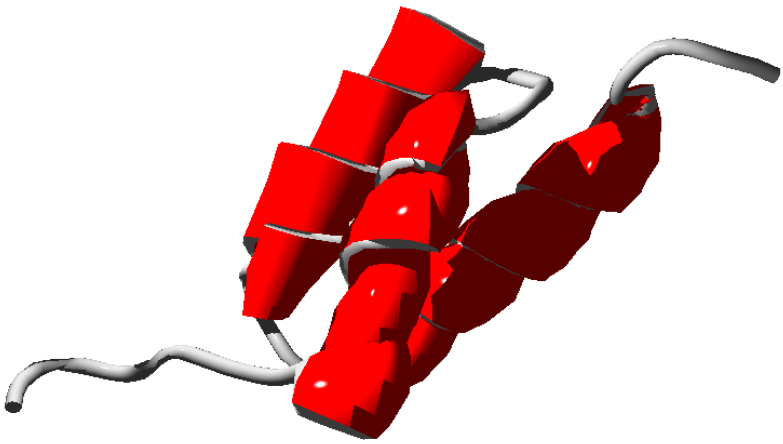

Figure 3.11. Protein crystal structure of B-domain of protein A from *S. aureus* (PDB ID: 1SS1).[197]

Table 3.2. The relative binding affinity of protein A to IgGs from different species.

IgG from species	Relative Binding Affinity
Rabbit, Guinea Pig	++++
Human, Pig	+++
Horse, Cow, Mouse	++
Sheep, Rat, Hamster	+
Goat, Chicken	-

Recombinant *S. aureus* protein A was covalently attached to the carboxyl-functionalised surface by amide bond formation using the one-step EDC coupling method as described in Chapter 2. To quantify the amount of immobilised protein A on GMA beads or SU-8 microparticles, a suspension of the solid supports was subjected to BCA protein assay (see Chapter 2 for details).

Table 3.3. Loading level of protein A-GMA and protein A-SU-8 measured by BCA protein assay.

Particle Type	Loading level (nmol/g)
Protein A-GMA	45 ± 7
Protein A-SU-8	
Code 1	287 ± 4
Code 2	854 ± 4
Code 3	540 ± 6
Code 4	243 ± 6

Table 3.3 summarises the amount of immobilised protein A on the two surfaces as estimated by BCA protein assay. From the absorbance measurement, the immobilised protein A was detected on both GMA beads and SU-8 microparticles. Since the amount of particles used in the assay was known, the loading level of protein A on the surface could therefore be calculated. On GMA beads, the protein A loading level was found to be 45 ± 7 nmol/g which corresponded to 0.6 ± 0.1 layers of protein A on the surface. In comparison, the loading level on SU-8 microparticles was found to be between 243 ± 6 and 854 ± 4 nmol/g (depends on the batch of microparticles used), which equates to 4-15 layers of protein A on the surface (see Appendix B for details). The variation in protein loading level on SU-8 microparticles could be due to batch-to-batch variation of the microparticles (e.g. from the fabrication process and the subsequent surface functionalisation steps). The

multiple layers of protein A found on the SU-8 surface could be due to the cross-linking effect as described in 0.

3.2.3 Selection of antibodies and antigens for the study

In this section, the process for selecting the antigens and antibodies for the proof-of-principle experiment is described. In order to demonstrate a multiplexed immunoassay, the chosen antigens and antibodies should fulfil the following requirements:

1. the antigens (IgG) should bind to the immunosorbent (protein A from *S. aureus*) with high affinity;
2. the detector antibodies should selectively bind to their complementary antigens and have little cross-reactivity with other antigens; and
3. the detector antibodies should have low affinity for the immunosorbent.

With the above requirements in mind, human IgG and rabbit IgG were selected as the antigens for the first proof-of-principle experiment (Figure 3.9). The assay panel could potentially be expanded to include IgGs from guinea pig, horse, pig, cow and mouse.[71] For the secondary antibodies, goat antibody was selected as they have poor affinity for protein A and hence less cross-reactivity with the immunosorbent. An alternative would be chicken antibody. Table 3.4 shows the primary antibodies (served as antigens) and labelled-secondary antibodies (served as target antibodies) to be used in the proof-of-principle experiments.

Table 3.4. Chosen antigens and antibodies for the multiplexed immunoassays and their modifications (if any).

Antibody	Produced from	Against	Modification
Polyclonal human IgG	Human	Multiple targets	None
Polyclonal rabbit IgG	Rabbit	Multiple targets	None
Cy3-anti human IgG	Goat	Human IgG	Cy3
Cy5-anti rabbit IgG	Goat	Rabbit IgG	Cy5

3.2.4 Immobilisation of IgGs to protein A-coated solid-supports

The protein A-coated particles provided a generic platform for immunoassay development. A wide range of IgGs could be attached onto these particles by affinity binding to the immobilised immunosorbent by a simple incubation step. This allowed flexibility in creating and expanding the assay panel.

To immobilise IgGs to the protein A-coated solid-supports, a solution of polyclonal IgG (human or rabbit, 6.67 μM in PBST) was added to the solid supports and agitated at room temperature for 1 h. After that, the microparticles were washed with PBST (1 mL x 4) to remove the unbound antibody. To confirm the presence of the immobilised IgG on the surface, the solid supports were stained with a fluorescently-labelled secondary antibody (667 nM) and then qualitatively analysed by fluorescence microscopy.

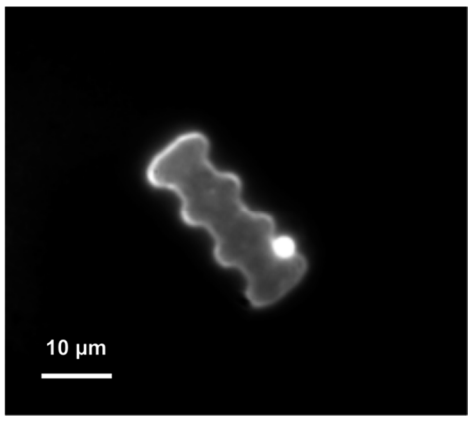

Figure 3.12. A fluorescence image of a human-IgG coated SU-8 particle stained with Cy5-labelled anti-human IgG antibody.

3.2.5 Cross-reactivity study on GMA beads

The cross-reactivity of the labelled target secondary antibodies to the immobilised IgGs (antigens), protein A (immunosorbent) and the non-coated solid support (carboxyl-functionalised GMA beads) was investigated. Protein A-, human IgG- and rabbit IgG-, and carboxyl-functionalised GMA beads were incubated with either Cy3-anti-human or Cy5-anti-rabbit antibodies. After removing the excess antibodies and washing the solid-supports with buffer, the fluorescence intensity of the beads was measured using a fluorescence flow cytometer.

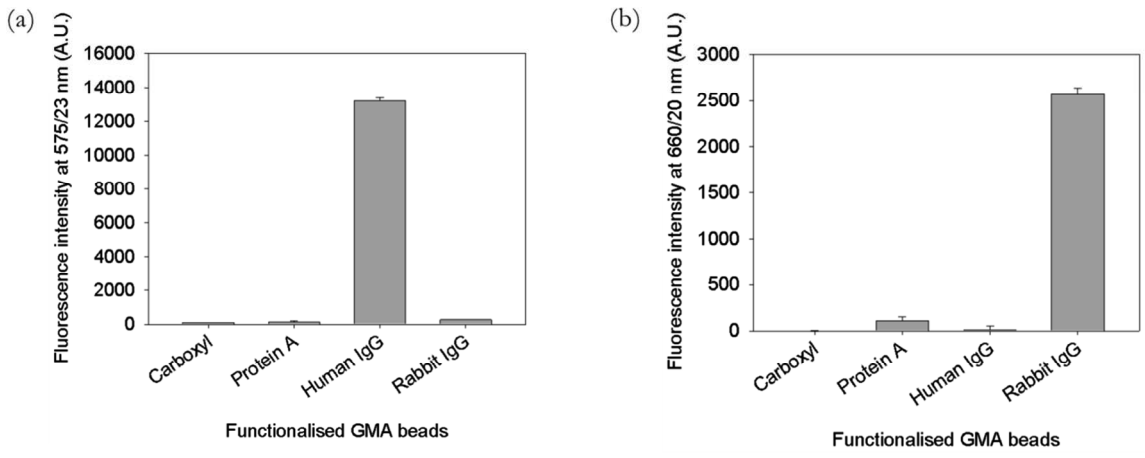

Figure 3.13. Cross-reactivity studies of Cy3-anti human (a) and Cy5-anti rabbit antibody (b) to different surface-functionalised GMA beads.

Figure 3.13 summarises the results of the cross-reactivity study on different functionalised GMA beads. Approximately 1000 particles were analysed by the fluorescence flow cytometer and the standard errors of the measurements are shown as error bars on the graph. The Cy3-labelled anti-human antibody predominantly reacted with the GMA beads coated with human IgG on the surface. The labelled secondary antibody had little cross-reaction with GMA beads functionalised with rabbit IgG, protein A or carboxylic acid. Similarly, the Cy5-labelled anti-rabbit IgG antibody selectively reacted with the rabbit IgG-coated surface and produced the highest fluorescence signal. It showed a slightly higher cross-reactivity with the protein-A coated GMA beads. However, it exhibited a relatively low cross-reactivity with the human IgG-coated and carboxyl-functionalised surfaces. Signal-to-noise ratios (S/N) of the two assays were calculated from Equation 3.1 and are summarised in Table 3.5.

$$S/N = \frac{F_{signal}}{F_{noise}} \qquad \text{Equation 3.1}$$

where S/N is the signal-to-noise ratio; F_{signal} is the fluorescence intensity of the target solid support; F_{noise} is the fluorescence intensity of the non-target solid support.

The results obtained from this study suggested that the chosen antigens and antibodies for the proof-of-principle multiplexed immunoassay had very high selectively towards the target and minimum cross-reactively with the non-target components in the assay.

Table 3.5. S/N on functionalised GMA beads as determined from the cross-reactivity study.

Functionalised GMA	S/N	
	Detection of Cy3-anti human IgG	Detection of Cy5-anti rabbit IgG
Carboxyl	118	856
Protein A	93	7
Human IgG	N/A*	36
Rabbit IgG	50	N/A*

*Specific signal produced from target solid support.

3.2.6 Proof-of-principle multiplexed immunoassays on GMA beads

From the cross-reactivity study described in the previous section, both fluorescently-labelled secondary antibodies bind to their target antigens with excellent selectivity and showed little cross-reaction to the non-target antigen. The next goal was to mix the IgG-coated particles and test their ability to capture the target antibodies in a duplexed format.

To demonstrate a multiplexed immunoassay, an equivalent amount of human- and rabbit-IgG coated GMA beads (0.3 mg each, ~2.52×10^6 beads) were mixed thoroughly. This mixture was agitated in a cocktail of Cy3-anti-human and Cy5-anti-rabbit antibodies (277 nM each, 50 μL). After 1 h the particles were washed with PBST and then analysed by fluorescence flow cytometry. Each bead passed through the detection zone where the size (measure by forward scattering) and fluorescence (at 575 ± 13 nm and 660 ± 10 nm) were measured. Approximately 1000 beads from the mixture were analysed and the results are represented in a dot plot below.

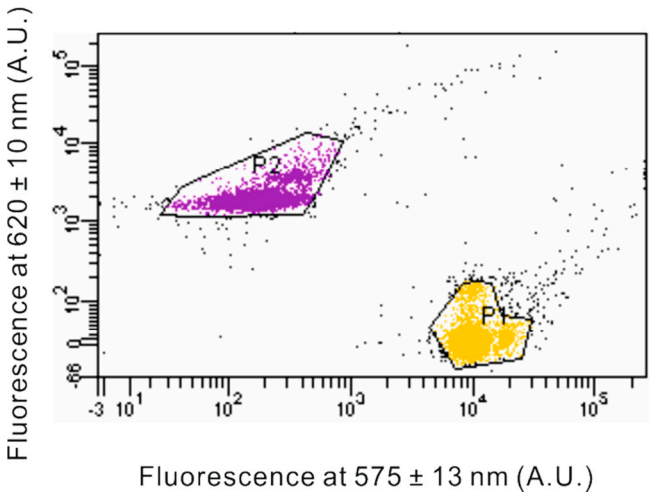

Figure 3.14. A two-dimensional fluorescence dot plot of the GMA beads from the multiplexed immunoassay.

Figure 3.14 shows the two-dimensional fluorescence dot plot of the GMA beads from the multiplexed immunoassays. Two well-defined populations, P1 (yellow) and P2 (purple), were clearly identified, in which P1 showed high Cy3 fluorescence and low Cy5 fluorescence, and vice versa for P2. This indicated that there were two sets of particles, each preferentially reacted with one of the two fluorescently-labelled antibodies. The absence of a third population with high fluorescence intensity in both Cy3 and Cy5 channels also suggested that the labelled antibodies had high specificity with one of the two sets of particles and little cross-reactivity with the other.

The multiplexed immunoassay result was compared to the corresponding mono-plexed assay from the cross-reactivity study. Table 3.6 shows the mean fluorescence intensity and the S/N of the two immunoassays. In both cases, the S/N between the monoplexed and multiplexed assays were very comparable.

Table 3.6. Relative S/N of monoplexed and multiplexed immunoassay.

		S/N	
Detection of		Monoplexed	Multiplexed
Cy3-anti-human	Human IgG-GMA *vs.* Rabbit IgG-GMA	50	48
Cy5-anti-rabbit	Rabbit IgG-GMA *vs.* Human IgG-GMA	36	33

This initial experiment demonstrated that the chosen antigens and antibodies were suitable for multiplexed suspension immunoassays. The labelled secondary antibodies were highly specific and had little cross-reactively with the non-target molecules. The signal obtained from the multiplexed immunoassay resembled the corresponding monoplexed assays, suggesting that the complexity of the assay panel had little impact on the quality of the result.

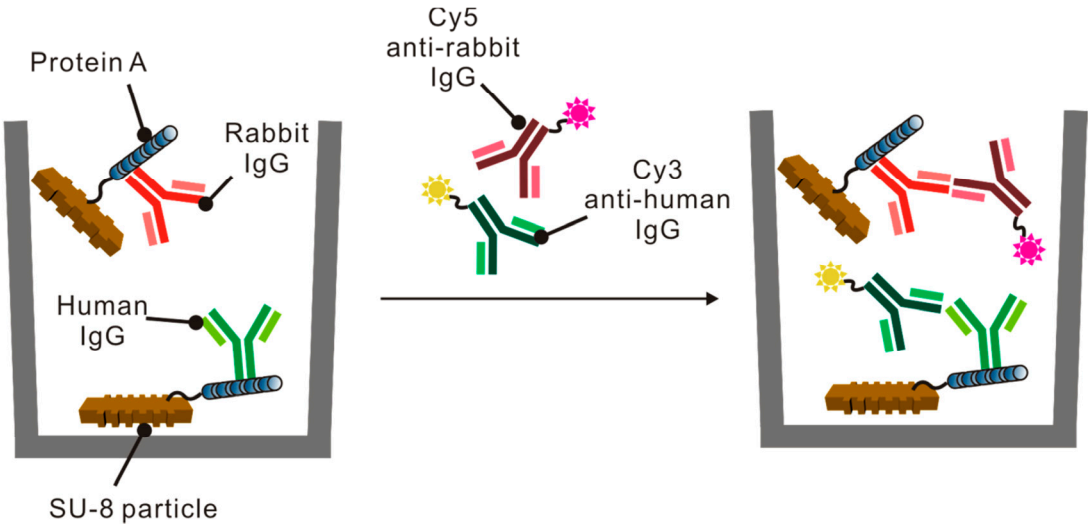

Figure 3.15. Schematic diagram of an multiplexed immunoassay on encoded SU-8 microparticles.

3.2.7 Multiplexed immunoassays on encoded SU-8 microparticles

The results obtained from the multiplexed immunoassays on GMA beads provided us with basic understanding of the suspension immunoassay. Our next objective was therefore to develop a similar immunoassay system on the encoded SU-8 particles (Figure 3.15).

To produce the protein A-coated SU-8 particles, the protein was covalently attached to carboxyl-SU-8 particles using the one-step EDC coupling chemistry. Human- or rabbit IgG were coated onto a specific set of code by affinity binding (1 h agitation). After washing away the excess IgG molecules that did not bind to the surface, the two sets of codes were mixed thoroughly (1 mg each, ~5.38×10^5 particles). To this suspension, a mixture of the fluorescently-labelled target antibodies (Cy3-anti human IgG and Cy5-anti rabbit IgG, 277 nM each) were added and the suspension was agitated at room temperature in the dark for 1 h. After removing the excess target antibodies and washing the particles with buffer, the particles were observed under a home-made fluorescence microscope equipped with a Cy3 and Cy5 filter sets.

Figure 3.16 shows a white light and fluorescence image of the encoded SU-8 particles from the multiplexed immunoassay. Two different SU-8 particles were clearly observed from the white light image (Figure 3.16a). Each of these particles contains a unique diffraction element on the surface that can be identified by naked eye in the image (left code 2; right code 4). From the Cy5 fluorescence image (Figure 3.16c), code 2 produced a relative high fluorescence level when illuminated with a red laser (633 nm) whereas code 4 showed little reaction. This showed the Cy5-labelled anti-rabbit antibody reacted specifically to the immobilised rabbit IgG on the SU-8 particles. Similarly, as seen from the Cy3 fluorescence image (Figure 3.16b), the Cy3-labelled anti-human antibody preferentially reacted to the human IgG-coated particles (code 4). The rabbit IgG-coated SU-8 particles

(code 2) also produced a low fluorescence in the Cy3 region. One possibility is that the secondary antibody reacted non-specifically with the rabbit IgG-coated surface, which was not observed on the GMA beads. Another possible cause to this elevated Cy3 fluorescence on the non-target particle is the intrinsic fluorescence property of the polymeric SU-8. Maire *et al.* demonstrated that after cross-linking, the polymeric SU-8 network produces high auto-fluorescence which overlapped with fluorescein and Cy3 fluorescence spectra.[113]

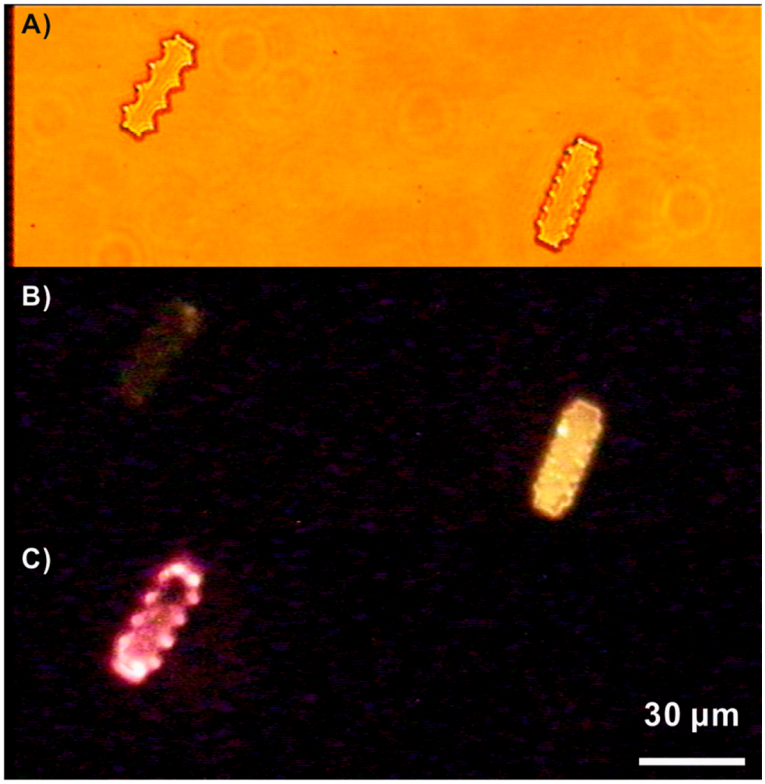

Figure 3.16. SU-8 microparticle from the multiplexed immunoassay. (A) White light image. (B) Cy3 fluorescence image. (C) Cy5 fluorescence image.

3.2.8 Fluorescence measurement by fluorescence flow cytometry

Potentially the SU-8 particles from the immunoassay could be easily measured and decoded using an automated analytical platform. This system would involve a motorised X-Y stage where a glass slide containing the particles could be placed. The on-board microscope then scans along the glass slide to locate a particle. Once a particle is identified, the system activates two laser beams, one for fluorescence illumination and the other for diffraction pattern generation. The fluorescence camera captured the fluorescence image and then transferred to the software to measure the fluorescence intensity. The diffraction pattern is also captured by an on-board camera and then decoded by the analytical software. The fluorescence measurement and the decoding data are coupled and presented to the user. Since the home-made analytical platform was only partially developed by the time this immunoassay was carried out, an alternative method was used to measure the fluorescence and decode the particles. A commercial fluorescence flow cytometer was used to measure the fluorescence of the SU-8 particles and a separate in-house analytical system was used for decoding the particles.

For the fluorescence measurement, the SU-8 particles from the immunoassay were injected into the flow cytometer, where the size of the particles and the fluorescence intensity at different wavelengths (Cy3: 575 ± 13 nm and Cy5: 660 ± 10 nm) were measured. During the measurement, we discovered that when illuminated with a green laser (488 nm), the SU-8 particles produced an intrinsic fluorescence that was too high and affected the scattering measurements. A neutral density filter with an optical density of 2 was therefore placed in front of the FSC and SSC detectors so that the transmitted light was reduced.

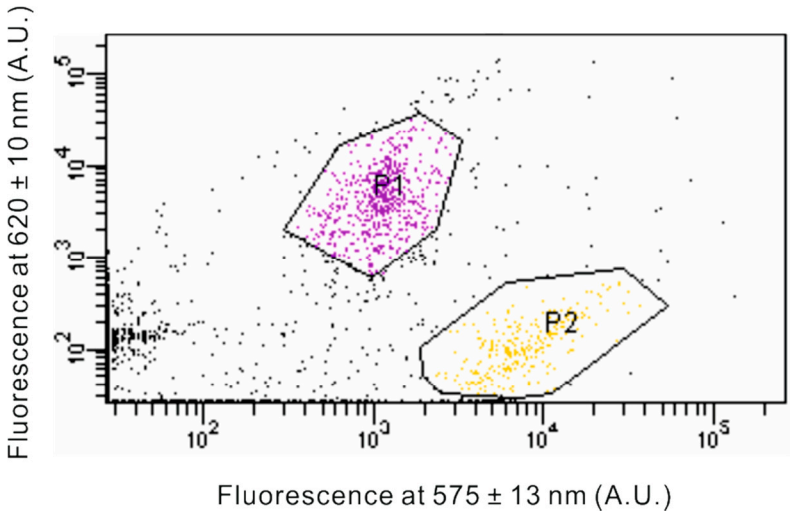

Figure 3.17. A two-dimensional fluorescence dot plot of the SU-8 microparticles from the multiplexed immunoassay.

Approximately 5000 particles from the multiplexed immunoassay were analysed by the FACS. Figure 3.17 shows the resulting 2-D fluorescence dot plot from the immunoassay. Similar to the immunoassays in GMA beads described above, two distinct fluorescent populations (P1 and P2) were identified. Table 3.7 compares the S/N of the multiplexed immunoassay on GMA beads and SU-8 particles. The two fluorescent SU-8 populations were not as well separated as in the GMA beads assay. The S/N of the Cy3-labelled anti-human reaction was reduced from 48 on GMA to 7 on SU-8. This might due to the fact that the SU-8 particles produced a higher Cy3 background fluorescence as seen in Figure 3.16.

Table 3.7. Comparison on S/N on GMA beads and SU-8 particles.

		S/N	
Detection of		On GMA	On SU-8
Cy3-anti-human	Human IgG-solid support *vs.* Rabbit IgG-solid support	48	7
Cy5-anti-rabbit	Rabbit IgG-solid support *vs.* Human IgG-solid support	33	50

3.2.9 Decoding and assay accuracy

To demonstrate the decoding system, the two fluorescent populations P1 and P2 were isolated by sorting using the cell sorter. From each isolated populations 50 particles were individually decoded by diffraction using the in-house analytical system. This system contained a stage where a single encoded particle was placed on top of a microscope objective. A laser beam was used to target the particle and an on-board CCD camera captured the resulting diffraction pattern which was projected onto a screen (Figure 3.18). After the image acquisition, the file was directly transferred to a PC where an in-house software package was used to analyse the diffraction pattern. First, it detected the zero-order beam on the image and assigned a directional vector. Then the software attempted to locate the first-order beams by comparing the contrast of individual pixels in a step-wise process. The distance between the zero- and first-order beams was calculated and used to identify a code.

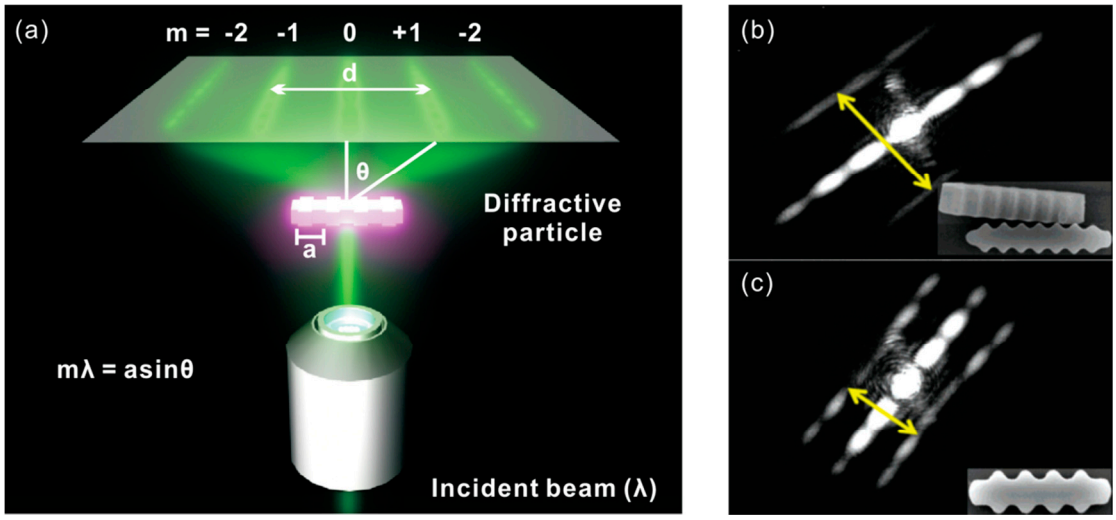

Figure 3.18. (a) A graphical illustration of an encoded SU-8 illuminated by an incident laser beam from the microscope objective. The fluorescently-labelled target on the surface emits fluorescence which is captured by the fluorescence microscope. In addition, the incident beam is also diffracted by the particles to generate a diffraction pattern on the screen. (b, c) Examples of different diffraction patterns generated by two encoded particles (photos shown in insets).

From each fluorescent population, around 50 particles were decoded using the in-house analytical software (Figure 3.19). Figure 3.20 summarises the results from the decoding analysis. In P1 (Cy5 channel – Cy5-anti-rabbit), 49 out of 50 particles were correctly identified as code 2 (rabbit IgG), whereas 50 out of 50 particles were found to be code 4 (human IgG) in P2 (Cy3 channel – Cy3-anti-human), so that the overall accuracy was calculated to be 98% for code 2 and 100% for code 4. There was no code 4 particle found in P1, or code 2 in P2, suggesting the demonstrated multiplexed immunoassay was highly specific and accurate.

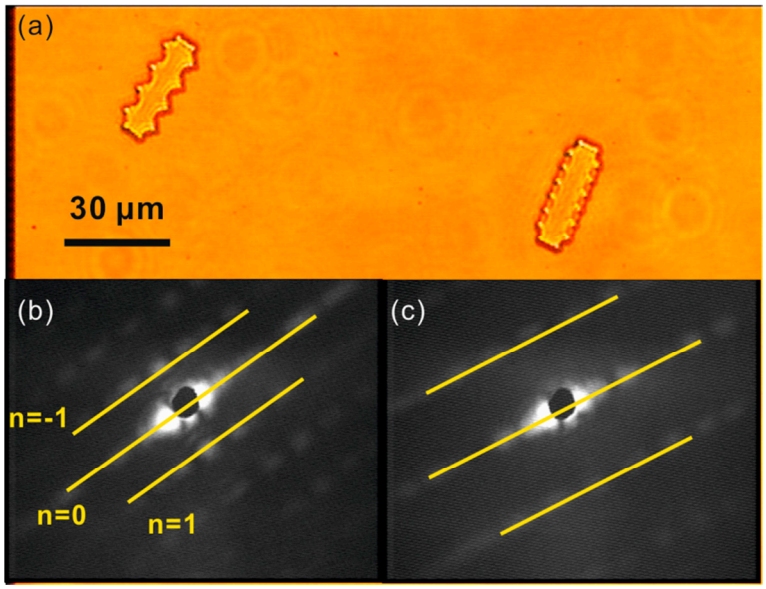

Figure 3.19. Examples of the diffraction patterns produced by two different codes. The white light image (a) shows code 2 (left) and code 4 (right) and the corresponding diffraction patterns (b) and (c). By measuring the distance between the zero order (n = 0) and first order (n = 1) the code can be identified.

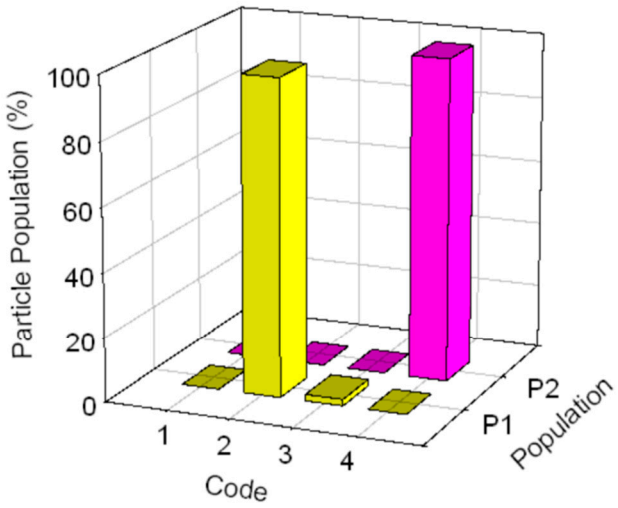

Figure 3.20. Fifty particles from each of the two fluorescent populations sorted by FACS were decoded by the in-house analytical software package. In population 1 (P1), 49 particles were correctly identified as code 2, whereas in population 2 (P2) all particles were recognised as code 4.

Interestingly, one particle in P1 was determined to be code 3 by the decoding system, which was not used in this assay. In order to understand the origin of this result, the raw

images of this particle were inspected thoroughly. Figure 3.21 shows the white light image of that particle and the corresponding diffraction pattern. By optical inspection the diffraction element on the particle was found to be similar to the others found in the same population. However, when illuminated by a laser beam the resulting diffractive pattern resembled a code 3 signature. This ruled out sample contamination and proved the particle contained a poorly define diffraction element and that resulted in being misidentified as a code 3 particle.

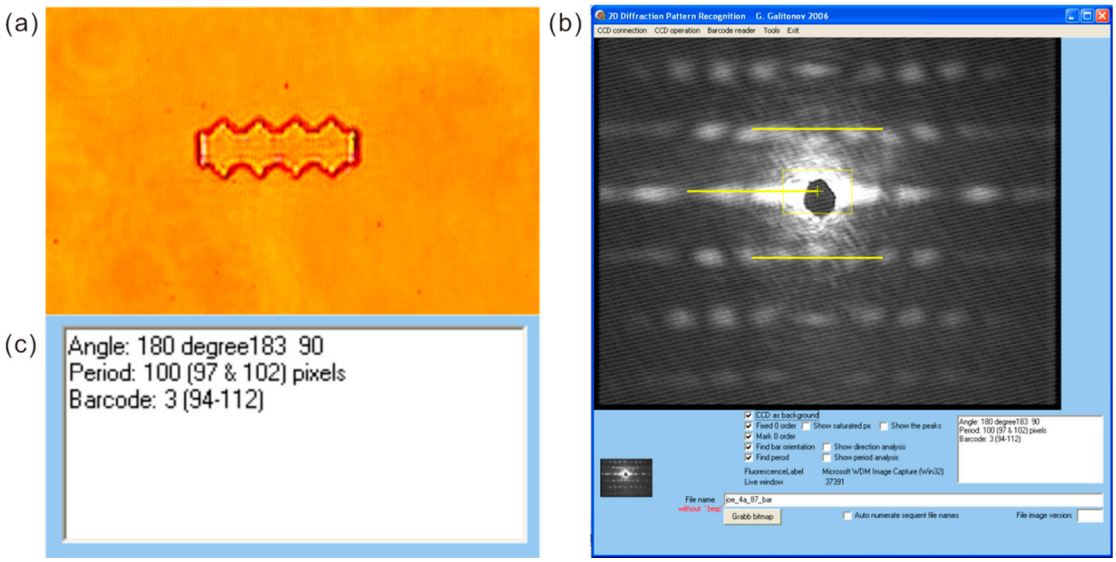

Figure 3.21. A code in P1 (a) was decoded by the in-house recognition system (b). After analysing the distance between the zero- and first-order diffraction beams the system determined the particle as code 3 (c).

In this experiment, code 3 was not used in the assay and therefore the outlier could be easily identified and omitted. However, it would soon become very difficult to identify the incorrect codes when the complexity of the panel increased. This would lead to false positive or negative results which has a profound impact on the quality of the data. In this example, the poor resolution of the diffraction element on the particles was causing the decoding problem. Potentially, this could be greatly improved during microfabrication

using prolonged exposure time. However this would dramatically reduce the amount of free epoxy groups for the subsequent chemical functionalisation. An alternative method is to produce the SU-8 encoded particles by nano-embossing, where the diffractive units are produced by stamping a negative mask on to the cross-linked SU-8 particles on a wafer. This method has been proven to produce diffraction features with sub-nanometre resolution.[198]

3.2.10 Thermodynamic studies

In order to understand the sensitivity of the assay platform, thermodynamics of human IgG:anti-human IgG interactions (Equation 3.4) on solid supports were determined by titration of analytes and fluorescence flow cytometry. Human IgG-coated particles (GMA beads or SU-8 particles, 1 mg) were incubated with increasing concentration of Cy5-labelled anti-human IgG antibody (3 pM – 1000 nM) at room temperature in the dark for 30 min. Subsequently, the particles were washed with PBST (200 μL) and then analysed by fluorescence flow cytometry. A comparative study was carried out in solution in which human IgG was incubated with Cy5-anti human IgG at different concentration for 30 min, after which the fluorescence polarisation of the reaction mixture was measured using a microplate reader (Safire^2, Tecan, Switzerland).

The resulting data obtained from the titration experiments were plotted and are illustrated in Figure 3.22 (a, b and c). In order to determine the equilibrium dissociation constants (K_d, Equation 3.3) for the human IgG/Cy5-anti-human IgG interactions in solution and on solid supports (Equation 3.4), the data were converted to a binding-curve (Figure 3.22d, e and f) and fitted to a one-site ligand binding curve (Equation 3.4) using SigmaPlot (version 10, Systat Software Inc., CA, USA).

$$[\text{Antibody}]_{\text{Free}} + [\text{Antigen}]_{\text{Free}} \leftrightarrow [\text{Antibody: antigen}] \quad \text{Equation 3.2}$$

$$K_d = \frac{[\text{Antibody}]_{\text{Free}} \times [\text{Antigen}]_{\text{Free}}}{[\text{Antibody: antigen}]} \quad \text{Equation 3.3}$$

$$[\text{Antibody: antigen}] = \frac{B_{max}[\text{Antibody}]_{\text{Free}}}{K_d + [\text{Antibody}]_{\text{Free}}} + Ns[\text{Antibody}]_{\text{Free}} \quad \text{Equation 3.4}$$

where $[\text{Antibody:antigen}]$ is the concentration of antibody bound to the immobilised antigen on the surface at equilibrium (M); $[\text{Antibody}]_{\text{Free}}$ is the concentration of free antibody at equilibrium (M); $[\text{Antigen}]_{\text{Free}}$ is the concentration of free antigen at equilibrium (M); K_d is the rate dissociation constant at equilibrium (M); B_{max} is the maximum concentration of functional antigen on the surface (M); Ns is the fraction of non-specifically bound antibody on the surface.

Figure 3.22 illustrates the antibody:antibody binding curves and the measured parameters are summarised in Table 3.8. In all three experiments, the binding curves demonstrated an initial linear response before reaching saturation. The K_d of the IgG/anti-IgG interaction was determined to be 14 ± 9 nM (R^2 = 0.894) in solution; 11 ± 2 nM (R^2 = 0.984) on GMA beads; and 9 ± 3 nM (R^2 = 0.949) on SU-8 particles. The amount of non-specifically bound labelled antibody, which was determined from Equation 3.4 (Ns), was estimated to be 9% on GMA beads and 6% on SU-8 particles. From the calculated B_{max}, the number of target antibody molecules bound to each particle at saturation was calculated. On GMA beads this value was ~7×10^6 molecules/bead (~12 amol), which roughly correspond to 0.8 layer. On SU-8 particles, B_{max} was determined to be ~6×10^7 molecules per particle (~10 amol), which also roughly relates to ~0.8 layer (see Appendix B for details).

Table 3.8. A summary of the measured thermodynamic parameters of the antibody:antigen interaction in solution; on GMA beads and on SU-8 microparticles.

	K_d (nM)	R^2	B_{max}	Ns
In solution	14 ± 9	0.894	ND	ND
On GMA	11 ± 2	0.984	48 ± 2	0.009
On SU-8	9 ± 3	0.949	90 ± 7	0.0059

ND = Not determined

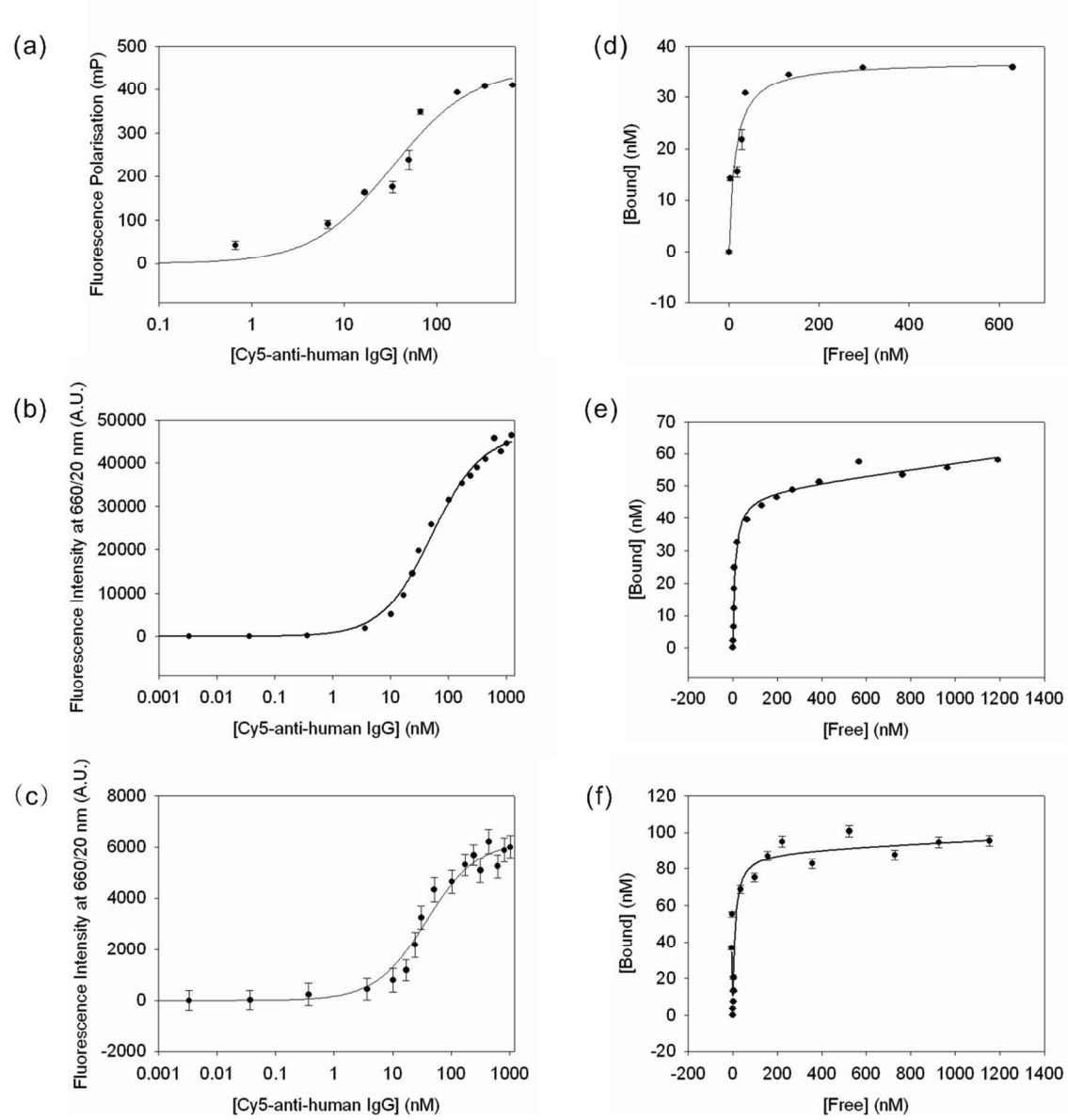

Figure 3.22. Binding curves of Cy5-labelled anti-human IgG to polyclonal human IgG in solution (a), on GMA beads (b) and on SU-8 particles (c). The binding curves were transformed into the corresponding [Bound] vs. [Free] curves (d-f).

The data obtained from the above thermodynamic studies confirmed that IgG/anti-IgG interaction on solid-supports (both GMA beads and SU-8 particles) resembled solution-like binding affinity. This demonstrated that the immobilised antigen retained its 3-D structure for binding and the surface did not affect the molecular interaction significantly. This finding was extremely important for developing sensitive immunoassay platform using high-affinity antibodies.

3.2.11 Assay kinetics on SU-8 particles

The binding kinetics of the Cy5-labelled anti-human IgG to the immobilised human IgG on protein A-coated SU-8 particles was analysed by carrying out a fluorescence time-course measurement. The IgG-coated particles were agitated in a solution of target antibody at 67 nM in PBST. At each time point, an aliquot of the suspension was withdrawn from the reaction and immediately washed with the assay buffer to stop the reaction. The fluorescence intensity of the particles from these samples were analysed by fluorescence flow cytometry. Figure 3.23 shows the results of the fluorescence time-course measurement. At an analyte concentration of 67 nM the binding reached equilibrium in <10 min. This measurement confirms that the binding assays on encoded SU-8 microparticles can be carried out in short time scales. Individual rate constants were not calculated due to the complexity of the sandwich system.

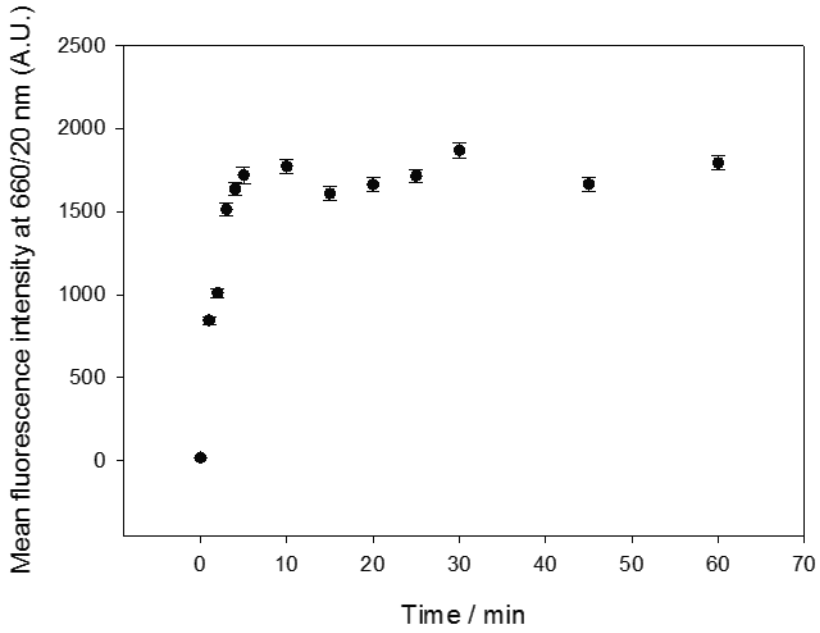

Figure 3.23. Kinetic analysis of the binding of target antibody at 67 nM to the IgG-coated SU-8 particles in suspension.

3.2.12 Theoretical detection limit and experimental verification

From the above thermodynamic studies, a theoretical detection limit on SU-8 particles could be calculated. A common method to determine the lowest detection limit (LDL) is by substituting a value which equates to three times the error from the background measurement (0 nM in this case) to the linear equation (Equation 3.5)

$$[\text{Cy5 anti-human IgG}] = \frac{\text{Fluorescence-c}}{\text{m}} \qquad \text{Equation 3.5}$$

where $[\text{Cy5 anti-human IgG}]$ is the original concentration of labelled antibody added to the reaction (nM); Fluorescence is the expected fluorescence signal obtained from the microparticles at such antibody concentration (A.U.); c is the intercept of the line; and m is the slope.

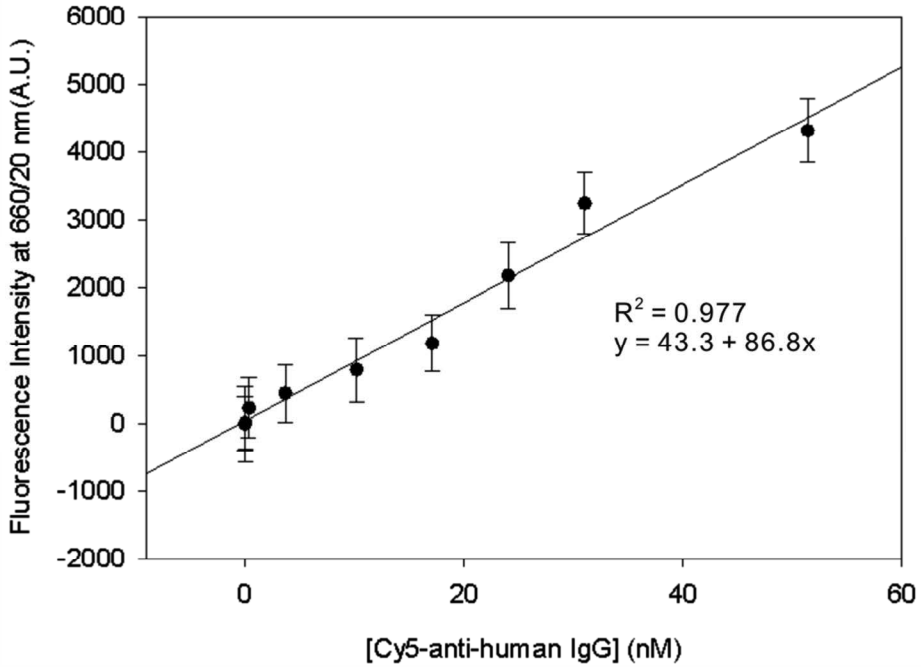

Figure 3.24. The antibody-antigen interaction on SU-8 particle produced a linear response at low antibody concentration.

The standard error (SE) of the background was determined to be 554 A.U. By substituting a value that equates to three times of the background error (554 × 3 = 1662 A.U.) into Equation 3.5, an LDL of 18.6 nM was obtained. Assuming 1 × SE of the background was sufficient to differentiate a positive signal from the background, then an LDL of 5.8 nM was calculated, which equates to a 1-μL solution containing 5.8 fmol Cy5-anti human IgG.

To validate this experimentally, human IgG- or rabbit IgG-coated SU-8 particles (20 particles each) were agitated in a solution of Cy5-anti-rabbit IgG (5.35 fmol, 1 μL). The particles were agitated at room temperature in the dark for 16 h and then washed with PBST. Fluorescence images of these particles were taken using a fluorescence microscope equipped with a Hamamatsu ORCA-ER digital camera. The fluorescence intensities of the images were analysed using an in-house software package.

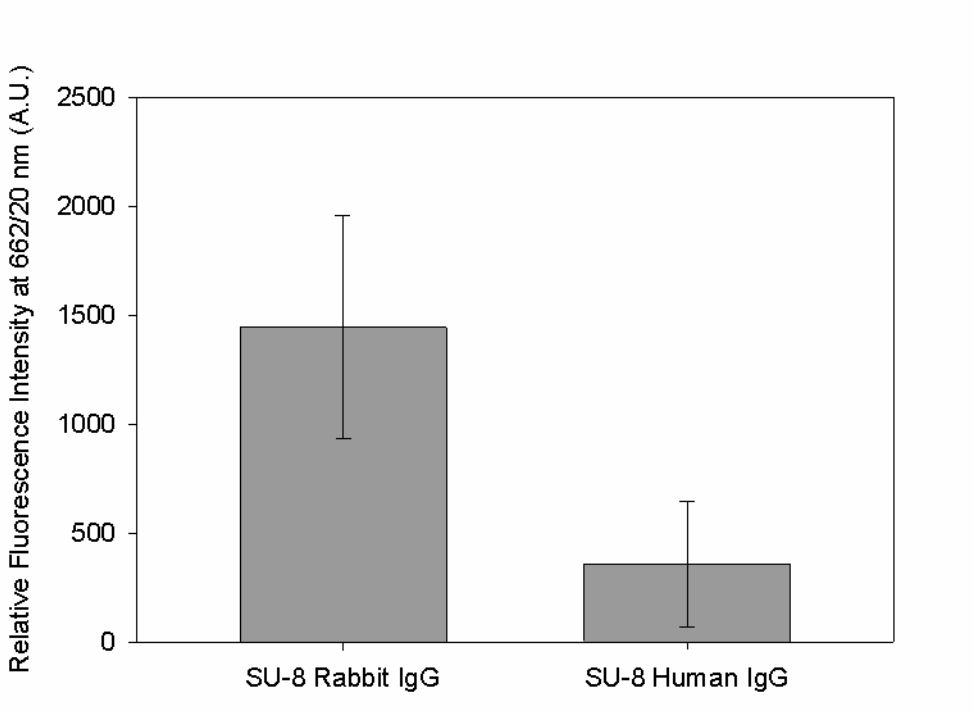

Figure 3.25. The mean fluorescence intensities of rabbit- or human-IgG coated SU-8 particles after reaction with a 1 μL solution containing 5.35 fmol Cy5-anti-rabbit IgG antibody.

Figure 3.25 summarises the result of the detection limit experiment. The mean fluorescence intensity of 20 particles from each set of SU-8 particles is shown and the standard deviation of the measurement is presented as error bars. This experiment demonstrated that a 1 μL solution of 5.35 fmol Cy5-antibody can be successfully detected on the SU-8 particles with a S/N of 4.

3.3 Conclusion

In this chapter we reported a novel method for detecting specific antigens in a multiplexed manner. This method was based on particle-based suspension immunoassay using encoded SU-8 particles. Each of these encoded particles contained a diffractive element on the surface which produced a code-specific diffraction pattern when illuminated

by a laser beam. We attempted the detection of fluorescently-labelled secondary antibody (anti-human and anti-rabbit) using primary antibody-coated solid supports. We used protein A from *S. aureus* as an immunosorbent to attach a wide range of IgGs to the particles. From the cross-reactivity study, the fluorescently-labelled antibodies interacted specifically with the target-functionalised surface and showed little cross-reactivity with the non-target solid supports. In a preliminary study, a multiplexed immunoassay was used to simultaneously detect Cy3-anti-human and Cy5-anti-rabbit antibodies. From the results obtained from a fluorescence flow cytometer, two distinct populations were identified, suggesting that the chosen biological reagents were suitable for such assay system. In the proof-of-principle experiment, this immunoassay system was transferred to the SU-8 platform. After analysing by fluorescence microscopy and fluorescence flow cytometry, the multiplexed immunoassay showed high specificity and low cross-reactivity. Decoding of SU-8 particles was demonstrated using an in-house analytical system. The particles were illuminated by a laser beam and the resulting diffraction pattern was analysed by the in-house software. The decoding accuracy was found to be >98%, consistent with the high accuracy required by these systems. In a comparative thermodynamic study, the IgG:anti-IgG interaction on solid supports was shown to resemble solution-like behaviour (K_d solution: 14 ± 9 nM; K_d on GMA beads: 11 ± 2 nM; K_d on SU-8: 9 ± 3 nM). The binding kinetics of the same interaction (67 nM) on SU-8 particles was found to be rapid and took less than 10 min to reach equilibrium. The sensitivity of the platform was also studied. If 1 × standard error (SE) of the background was required to discriminate a positive signal from the background, then a theoretical Lowest Detection Limit (LDL) of 5.8 nM was achieved. An experimental validation using 5.35 nM of Cy5-anti human confirmed this estimation with a S/N of 4.

Chapter 4 Simultaneous quantification of multiple human cytokines on encoded SU-8 particles

Multiplexing immunoassay is a powerful technique that detects and quantifies multiple analytes simultaneously in a single reaction mixture. In Chapter 3, a proof-of-principle immunoassay for detecting goat anti-human IgG and goat anti-rabbit-IgG was demonstrated. This experiment showed that the immunoassay on SU-8 particles was very specific and showed little cross-reactivity. In this chapter, the detection of multiple small proteins (MW ~20 kDa) in a sandwich immunoassay format on SU-8 particles is described.

4.1 Introduction

4.1.1 Cytokine

Cytokines are a group of small signalling proteins that play an important rôle in the regulation of the immune system. They are produced *in situ* by a variety of cell types, including macrophages, monocytes, B cells and T cells.[199] Their primary function is to aid the intercellular communication between the immune cells by altering their behaviours and properties.[200] Their effects include induction of inflammation, development of cell-mediated and humoral responses, induction of cellular proliferation and differentiation, promotion of apoptosis, and triggering of tissue repair.[201] These molecules are biomarkers for a wide range of diseases and their multiplexed analysis may serve for diagnostic purposes.[202]

4.1.2 Functions

A cytokines can have multiple, overlapping and sometimes contradictory functions depending on its concentration, the cell type it is acting upon and the presence of other cytokines.[201] Often, two or more cytokines work in synergy in order to stimulate target cells. For example, T cells secret both interleukin (IL)-4 and IL-5 which co-stimulate B cells for the production of immunoglobulin E (IgE).[203] Many cytokines regulate the immune response through specific cell surface receptors. An example is the Janus kinase-signal transducer and activator of transcription (JAK-STAT) pathway (Figure 4.1).[204] When the cytokine binds to the target cell receptor, the receptor undergoes conformational changes, in which it activates a tyrosine kinase, JAK, to phosphorylate the receptor and a transcription factor, STAT. This process causes STAT to dimerise and promotes the dimerised protein to translocate to the nucleus. The internalised STAT dimer then initiates the transcription of target genes. Some cytokines inhibit other cytokine activity by blocking the cell-signalling pathway.[205] For example, IL-1 receptor antagonist (IL-1ra), a member of the IL-1 family, blocks the cell surface IL-1 receptor and hence inhibits other IL-1 activities, such as IL-1α and IL-1β.[206]

4.1.3 Classification

There are a number of methods to classify cytokines. One of these is by their cellular source; for example, lymphokines are cytokines secreted mainly by activated T_h lymphocytes whereas monokines are produced by macrophages and monocytes.[199] Besides these terms expressing their cellular origin, cytokines may also be named according to their functions, these includes interferons (IFN),[207] which have anti-viral properties, and tumour necrosis factors (TNF), which promote programmed cell death (apoptosis).[208]

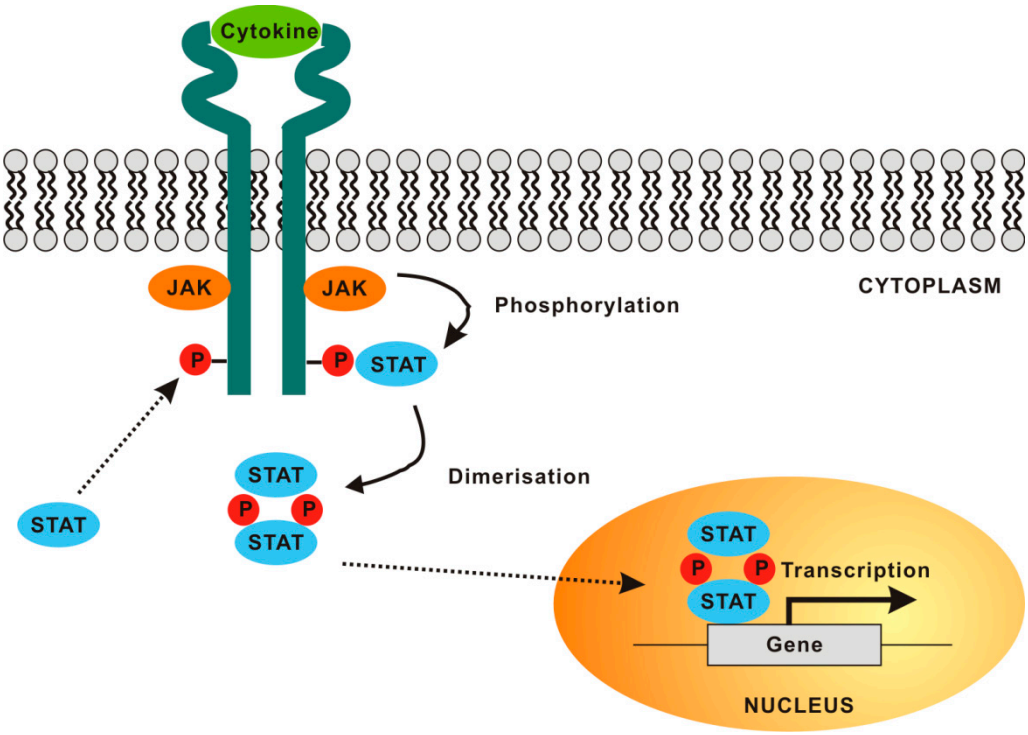

Figure 4.1. A schematic diagram showing the JAK-STAT cell signalling pathway.

4.1.3a Pro-inflammatory

Pro-inflammatory cytokines are predominantly produced by activated macrophages and are involved in the up-regulation of inflammation.[209,210] Most of these cytokines, including IL-1 and TNF-α, induce the expression of a number of enzymes so that the synthesis of the inflammatory mediators is initiated.[211] These mediators then cause a cascade of cellular events to induce inflammation, which causes fever, an increase of local blood flow and tissue destruction.

4.1.3b Anti-inflammatory cytokines

Sustained or excess inflammatory reactions can cause serious damage to the host body.[209] There is another group of cytokines, termed anti-inflammatory cytokines which down-regulate inflammation and limit the damage caused.[212,213] They accomplish this by a number of methods: they down-regulate or inhibit the production of pro-inflammatory cytokines; promote target-specific immune responses; and trigger tissue repair (Table 4.1).

Table 4.1. A summary of a selection of anti-inflammation cytokines. This material was adapted from references 210 and 211.

Cytokines	Cellular Sources	Major Activities
IL-1a	Monocytes, macrophage	IL-1 receptor blocker. Inhibits IL-1α and IL-1β activates.
IL-4	T cells, B cells, stromal cells	Inhibition of proinflammatory cytokine synthesis.
IL-6	T cells, B cells, monocytes	Inhibition of TNF and IL-1 production by macrophage.
IL-10	Monocytes, macrophage, T cells, B cells	Inhibits the production of cytokines from monocytes/macrophage.

4.1.4 Quantification methods

There are two common methods used to quantify cytokines. One method is by detecting the mRNA level by quantitative reverse transcriptase-PCR (qRT-PCR).[214,215] In this approach, cDNA is produced from the mRNA by reverse transcription. The cDNA is then used as a template for qPCR. The amount of cDNA, and hence the mRNA level, is then quantified by qPCR. Another commonly used method is by immunoassay, such as ELISA.[216] In this method, the soluble cytokines in serum, plasma or tissue culture are quantified directly. Although these methods are widely used for cytokine quantification, they show certain disadvantages. In general, the methods are very time consuming and can only quantify one target cytokine at a time. In addition, the principle of these assays does

not permit the study of the complex relationship within the cytokine network, especially with cytokines that exhibit contradictory functions. The ability to monitor multiple cytokines in an efficient manner is therefore highly desirable.

4.1.5 Aims of this chapter

This chapter focuses on the development of particle-based suspension immunoassays and to demonstrate the feasibility on simultaneous quantification of multiple analytes from a single target.

4.2 Results and Discussions

4.2.1 Principle of the assay

The approach for detecting multiple target proteins simultaneously was as follow: single capture antibody molecules were covalently attached to a set of SU-8 microparticles. These particles were suspended in the sample and captured the target analyte. A biotinylated detection antibody was used to form an antibody:antigen:antibody sandwich complex on the surface. In order to visualise and quantify the immuno-sandwich, the bound complex was fluorescently labelled with Cy5-streptavidin. The accumulated fluorescence on the solid support was then measured (Figure 4.2).

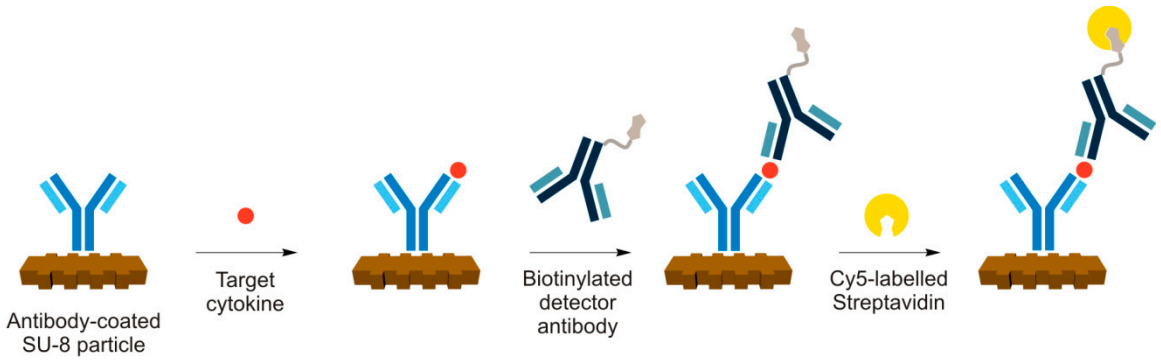

Figure 4.2. The principle of the microparticle-based suspension sandwich immunoassay.

For the proof-of-principle sandwich immunoassays, the quantification of human TNF-α and human IL-6 was chosen. The capture antibodies and the biotinylated detection antibodies (Table 4.2, kindly provided by SPI-BIO, Paris, France) against these analytes were used in a commercially available ELISA (see Appendix C for standard curves in ELISA format).

Table 4.2. The capture and detection antibodies used in the microparticle-based suspension immunoassay for human cytokines.

Analyte	Antibody ID	Function	Source	Type
TNF-α	TNF-α0306	Capture	Mouse	Monoclonal
	TNFαD-0107	Detection	Mouse	Monoclonal
IL-6	IL6C-0307	Capture	Mouse	Monoclonal
	IL6D-0307	Detection	Mouse	Monoclonal

4.2.2 Attachment of capture antibodies

The capture antibodies were covalently attached to the solid support by the 2-step EDC/sulfo-NHS coupling method described in Chapter 2. To estimate the loading level

of the immobilised antibody, a known amount of the particles was subjected to BCA protein assay. From this measurement, the loading level was estimated to be 23 ± 9 nmol/g, which was equivalent to 2.0 ± 0.7 layers of proteins on the surface.

4.2.3 Conjugation of detection antibody with biotin or biotin-LC

The detection antibodies were biotinylated using 1) sulfo-NHS-LC-biotin (contained a hexacarbon spacer) or 2) sulfo-NHS-biotin (Figure 4.3, both obtained from Pierce Biotechnology[217,218]). The biotinylated antibody was purified by gel chromatography. The number of biotins conjugated to the antibody was quantified by the HABA assay (Figure 4.4), which was based on the displacement of HABA with the biotinylated-antibody from the spectroscopically active HABA:avidin complex. The decrease in the absorbance at 500 nm was used to calculate the total amount of biotin in the antibody solution. From this measurement, the biotinylation level was determined to be 12.7 ± 0.3 and 10.1 ± 0.7 for biotin and biotin-LC respectively (Table 4.3).

Table 4.3. The number of biotin molecules conjugated to the antibody as estimated by the HABA:avidin assay.

	Biotin:IgG	
	Biotin	Biotin-LC
Anti-human IL-6 detection Ab	12.7 ± 0.3	10.1 ± 0.7

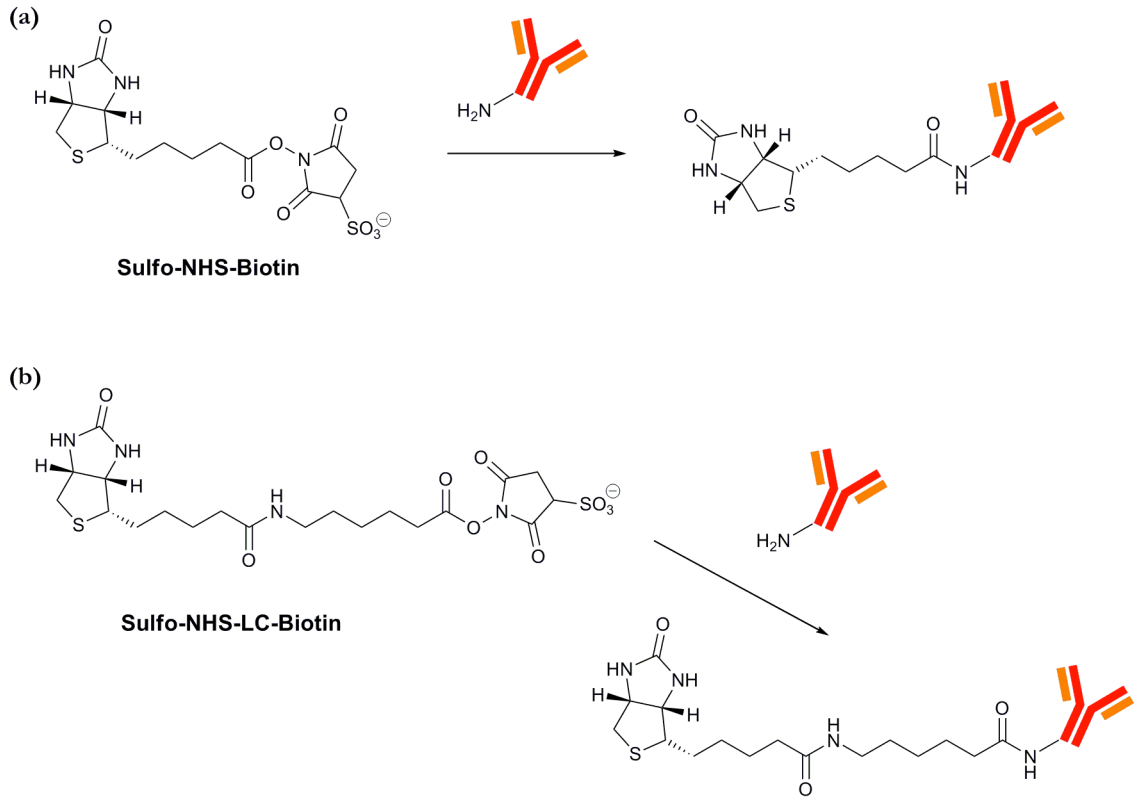

Figure 4.3. Schematic diagram of the biotinylation of antibody using sulfo-NHS-biotin (a) and sulfo-NHS-LC-biotin (b).

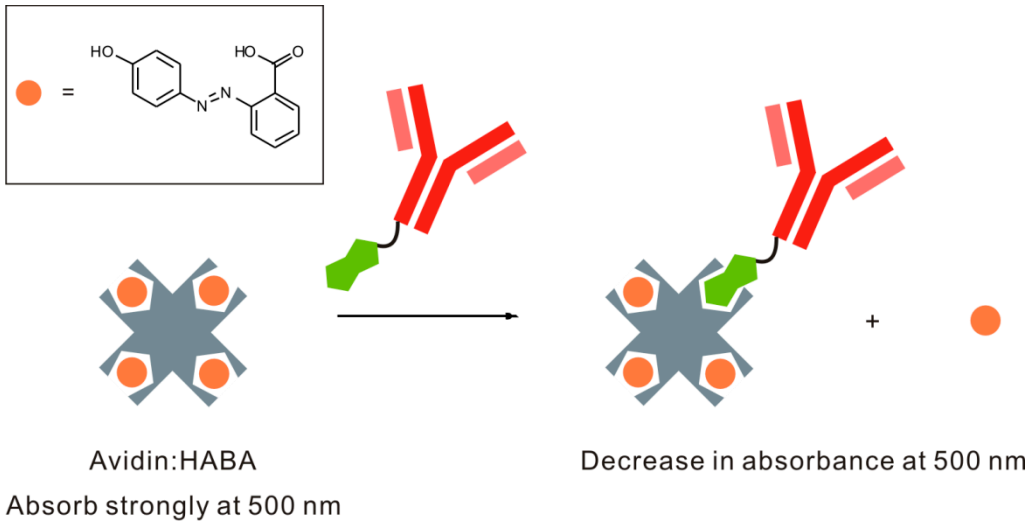

Figure 4.4. The principle of the HABA:avidin assay. The HABA:avidin complex absorbs strongly at 500 nm. The biotin conjugated to the antibody displays the weekly bound HABA from avidin and causes a decrease in absorbance at 500 nm.

4.2.4 Particle-based suspension sandwich immunoassay

Aspects of a proof-of-principle particle-based suspension immunoassay were investigated. To assess the specificity in this assay, recombinant human IL-6 or TNF-α at a concentration of 238 pM and 287 pM respectively (both at 5000 pg/mL) was measured using the anti-IL6 particles according to the method described in section 4.2.1. The non-specific binding of the detection antibody and Cy5-streptavidin to the SU-8 particles was measured from the "buffer" sample, which contained no cytokine. Figure 4.5 shows the assay readouts of the suspension immunoassay. The results are reported as the mean of fluorescence intensity of 1000 particles for each analyte. From the measurements, the use of biotin- or biotin-LC-conjugated detection antibody showed similar behaviour in the assay. The extra C6 spacer in biotin-LC did not show a significant improvement on streptavidin binding. The non-specific binding signal of the recombinant human TNF-α was higher than the detection antibody and Cy5-streptavidin. This might be due to the cross-reactivity of the antibody pairs to the non-target cytokine, which was reported to be <0.5% by the supplier. A strong fluorescence signal was observed on particles with the specific cytokine. The signal-to-noise ratio was found to be ~10:1.

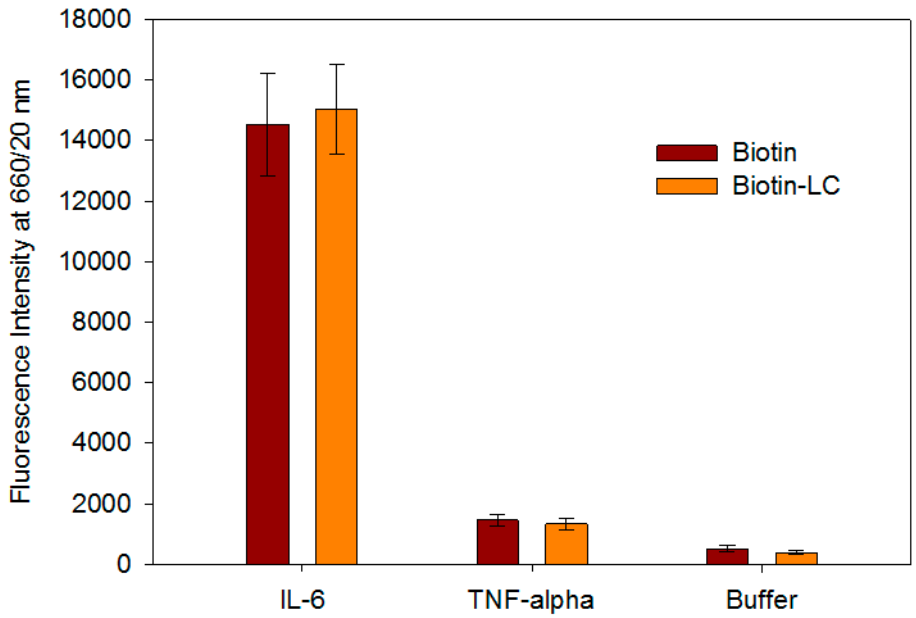

Figure 4.5. A fluorescence histogram of the specificity study of the anti-IL-6 SU-8 microparticles in a sandwich suspension immunoassay.

4.2.4a Quantification by fluorescence flow cytometry

To gain insight into the sensitivity of the particle-based suspension sandwich immunoassay, standard human IL-6 solutions with concentration ranging from 90 fM to 48 nM were assayed using the method described above. Mean fluorescence intensity of each target concentration was measured and was shown as a standard curve (Figure 4.6). The standard curve followed a Langmuir binding behaviour with a 4-log dynamic range. The data points were fitted to a 4-parameter logistic nonlinear regression model (Equation 4.1) with a correlation coefficient (R^2) of 0.969. The sample contained no cytokine provided a background signal for the assay, which was contributed by the non-specific binding of the detection antibody and Cy5-streptavidin. The lowest detection limit (LDL) was determined by extrapolating the cytokine concentration at a signal equal to the background plus 3 × standard error of the background signal, which was 22 pM. For comparison, similar IL-6

immunoassay in ELISA format had a LDL of 0.47 pM (Appendix C1). This indicated that the SU-8 particles were ~47 times less sensitive than the ELISA counterpart format.

$$f = \frac{A - D}{1 + (\frac{x}{C})^B} + D \qquad \text{Equation 4.1}$$

where *f* is the fluorescence intensity (A.U.); *x* is the concentration of the cytokine (pM); *A* is the minimum asymptote; *B* is the slope factor; *C* is the inflection point; and *D* is the maximum asymptote.

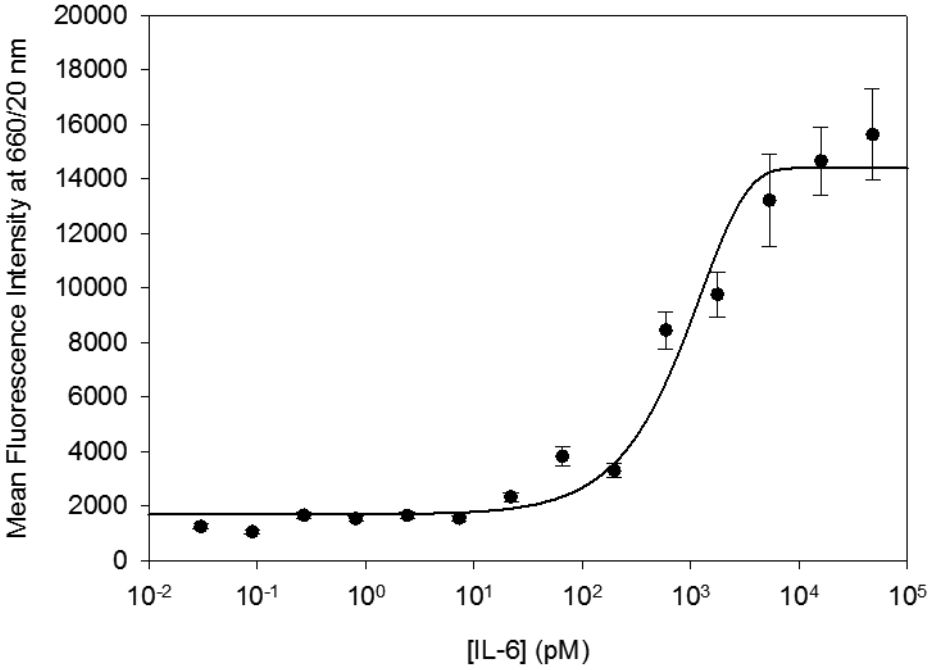

Figure 4.6. A binding curve showing the detection dynamic range and sensitivity of the anti-IL-6 SU-8 microparticles in a suspension immunoassay for recombinant human IL-6.

A similar immunoassay for the quantification of human TNF-α was carried out using the SU-8 particles coated with the anti-human TNF-α capture antibody. To demonstrate the assay specificity the standard TNF-α solution was assayed with the anti-human IL-6 SU-8 particles in parallel. Figure 4.7 shows the resulting titration curves. As anticipated,

the fluorescence signal on the anti-TNF-α SU-8 particles increased in response to the increasing concentration of the target analyte. In contrast, the anti-IL6 particles showed little or no reaction against TNF-α. The data points were fitted into Equation 4.1 and showed linearity between 1 pM and 800 pM with a LDL of 3.83 pM. In comparison, a similar immunoassay in ELISA format produced a LDL of 57.5 fM (Appendix D2). Similarly, the SU-8 particles were ~66 times less sensitive than the ELISA format.

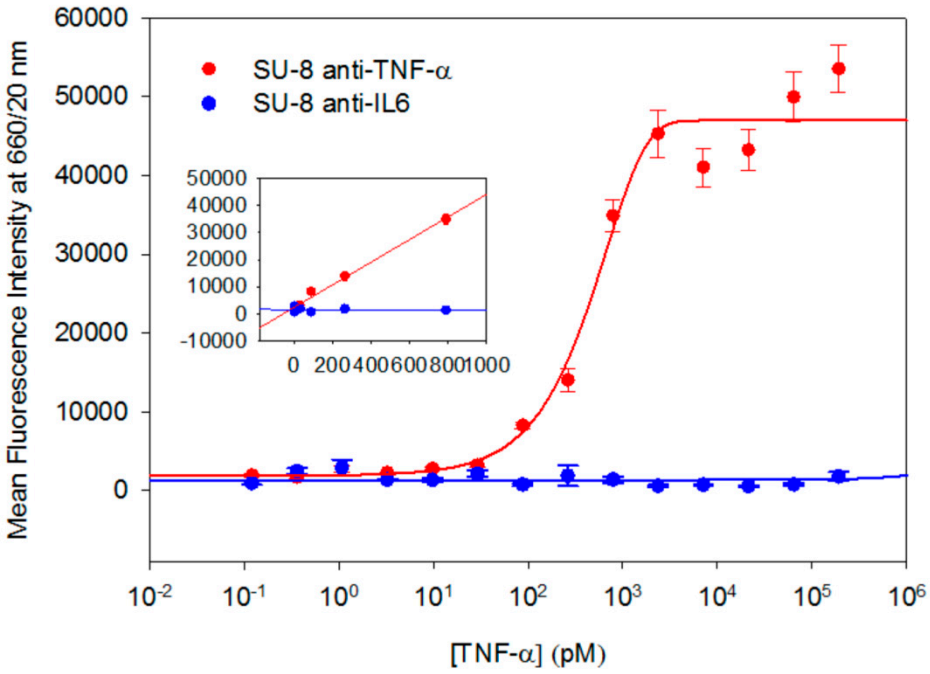

Figure 4.7. A binding curve showing the detection dynamic range and sensitivity of the anti-TNF-α SU-8 microparticles (red) in a suspension immunoassay for recombinant human TNF-α. Anti-IL-6 particles (blue) showed minimal cross-reaction with the analyte.

The particle-based suspension sandwich immunoassay demonstrated above showed good specificity against the target analyte. However, the assay was found to be ~66 times less sensitive than the ELISA format. Part of this relatively poor sensitivity might be due to the instrument used for the assay readout. The use of a fluorescence flow cytometer to analyse the particles had a number of disadvantages. Since the encoded SU-8 particles had an anisotropic shape, the flow cytometer produced a large standard deviation when

measuring the size and fluorescence of the particles in flow. As a result, a large amount of microparticles had to be analysed (at least 1000 particles) from a single assay in order to produce a statistically valid measurement. The high standard deviation also affected the measurement at low target concentrations. In addition, commercially available flow cytometer could not be used to decode the particles and so could not be used for analysing multiplexed immunoassay.

4.2.4b Suspension immunoassay analysed by fluorescence microscopy

Instead of analysing the assay by fluorescence flow cytometry, the use of fluorescence microscopy for assay measurement for improved data quality was assessed. To demonstrate this concept, human IL-6 solutions with concentrations ranging between 0.04 pM and 47.8 pM were assayed with the anti-IL6 particles. Approximately 20 particles (*c.f.* ~1000 with the flow cytometry system) from each concentration were analysed with an inverted fluorescence microscope. A broadband mercury lamp and a Cy5-filter set were used to excite the particles. The fluorescence images were acquired using an on-board cooled digital camera (ORCA-ER, Hamamatsu, Japan) and saved as 16-bit TIFF format. To measure the fluorescence intensity, these images were analysed using an open-source image analysis software package (ImageJ version 1.48o, National Institutes of Health, USA). Figure 4.8 shows the standard curve of human IL-6. Overall, the quality of the data was improved with a lower variability (with CV ranged from 1% - 8%, mean 2.8%). The data points were also fitted to Equation 4.1 with an increase of confidence ($R^2 = 0.974$). At low target concentration (up to 24 pM), the linearity was greatly improved ($R^2 = 0.902$). With the combination of these improvements, the LDL was lowered to 3 pM (*c.f.* 22 pM from flow cytometry setup and 0.47 pM from commercial ELISA).

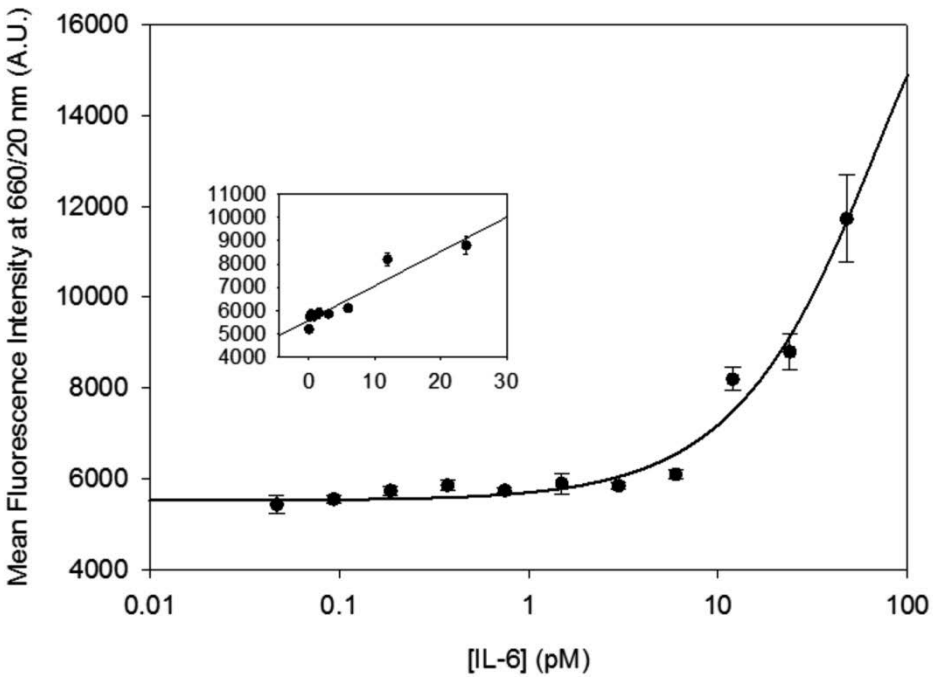

Figure 4.8. The sensitivity of the human IL-6 immunoassay on anti-IL-6 SU-8 microparticles was improved when fluorescence microscopy was used for assay readout.

To assess the reproducibility of the cytokine assay, TNF-α at concentrations between 14 fM and 57 pM was assayed in triplicates with a fluorescence microscope. Figure 4.9shows the standard curves of all three assays. Intra-assay variability, expressed as a coefficient of variation (CV), was calculated based on the fluorescence intensity against the standard deviation of each concentration per assay. This was found to be consistent between the triplicates. Inter-assay variation was evaluated by comparing the mean fluorescence intensity with the SD of each concentration between the assays. The variability was between 15-316%, with an average of 90%. In comparison, a similar immunoassay carried out with the Luminex system produced an intra- and inter-assay CV of ~10%.[219] The cause of this relatively large intra- and inter-assay CVs will be discussed in the following sections.

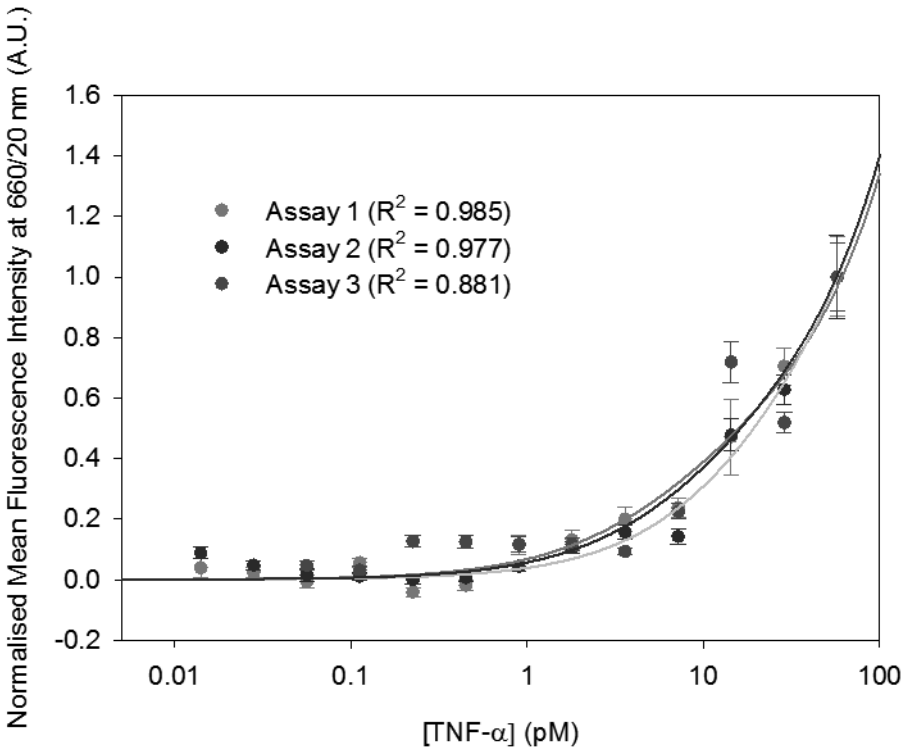

Figure 4.9. The titration of recombinant human TNF-α was repeated in triplicate.

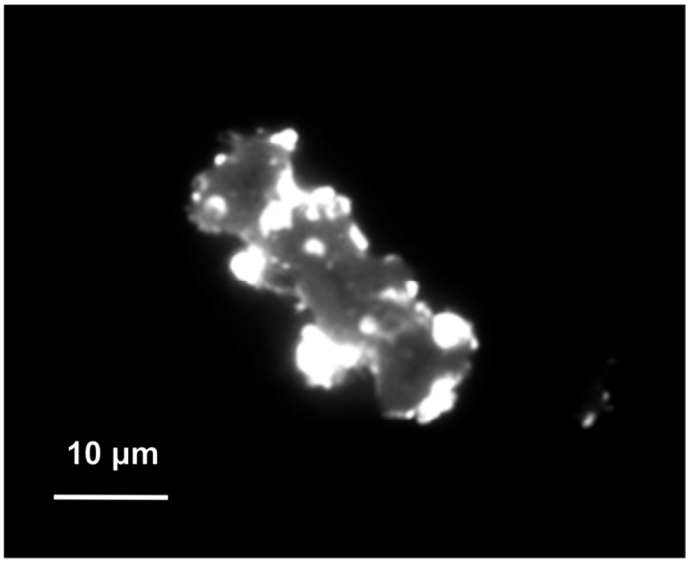

Figure 4.10. A fluorescence micrograph showing an encoded SU-8 microparticles from the immunoassay with highly fluorescent protein aggregates on the surface.

4.2.5 Optimisation

4.2.5a Reducing protein precipitates

As discussed above, the suspension sandwich immunoassay produced relatively large intra- and inter-assay variations. Figure 4.10 shows a fluorescence micrograph of a SU-8 microparticle from the sandwich immunoassay. The microparticle was contaminated with highly fluorescent protein precipitates which saturated the detector (maximum pixel value 4016 A.U.). During image analysis, the edge of each microparticle was identified and the mean value of the grey-scale pixels within this barrier was reported as the fluorescence intensity. The highly fluorescent protein precipitates affected the image quality and, as a result, overestimated the fluorescence intensity.

This phenomenon was not observed with the IgG immunoassay described in Chapter 3, in which the fluorescently labelled IgG was directly bound to the antigen-coated SU-8 microparticle. The precipitates found in the sandwich immunoassay had probably arisen from an undesired cross-linking reaction of the multivalent streptavidin with the residual biotinylated detection antibody in the reaction mixture. In order to produce a cleaner surface, the washing steps were optimised. To this end, the use of spin-columns for efficient washing was assessed.

The SU-8 particles were agitated in the test sample in this column. After each incubation step, the column was centrifuged at low speed (<1000 *g*) so that the majority of the solution was isolated from the particles. Figure 4.11 shows the relative number of particles contaminated with the highly fluorescent protein precipitates. From this result, it is clear that the use of spin-columns was advantageous in preventing the formation of fluorescent protein aggregates on the particles' surfaces. The number of contaminated particles was greatly reduced from ~70% to <10%.

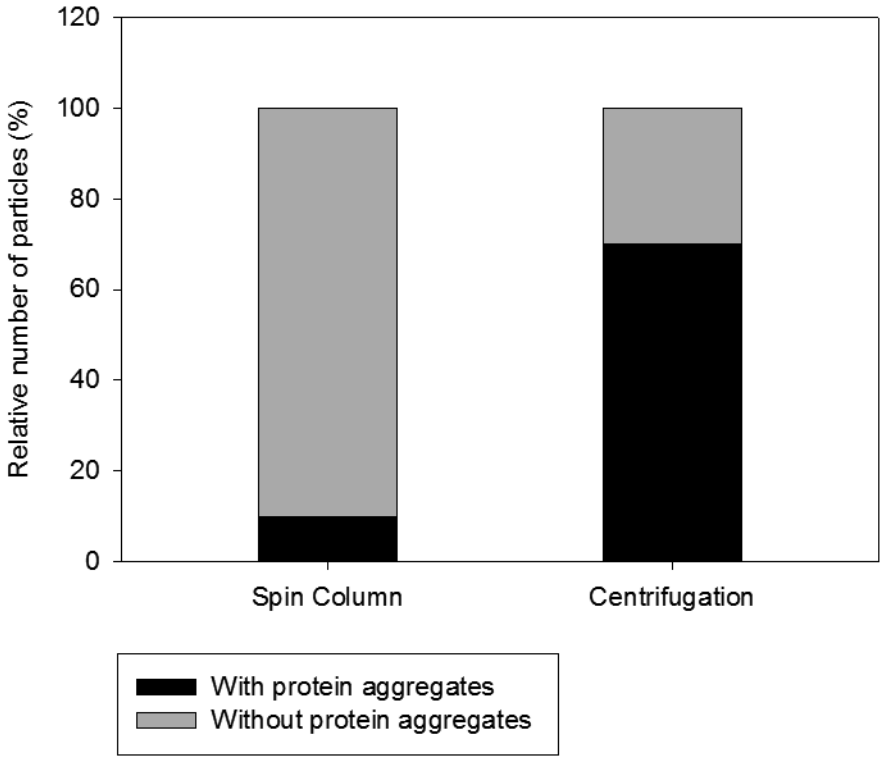

Figure 4.11. A histogram showing the relative number of particles contaminated by highly fluorescent protein aggregates when different washing strategies were used.

4.2.5b Data quality: Jeffamine vs. PEG_{3000}

Apart from improving the washing procedure, the quality of the particles' surfaces was also taken into consideration. In Chapter 2, the use of various spacers for attaching antibodies, and their effect on non-specific binding was described. Jeffamine was found to produce high level of non-specific protein binding. The use of a poly(ethylene)glycol (PEG_{3000}) as a spacer was found to be an effective alternative, in which the amount of non-specific binding was decreased.

The PEGylated SU-8 microparticles were used in a suspension sandwich immunoassay, in which human TNF-α solutions at concentrations between 49 fM and 319 pM were assayed. Figure 4.12 illustrates the standard binding curve for this experiment. The data points were fitted to Equation 4.1 with high confidence ($R^2 = 0.979$). The standard errors

of the data points were reduced when compared to the previous titrations (Intra-assay CV was determined to be 8-20%, mean 12%). The linearity of the standard curve at low target concentration (<12 pM) was greatly improved (R^2 = 0.997). The sensitivity of the assay platform was also improved with a LDL of 130 fM (*c.f.* 3.83 pM from Jeffamine-SU-8 particles and 57.5 fM from commercial ELISA).

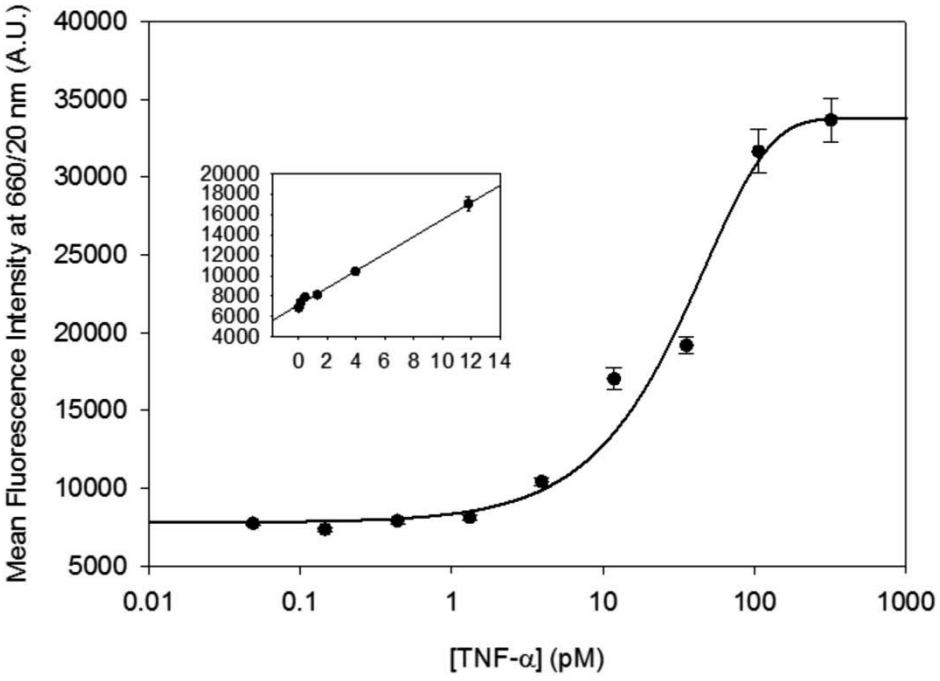

Figure 4.12. The sensitivity and data quality for the quantification of recombinant human TNF-α were greatly improved on PEGylated-SU-8 particles.

4.2.6 Multiplexed assay format

The next goal was to demonstrate a multiplexed immunoassay for the simultaneous quantification of human IL-6 and TNF-α from a single sample. In this experiment, a mixture of the antibody-coated SU-8 particles was suspended in a solution of a mixture of TNF-α and IL-6 at various concentrations (Table 4.4). After removing the excess antigens and washing the particles with assay buffer, a mixture of the detection antibodies was added. Finally, the particles were reacted with Cy5-streptavidin after washing.

Table 4.4. The concentrations of human TNF-α and human –IL-6 in each sample.

Sample number	[TNF-α] (pM)	[IL-6] (pM)
1	287.4	0
2	95.8	0.0364
3	31.9	0.109
4	10.6	0.328
5	3.55	0.984
6	1.18	2.95
7	0.394	8.86
8	0.131	26.6
9	0.0438	79.7
10	0	239.2

Figure 4.13 shows the mean fluorescence intensity of the two sets of particles as a function of sample number. The two sets of SU-8 microparticles responded accordingly to the target analyte concentration, in which the fluorescence intensity increased in opposite direction. The graph shown in Figure 4.13 was transformed into the standard binding curves (Figure 4.14). Both sets of data point were fitted into the 5-parameter equation (Equation 4.1) with high confidence (R^2: TNF-α = 0.978; IL-6 = 0.960). Human IL-6 and human TNF-α showed linearity between to at least 12 pM. The LDL was determined to be 1.47 pM and 379 fM for human IL-6 and human TNF-α respectively. The multiplexed immunoassay was found to be less sensitive when compared with the monoplexed counterpart assays (*c.f.* monoplex TNF-α: 130 fM). One potential possibility was that the reagents (e.g. capture antibodies, analytes, detection antibodies and Cy5-streptavidin) had detectable cross-reactivity and therefore reduced the overall sensitivity when both targets were being detected and quantified.

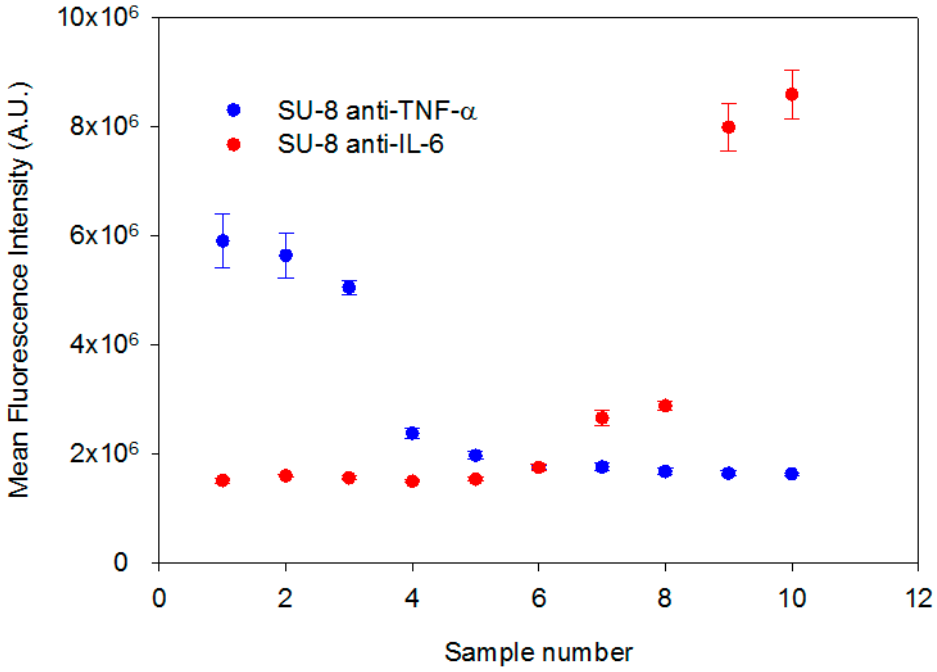

Figure 4.13. The fluorescence intensity of the SU-8 microparticle population as a function of sample number.

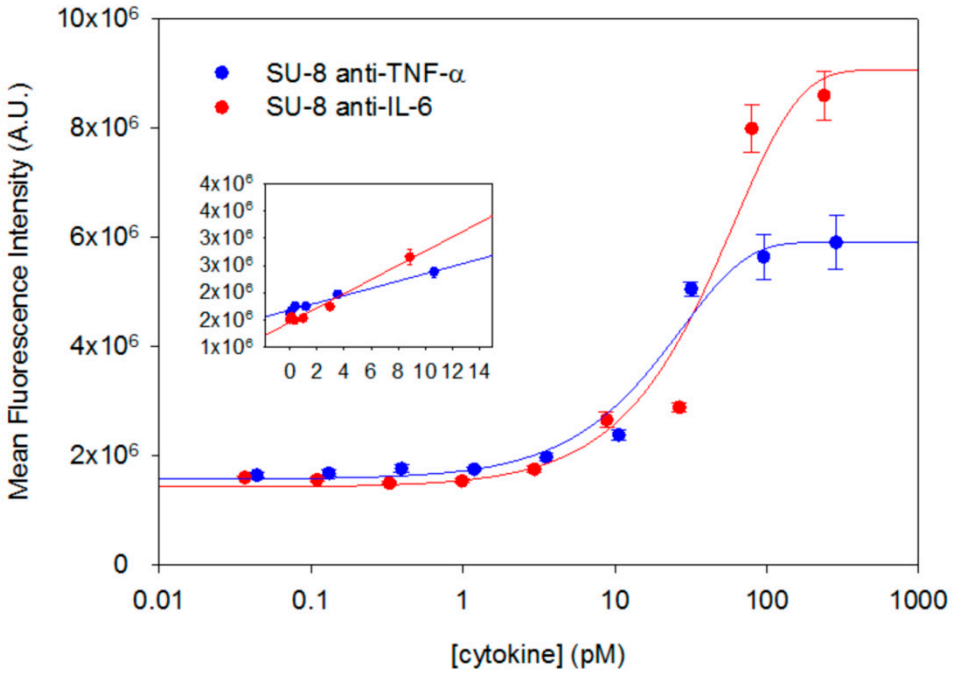

Figure 4.14. Titration curves of recombinant human TNF-α and human IL-6 of the multiplexed suspension immunoassay.

4.3 Conclusion

In this chapter a particle-based suspension sandwich immunoassay on encoded SU-8 microparticles was demonstrated. The use of fluorescence flow cytometry was found to be inadequate for particle recognition and assay readout. Due to the anisotropic shape of the encoded particles, the flow cytometer produced a large error in both forward-scattering and fluorescence measurements. This resulted in apparent poor assay sensitivity. In addition, the flow cytometer could not be used for particle decoding. As an alternative, fluorescence microscopy was tested for assay quantification. Particle decoding was archived by optical detection from the bright-field micrograph. Fluorescence intensity was quantified from the grey-scale 24-bit fluorescence images. With this system, the sensitivity of the detection of TNF-α was determined to be 1.45 pM. The immunoassay was further optimised, including the use of spin-columns for efficient washings. With this improvement, the amount of protein precipitates found of the particles' surfaces was greatly reduced. In addition, the use of PEG_{3000} as a spacer between the solid support and the capture antibody further reduced undesired non-specific binding. The sensitivity of the TNF-α detection was improved with a LDL of 130 fM. Finally, a multiplex immunoassay for the co-detection of TNF-α and IL-6 was demonstrated on this system. The standard curves were comparable to the monoplexed counterpart assays with a LDL of 379 fM and 1.47 pM for TNF-α and IL-6 respectively.

Chapter 5 Conclusion

SU-8 was found to be a suitable material for the microfabrication of diffractive microparticles by conventional photolithography. A number of functional groups were incorporated onto the particles' surface to enable the attachment of different biomolecules for various biological assays.

5.1 Surface modification of SU-8 microparticles

Several colorimetric-based analytical tests were developed for monitoring different chemical reactions on the polymeric SU-8 microparticles. These tests were found to be suitable to detect a variety of functional groups (e.g. –OH and $–NH_2$) or proteins on the particle's surface. With the aid of these analytical techniques, amino-, azido-, carboxyl- and hydroxyl-functionalised SU-8 microparticles were prepared from different types of surface modification chemistry.

Non-specific binding of proteins to the SU-8 particles was reduced by inserting PEG_{3000} or star-shaped PEG_{12000} between the surface and the biomolecules ("grafting to" method). An alternative method was to synthesise the non-fouling polymer directly from the surface by radical polymerisation ("grating from" method). However, the reaction conditions tested were found to be not suitable and required further optimisation.

5.2 Proof-of-principle multiplexed immunoassays

SU-8 microparticles bearing micrometre-sized diffractive elements were functionalised with IgGs to demonstrate multiplexed immunoassays. In a preliminary study, a

multiplexed immunoassay was developed to simultaneously detect Cy3-anti-human and Cy5-anti-rabbit antibodies. The multiplexed immunoassay showed high specificity and low cross-reactivity. Decoding of SU-8 microparticles was demonstrated using an in-house analytical system with high accuracy (>98%). A comparative thermodynamic study showed that the IgG:anti-IgG interaction on the encoded particles resembled solution-like behaviour (K_d solution: 14 ± 9 nM; K_d on SU-8: 9 ± 3 nM). From these results, a theoretical Lowest Detection Limit (LDL) of 5.8 nM on SU-8 particles was estimated. An experimental validation using 5.35 nM of Cy5-anti human confirmed this estimation.

5.3 Simultaneous quantification of human cytokines

A particle-based suspension sandwich immunoassay on encoded SU-8 microparticles was demonstrated. In this assay, human TNF-α and IL-6 were being detected and quantified simultaneously from a single sample. The use of fluorescence flow cytometry was found to be inadequate for code recognition and assay readout. As an alternative, fluorescence microscopy was employed for assay quantification. The use of spin-columns for washing the microparticles between the incubation steps was found to be necessary to prevent undesired protein precipitation, which greatly affected the quality of the data. To further reduce non-specific binding on the particles' surfaces, a PEG_{3000} spacer was inserted between the microparticle and the capture antibody. With these improvements, the sensitivity of TNF-α detection with a LDL of 130 fM was achieved. Finally, a multiplex immunoassay for the co-detection of TNF-α and IL-6 was demonstrated on this system. The standard curves were comparable to the monoplexed counterpart assays with a LDL of 379 fM and 1.47 pM for TNF-α and IL-6 respectively.

5.4 Future Work

Throughout the studies described herein, the time needed for code reading and signal analysis were limiting the assay throughput. Although an in-house optical system was developed for code recognition and fluorescence measurement, each particle still required no less than 1 minute for decoding and fluorescence measurement. With the aid of advanced optical hardware, a reading chamber and image recognition algorithm, the analysis time could be greatly reduced. Together with an integrated microfluidic system, libraries of molecules (e.g. peptides and oligonucleotides) could be directly synthesised from the encoded particles in an automated manner by pre-programmed combinatorial chemistry. The immobilised molecules could then be used for multiplexed biological assays, such as drug screening, diagnostic tests and genome sequencing in a high-throughput manner.

Chapter 6 Experimental methods

6.1 Materials

6.1.1 Reagents

SU-8 microparticles were provided by S. Banu (University of Southampton). Glycidyl methacrylate (GMA) beads (5.6 μm diameter) were purchased from Bangs Laboratories (IN, U.S.A.). MF-319 developer solution (contains tetramethylammonium hydroxide, 2.2% w/v in water) was obtained from Chestech Ltd. (Ruby, U.K.).

Boc-NH-PEG_{3000}-NH_2 was purchased from Iris Biotech (Marktredwitz, Germany). Ethylenediamine, Jeffamine ED-900 and H_2N-PEG_{3000}-NH_2 were obtained from Sigma Aldrich (Dorset, U.K.). Isocyanate-functionalised starPEG (NCO-sPEG) was donated by T. Newman (University of Southampton) and M. Moeller (RWTH Aachen University). Rhodamine B, piperazine, trimethylaluminum, succinic anhydride, 4-pentynoic acid, (*N*-(3-Dimethylaminopropyl)-*N*'-ethylcarbodiimide hydrochloride) (EDC. HCl), *N*-hydroxysulfosuccinimide sodium salt (sulfo-NHS), triethylamine, *N,N*-diisopropylethylamine (DIPEA), Tween-20 and other reagents and solvents were obtained from Sigma-Aldrich (Dorset, U.K.), Acros (Leicestershire, U.K.), Alfa Aesar (Lancashire, U.K.) and Fisher Scientific (Leicestershire, U.K.).

Wang resin, DIC, HOBt, Fmoc-Gly-OH, Fmoc-L-Lys(Boc)-OH and Fmoc-L-Ala-OH were obtained from AGTC Bioproducts Ltd. (Hessle, U.K.). Fmoc-L-Lys(Dde)-OH was purchased from Novabiochem (Darmstadt, Germany). ETT activator (0.25 M 5-ethylthio-1*H*-tetrazole in MeCN), oxidiser (0.1 M I_2 in THF/pyridine/water 78:20:2), deblock mix (3% trichloroacetic acid in DCM), anhydrous MeCN, 5'-DMT-deoxynucleoside

phosphoramidite and DMT-hexaethyleneglycol-phosphoramidite were purchased from Link Technologies (Lanarkshire, U.K.).

Cy3-labelled goat anti-human IgG and Cy5-labelled goat anti-rabbit IgG were purchased from Abcam (Cambridge, U.K.). Polyclonal human IgG and polyclonal rabbit IgG were obtained from Sigma Aldrich (Dorset, U.K.). Recombinant protein A was purchased from Cambridge Bioscience (Cambridge, U.K.). Recombinant human TNF-α and human IL-6 were obtained from PeproTech (London, U.K.). Capture and detection antibodies for human TNF-α and human IL-6 were donated by SPI-Bio (now Bertin Pharma, Montigny-le-Bretonneux, France). Cy5-labelled streptavidin was purchased from Invitrogen (Paisley, U.K.).

EZ-Link Sulfo-NHS-LC-Biotin, EZ-Link Sulfo-NHS-Biotin, BCA protein assay kit, Biotin quantitation kit and Pierce Micro-Spin Columns were purchased from Pierce Biotechnology (now part of Thermo Fisher Scientific, Northumberland, U.K.). Kaiser test kit was obtained from Sigma-Aldrich (Dorset, U.K.).

The compositions of the buffers used throughout this thesis are shown in Appendix A.

6.1.2 Instruments

Mass spectrometry was acquired on Micromass Platform II (ES) or Micromass TofSpec2E (MALDI-TOF).

Fluorescence micrographs were acquired on a Zeiss Axiovert 200 fluorescence microscope with mercury vapour lamp illumination and FITC, Cy3 or Cy5 filter sets. Images were captured on a Hamamatsu ORCA-ER digital camera.

Fluorescence flow cytometry data were obtained from BD FACSAria (Becton Dickson, Oxford, U.K.) equipped with a 488 nm solid state and 633 HeNe lasers. FACSFlow sheath fluid was used and samples were delivered at a pressure of 70 psi through a 70 μm nozzle. Data acquisition and analysis were carried out with FACSDiVa software package.

6.2 General Methods

6.2.1 Preparation of carboxyl-functionalised GMA microparticles

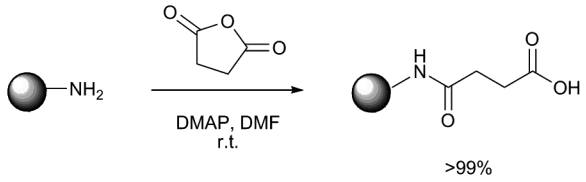

To a suspension of amino GMA beads (100 mg, 0.53 μmol based on amino groups, suspended in dry DMF, 100 μL), was added a solution of succinic anhydride (1 mg, 10 μmol), DMAP (0.1 mg, 0.82 μmol) and DIPEA (1.35 μL, 7.74 μmol) in dry DMF (1 mL). The reaction mixture was agitated at room temperature for 1 h. The reaction mixture was concentrated by centrifugation (12500 *g*, 1 min), the supernatant discarded and reaction repeated with fresh reagent for a further 1 h. The microparticles were then washed with DMF (1 mL × 4) followed by MeOH (1 mL × 4) before being dried *in vacuo* to afford carboxyl-functionalised GMA. The completeness of the reaction was monitored by ninhydrin test, which was negative on completion (absorbance < 0.01).

6.2.2 Release of SU-8 microparticles from aluminium-coated silicon wafer

Encoded SU-8 microparticles adhered to silicon wafers were released by sonication in MF-319 developer solution (5-10 mL/wafer) until the aluminium layer was completed dissolved (between 15 min and 3 h, depending on the size of the microparticles). The suspended SU-8 microparticles were collected by centrifugation (12500 *g*, 1 min) and then washed with MeCN (1 mL × 4).

6.2.3 Preparation of amino-functionalised SU-8 microparticles

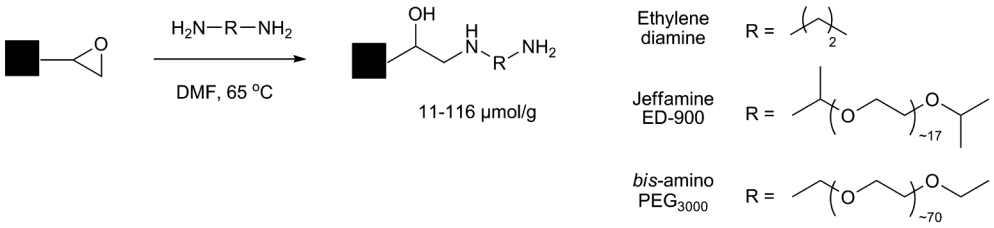

To a suspension of epoxy SU-8 microparticles (~ 10 mg, suspended in dry DMF, 500 μL), was added a solution of the *bis*-amino spacer (>2 μmol) in DMF (500 μL). The suspension was agitated at 50 °C for 16 h. The reaction mixture was concentrated by centrifugation (12500 *g*, 1 min) and the supernatant discarded. The microparticles were washed with DMF (1 mL × 4) and the supernatant separated by centrifugation (12500 *g*, 1 min) to afford amino-functionalised SU-8.

6.2.4 Preparation of carboxyl-functionalised SU-8 microparticles

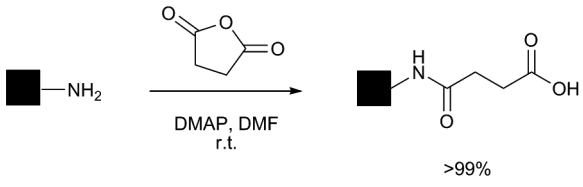

To a suspension of the amino-functionalised SU-8 (2 mg, 40-50 nmol based on amino groups, suspended in dry DMF, 100 μL), was added a solution of succinic anhydride (10 mg, 100 μmol), DMAP (1 mg, 8.18 μmol) and DIPEA (13.5 μL, 77.4 μmol) in dry DMF (1 mL). The suspension was agitated at room temperature for 1 h. The reaction mixture was concentrated by centrifugation (12500 *g*, 1 min), the supernatant discarded and the reaction repeated with fresh reagents for a further 1 h. The microparticles were washed with DMF (1

mL × 4), the supernatant separated by centrifugation (12500 *g*, 1 min), followed by washing with MeOH (1 mL × 4), and drying in vacuo to afford carboxyl-functionalised SU-8 (3). The reaction was monitored by the ninhydrin test, which was negative on completion. (absorbance < 0.01).

6.2.5 Preparation of hydroxyl-functionalised SU-8 microparticles

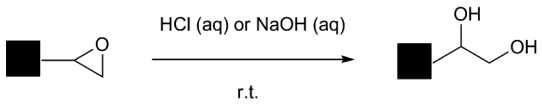

To a suspension of epoxy SU-8 microparticles (~10 mg, suspended in 0.1% (v/v) Tween-20 solution in water, 500 μL), was added a solution of 1 M HCl (aq.) or NaOH (aq.) (500 μL,). The suspension was agitated at room temperature for >16 h. The reaction mixture was concentrated by centrifugation (12500 *g*, 1 min) and the supernatant discarded. The microparticles were washed sequentially with 0.1% (v/v) Tween-20 solution (1 mL × 4), MeOH (1 mL × 4) and DMF (1 mL × 4) to afford hydroxyl-functionalised SU-8.

6.2.6 Preparation of DMT-protected SU-8 microparticles

To a suspension of hydroxyl SU-8 microparticles (~1 mg), was added a mixture of DMT- HEG phosphoramidite (or 5'-DMT-deoxynucleoside phosphoramidite, 1 μmol) and 5-ethylthio-1*H*-tetrazole (10 μmol) in anhydrous MeCN (1 mL). The microparticles were gentle agitated at room temperature for 1 h. After that, the microparticles were pelleted by centrifugation (12500 *g*, 1 min) and the supernatant was discarded. The microparticles were washed with anhydrous MeCN (1 mL × 4). Subsequently, a solution of 0.1 M I_2 in a

mixture of THF/pyridine/water (78:20:2) was added to the microparticles. The reaction mixture was gently agitated at room temperature for 20 min and then washed with anhydrous MeCN (1 mL × 4).

6.2.7 Immobilisation of proteins to carboxyl-functionalised particles *via* one-step EDC chemistry

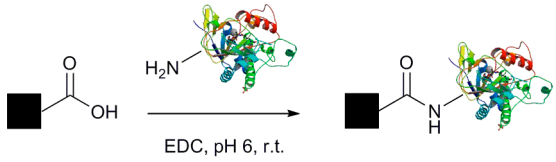

To carboxyl-functionalised microparticles (GMA: 10 mg; SU-8: 2 mg, 40-50 nmol based on carboxyl groups, suspended in 0.1 M MEST buffer, 600 μL), was added a solution of protein (>1.7 nmol) and EDC.HCl (9.3 mg, 48.5 μmol) in 0.1 M MEST buffer (400 μL). The reaction mixture was agitated at room temperature for 2 h. The microparticles were washed with PBST (1 mL × 4) and the supernatant separated by centrifugation (12500 *g*, 1 min) to afford protein-immobilised solid supports. The amount of immobilised protein was determined by BCA protein assay.

6.2.8 Immobilisation of proteins to carboxyl-functionalised particles *via* two-step EDC chemistry

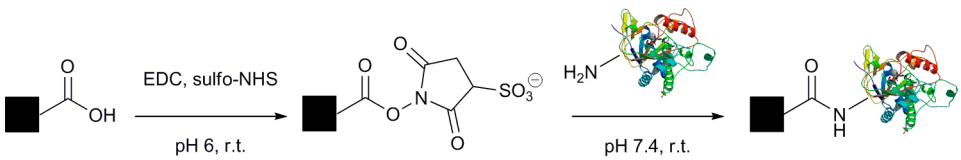

To carboxyl-functionalised microparticles (GMA: 10 mg; SU-8: 2 mg, 40-50 nmol based on carboxyl groups, suspended in 0.1 M MEST buffer, 600 μL), was added a solution of EDC.HCl (9.3 mg, 48.5 μmol) and sulfo-NHS (10.8 mg, 50 μmol) in 0.1 M MEST buffer (400 μL). The reaction mixture was agitated at room temperature for 30 min. The microparticles were washed with PBST (1 mL) and the supernatant separated by centrifugation (12500 *g*, 1 min). After that, a solution of the protein (>1.7 nmol) in PBST (400 μL) was added and the microparticles were agitated at room temperature for 2 h. The microparticles were washed with PBST (1 mL × 4) and the supernatant separated by centrifugation (12500 *g*, 1 min) to afford protein-immobilised solid supports. The amount of immobilised protein was determined by BCA protein assay.

6.2.9 Quantitative Kaiser test

A known amount of microparticles (GMA: ~5 mg; SU-8: ~0.5 mg) was washed with EtOH (1 mL × 4) before being heated in commercially available Kaiser test solution (Sigma-Aldrich, Poole, U.K., 300 μL total volume) at 120 °C for 5-10 min. After this the suspension was centrifuged (12500 *g*, 1 min) and the supernatant was isolated. To ensure all the chromophore molecules were recovered, the particles were washed with EtOH (50 μL × 2) and the wash through was collected. The absorbance of the combined supernatant was measured at 570 nm using a microplate reader (Safire^2, Tecan, Switzerland).

6.2.10 DMT quantification

To DMT-protected hydroxyl-SU-8 microparticles (~1 mg), was added a solution of 3% TCA in DCM. The suspension was agitated at room temperature for 15-30 min. After which, the orange DMT cation released by the acidic treatment was isolated by centrifugation (12500 *g*) and then measured spectroscopically at 498 nm (ε = 71700 M^{-1} cm^{-1}).

6.2.11 Fmoc quantification

To Fmoc-protected solid supports (Wang resin: 1 mg; GMA: 10 mg; SU-8 10 mg), was added 20% (v/v) piperidine in DMF. The reaction mixture was agitated at room temperature for 30 min. After that, the released dibenzofulvene-piperidine adduct was isolated by centrifugation (12500 *g*) and then measured by UV/Vis spectroscopy at 290 nm (ε = 7800 M^{-1} cm^{-1}).

6.2.12 BCA protein assay

To protein immobilised solid-supports (GMA: 2 mg; SU-8: 0.5 mg), suspended in storage buffer (50 μL, 10 mM NaH_2PO4, 150 mM NaCl, 0.1% Tween 20, pH 7.8), was added working reagent (200 μL, 98% v/v BCA™ Reagent A, 2% v/v BCA™ Reagent B). The reaction was carried out at 60 °C for 30 min and then allowed to cool to room temperature. The microparticles were removed by centrifugation (15000 *g*, 1 min) and the absorbance of the supernatant was measured at 562 nm. Protein solutions with known concentration were used as standards.

6.3 Methods for Chapter 2

6.3.1 Rhodamine B 4-(3-Carboxypropionyl)piperazine amide

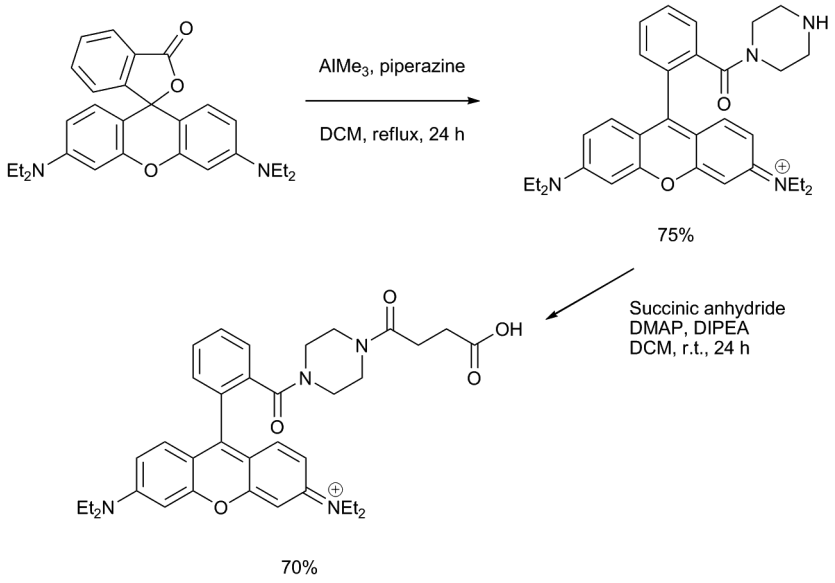

Rhodamine B 4-(3-Carboxypropionyl)piperazine amide (rhodamine-piperazine-carboxylic acid) was kindly supplied by Rachael Robbins (School of Chemistry, University of Southampton) according to the method of Nguyen *et al.*[220]

6.3.2 Peptide synthesis

The hexapeptide was constructed using standard Fmoc solid phase peptide synthesis protocol, using a sintered glass bubbler device. Deprotection of Fmoc-Gly-Wang resin (0.5 g, 0.5 mmol/g) was accomplished using 20% (v/v) piperidine in DMF at room temperature for 30 min, followed by washing with DMF (5 × 10 mL). The completion of the deprotection reaction was monitored by quantitative Fmoc analysis. To a solution of Fmoc-Lys(Dde)-OH (5 mol eq.) dissolved in minimum amount of DMF, was added DIC (5 mol eq.) and HOBt (5 eq.). The resultant reaction mixture was stirred at room temperature for 10 min before being transferred to the deprotected resin and then manually agitated for 1 h. The completion of the coupling was monitored by qualitative Kaiser test. The removal

of Dde group was achieved using a mixture of hydroxylamine hydrochloride and imidazole in NMP:DMF (5 mL, 1:1) at room temperature for 2 h. 4-Pentynoic acid (5 mol eq.) was coupled to the lysine side-chain in the presence of DIC (5 mol eq.) and HOBt (5 mol eq.) in minimum amount of DMF. Fmoc-L-Ala-OH, Fmoc-L-Lys-OH, Fmoc-Ala-OH, Fmoc-L-Lys-OH, *N*-Fmoc-8-aminooctanoic acid and Rhodamine-piperazine-carboxylic acid were sequentially conjugated to the resin using the DIC/HOBt coupling and Fmoc deprotection steps as described above. The peptide was cleaved from the resin by stirring in a mixture of TFA/anisole/water (10 mL, 95:2.5:2.5) at room temperature for 30 min. The mixture was filtered and the filtrate was concentrated by evaporation in vacuo. The crude peptide was dissolved in water (5 mL) and purified by reverse phase HPLC. MALDI-TOF MS m/z: found (M^+) 1415.9, expected (M^+) 1415.8 (see Appendix C for details).

6.3.3 Preparation of trifyl-azide

The preparation of trifyl-azide was according to the method of Cavender *et al.*,[131] and the product was used for the next step without further purification.

6.3.4 Preparation of azido-functionalised SU-8 microparticles

To a suspension of amino-functionalised solid support (GMA: 10 mg; SU-8: 1 mg, suspended in Tris-HCl buffer, 400 μL), was added either a solution imidazole-1-sulfonyl azide (1.73 mg, 10 μmol) in water (100 μL) or freshly prepared TfN_3 (~10 μmol) in DCM (100 μL), in the presence of $CuSO_4$ (cat) or $ZnSO_4$ (cat). The suspension was agitated at room temperature for 16 h. After that, the microparticles were washed with Tris-HCl buffer (1 mL × 4).

6.3.5 Attachment of peptide to solid support by Click chemistry

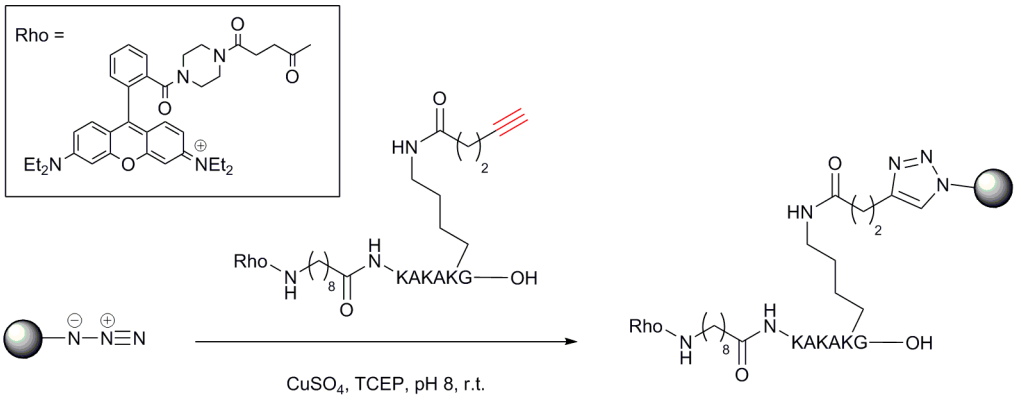

To a suspension of azido-functionalised solid support in Tris-HCl buffer (100 mM Tris-HCl, 150 mM NaCl, pH 8, 100 μL), was added a mixture of the alkyne-functionalised peptide (10 nmol), $CuSO_4$ (1 nmol) and TCEP (5 nmol). The suspension was agitated in the dark at room temperature for 20 h. After that, the microparticles were washed with Tris-HCl buffer (1 mL × 4) and then analysed by fluorescence flow cytometry.

6.3.6 Preparation of NH_2-PEGA

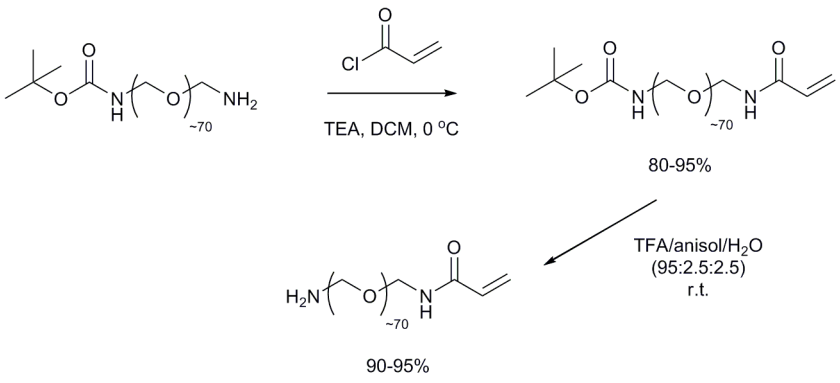

PEGA monomer was synthesised using a method developed by Won.[154] To prepare the heterobifunctional PEG, acryloyl chloride (1 μL, 12.2 μmol) was reacted with the terminal amino group of t-Boc-PEG_{3500}-NH_2 (2 mg, 571 nmol) in the present of TEA (1 μL, 7.17 μmol) in anhydrous DCM (5 mL) at 0 °C for 12-18 h. The reaction was monitored by the disappearance of amino group by a combination of TLC and Kaiser test. The acryloyl product was isolated by cold ether precipitation method with a yield of 80-95%. Boc deprotection was achieved by reacting the protected monomer with a solution of TFA/anisole/water (5 mL, 95:2.5:2.5) at room temperature for 1 h. After solvent evaporation, the deprotected product was precipitated in cold ether and then dried *in vacuo* overnight to give the product in 90-95% yield.

6.3.7 Solution-phase polymerisation of PEGA

To a solution of the PEGA monomer (100 nmol) in water (500 μL), was added a solution of APS (0.003-30 mol%) in water. The reaction mixture was allowed to stand at room temperature for 5-30 min. The polymerisation of PEGA was indicated by the gel formation.

6.3.8 Grafting of PEGA on SU-8 microparticles

The PEGA monomer was conjugated to the particle surface as described in section 6.2.3. After this step, the particles were washed thoroughly with water and the suspension degassed with N_2. A solution of APS (3 mol% to typical amine loading level) in water was added to the particles to activate the PEGA monomer on the surface. After 1 min of agitation at room temperature, a solution of PEGA monomer (500 μL, 300 μM) was added and the polymerisation was allowed to proceed at room temperature for 18 h. After that

the particles were washed thoroughly with water and MeOH. The polymerisation reaction was monitored by the Kaiser test.

6.3.9 Non-specific binding study by protein adsorption

To the functionalised SU-8 microparticles (~5000 particles), was added a solution of Cy5-labelled Streptavidin in PBST (862 nM, 30 μL). The suspension was agitation in the dark at room temperature for 30 min. After that, the microparticles were washed with PBST (500 μL × 4) and then analysed by fluorescence microscopy (5 s exposure time and gain set to 200). The fluorescence intensity of the particles were analysed by an open-source software package (ImageJ 1.41o, National Institute of Health, U.S.A.).

6.4 Methods for Chapter 3

6.4.1 Immobilisation of IgGs to protein A-coated solid supports

To protein A coated solid support (GMA: 0.3 mg, bearing 28.5 pmol of immobilised protein A; SU-8: 1 mg, 284-575 pmol of immobilised protein A), suspended in storage buffer (10 μL), was added a solution of human or rabbit IgG (~350 pmol) in storage buffer (180 μL). The reaction mixture was allowed to stand at room temperature for 1 h with periodic gentle manual mixing. The microparticles were washed with storage buffer (1 mL × 4), the supernatant separated by centrifugation (12500 *g*, 1 min) and resuspended in the same buffer (200 μL), to provide IgG functionalised microparticles.

6.4.2 Cross-reactivity study on GMA beads

A solution of Cy3-labelled anti-human IgG (2 μL, 13.3 pmol) or Cy5-labelled anti-rabbit IgG (2 μL, 13.3 pmol) was added to GMA beads functionalised with carboxylic acid, protein A, human IgG or rabbit IgG (0.3 mg). The reaction mixture was agitated in the dark at room temperature for 1 h. After that, the beads were washed with PBST (1 mL × 4), the supernatant separated by centrifugation (12500 *g*, 1 min), and resuspended in the same buffer (200 μL). The fluorescence intensity of the beads was analysed by fluorescence flow cytometry.

6.4.3 Multiplexed IgG detection on GMA beads

A solution of Cy3-labelled anti-human IgG (2 μL, 13.3 pmol) and Cy5-labelled anti-rabbit IgG (2 μL, 13.3 pmol) in storage buffer (46 μL) was added to a mixture of human

IgG and rabbit IgG conjugated GMA (0.3 mg each) at room temperature for 1 h with gentle mixing. The microspheres were washed with buffer B (1 mL × 4), the supernatant separated by centrifugation (12500 *g*, 1 min), and resuspended in the same buffer (200 μL). The fluorescence intensity of the sample was analysed by fluorescence flow cytometry.

6.4.4 Multiplexed IgG detection on SU-8 microparticles

A solution of Cy3-labelled anti-human IgG (2 μL,13.3 pmol) and Cy5-labelled anti-rabbit IgG (2 μL,13.3 pmol) in storage buffer (46 μL) was added to a mixture of human IgG and rabbit IgG conjugated SU-8 (1 mg each) at room temperature for 1 h with gentle mixing. The microparticles were washed with buffer B (1 mL × 4), the supernatant separated by centrifugation (12500 *g*, 1 min), and the particles resuspended in the same buffer (200 μL). The fluorescence intensity of the sample was analysed by fluorescent-activated cytometry.

6.4.5 Assay readout by fluorescence flow cytometry

Flow cytometric analyses and sorting were carried with BD FACSAria. Each particle was excited at 488 nm and 633 nm, and resulting emissions were acquired and analysed using BD FACSDiVa software. If required, desired particle populations were sorted on to glass microscope slides.

6.4.6 Decoding of SU-8 microparticles

A glass microscope slide containing the encoded SU-8 microparticles was analysed using the in-house decoding system (developed by G. S. Galitonov, University of

Southampton). A green laser beam (532 nm) was used to target a single microparticle and the resulting diffraction pattern was captured and analysed using the in-house decoding software package.

6.4.7 Thermodynamic study by fluorescence polarisation

To a solution of Cy5-labeled goat anti-human IgG (0.67 nM) in buffer (10 mM NaH2PO4, 150 mM NaCl, 0.01% NaN3, pH 7.8) was added human-IgG (final concentration 0-666 nM), and the reaction mixture was incubated at room temperature in the dark for 16 h. The fluorescence polarization of each of the samples was recorded using a microplate reader (Safire^2, Tecan, Switzerland, λ_{ex} = 635 nm, λ_{em} = 666 nm).

6.4.8 Thermodynamic study on SU-8 particles

Human IgG-coated SU-8 microparticles (1 mg), suspended in storage buffer (10 mM NaH2PO4, 150 mM NaCl, 0.1% Tween-20, pH 7.8, 100 μL, giving a 0.75 μM concentration of immobilized human IgG) were incubated with Cy5-labeled detector antibody (3 pM) at room temperature for 15-30 min. An aliquot of the sample (5 μL) was withdrawn, immediately washed with PBS (200 μL), and stored at 4 °C in the dark. The microparticles were separated from the reaction mixture by centrifugation (12500 *g*, 1 min), and an aliquot of the supernatant (5 μL) was removed. A further aliquot of Cy5-labelled anti-IgG was added, and the above procedures were repeated. The fluorescence intensity of the samples was measured by fluorescence-activated cytometry.

Table 6.1. Concentration of the Cy5-anti-human antibody stock solutions.

Final [Cy5-antibody] (nM)	Stock [Cy5-antibody] (nM)	Final reaction volume (μL)
0.003	0.067	100
0.037	0.640	95
0.369	6.067	90
3.69	57.3	85
10.2	113	80
17.1	163	75
24.0	207	70
31.0	243	65
51.4	433	60
103	800	55
173	1133	50
244	1400	45
317	1600	40
440	2083	35
625	2500	30
817	2750	25
1021	2833	20
1250	2750	15
1705	2833	10

6.4.9 Kinetic measurement

Human IgG immobilised SU-8 (1 mg), suspended in storage buffer (99 μL), were incubated with Cy5-labelled detector antibody (1 μL, 6.67 pmol) at room temperature. After fixed time intervals, samples (5 μL) were withdrawn, immediately washed with storage buffer (200 μL) and stored at 4 °C in the dark. The fluorescence intensity of the samples was measured by fluorescent-activated cytometry (section 3.1.4).

6.4.10 Immunoassay close to the theoretical detection limit

To human or rabbit IgG-coated SU-8 particles (~20 particles each) was added Cy5-anti-rabbit IgG (5.35 fmol, 1 μL). The particles were gently agitated at room temperature in the dark for >16 h and then washed with PBST buffer (PBS + 0.02% Tween-20, pH 7.4, 100 μL). Fluorescence images of the particles were taken using a fluorescence microscope. The fluorescence intensity of the images were analysed using an in-house software package.

6.5 Methods for Chapter 4

6.5.1 Biotinylation of IgG

To a solution of the detection antibody in PBS (1 mL, 13.3 μM) was added a solution of the biotin derivative in water (27 μL, 10 mM). The reaction mixture was allowed to stand at room temperature for 30 min. After that, the conjugated antibody was purified from the reaction mixture by gel chromatography (Sephadex G-25 resin).

6.5.2 HABA assay

The quantification of biotinylation level was carried out according to the manufacturer's protocol.[221]

6.5.3 Sandwich immunoassay

To the capture antibody-coated SU-8 particles (anti-human TNF-α or anti-human IL-6, 10 μg, ~5000 particles), was added a solution of the target antigen (human TNF-α or IL-6) in PBST (30 μL) at various concentration. The particles were gently agitated at room temperature for >2 h and then washed with PBST (500 μL × 3). Washing was achieved by resuspending the microparticles in fresh PBST (500 μL). The resulting supernatant was isolated either by pipetting or centrifugation with a spin-column (<1000 *g*, 1 min). After that, a solution of the biotinylated detection anybody in PBST (anti-human TNF-α or anti-human IL-6, 330 nM, 30 μL) was added and the microparticles resuspended at room temperature for 1 h. After washing the microparticles with PBST (500 μL × 3), a solution of Cy5-labelled streptavidin in PBST (30 μL, 862 nM) was added. The particles were resuspended in this solution in the dark at room temperature for 30 min. Finally, the

microparticles were washed with PBST (500 μL × 3), and then analysed by fluorescence flow cytometry or fluorescence microscopy.

6.5.4 Multiplexed sandwich immunoassay

Equivalent amounts of each set of antibody-coated SU-8 particles (anti-human TNF-α or anti-human IL-6, ~200 μg) in PBST (200 μL) were mixed thoroughly. To a suspension of these particles (10 μg, ~5000 particles) was added a mixture of human cytokines (TNF-α and IL-6, 30 μL, 1-2000 pg/mL each) in PBST. The reaction mixture was agitated at room temperature for 2 h. The particles were separated from the reaction mixture by centrifugation (12500 *g*, 1 min) and then resuspended in a solution of biotinylated detection antibodies (anti-TNF-α and anti-IL-6, 30 μL, 50 μg/mL each). The reaction mixture was agitated at room temperature for 1 h and then the particles separated. A solution of Cy5-streptavidin (30 μL, 860 nM) was added to the particles and the reaction mixture agitated at room temperature in the dark for 30 min. After the particles were washed with PBST (4 × 200 μL) fluorescence images were captured by fluorescence microscopy.

Chapter 7 References

(1) Renault, N. K.; Gaddipati, S. R.; Wulfert, F.; Falcone, F. H.; Mirotti, L.; Tighe, P. J.; Wright, V.; Alcocer, M. J. *J. Immunol. Methods* **2010**, *364*, 21.

(2) Hermle, J.; Anders, M.; Heuser, A. M.; Muller, B. *BMC Biotechnol.* **2010**, *10*, 32.

(3) Krishnan, S.; Mani, V.; Wasalathanthri, D.; Kumar, C. V.; Rusling, J. F. *Angew. Chem., Int. Ed.* **2011**, *50*, 1175.

(4) Douglas, P.; Kriek, M.; Bryant, P.; Roach, P. L. *Angew. Chem., Int. Ed.* **2006**, *45*, 5197.

(5) Wood, R. J.; McKelvie, J. C.; Maynard-Smith, M. D.; Roach, P. L. *Nucleic Acids Res.* **2010**, *38*, e107.

(6) Fiehn, O.; Garvey, W. T.; Newman, J. W.; Lok, K. H.; Hoppel, C. L.; Adams, S. H. *PLoS One* **2010**, *5*, e15234.

(7) Puneeth Kumar, A.; Nandini, C. D.; Salimath, P. V. *FEBS J.* **2011**, *278*, 143.

(8) Dale, S. E. *Mol. Diagn. Ther.* **2010**, *14*, 205.

(9) Evensen, L.; Link, W.; Lorens, J. B. *Curr. Pharm. Des.* **2010**, *16*, 3958.

(10) Bromage, E. S.; Lackie, T.; Unger, M. A.; Ye, J.; Kaattari, S. L. *Biosens. Bioelectron.* **2007**, *22*, 2532.

(11) Francois, P.; Pittet, D.; Bento, M.; Pepey, B.; Vaudaux, P.; Lew, D.; Schrenzel, J. *J. Clin. Microbiol.* **2003**, *41*, 254.

(12) Schwikowski, B.; Uetz, P.; Fields, S. *Nat. Biotechnol.* **2000**, *18*, 1257.

(13) Chan, L.; Cross, H. F.; She, J. K.; Cavalli, G.; Martins, H. F.; Neylon, C. *PLoS One* **2007**, *2*, e1164.

(14) Malinowsky, D.; Lundkvist, J.; Laye, S.; Bartfai, T. *FEBS Lett.* **1998**, *429*, 299.

(15) Engvall, E.; Perlmann, P. *Immunochemistry* **1971**, *8*, 871.

(16) Kriek, M.; Martins, F.; Leonardi, R.; Fairhurst, S. A.; Lowe, D. J.; Roach, P. L. *J. Biol. Chem.* **2007**, *282*, 17413.

(17) Lake, B. G.; Price, R. J.; Giddings, A. M.; Walters, D. G. *Methods Mol. Biol.* **2009**, *481*, 47.

(18) Zaninotto, M.; Plebani, M. *Clin. Chem. Lab. Med.* **2010**, *48*, 911.

(19) Brocklehurst, P.; Kujan, O.; Glenny, A. M.; Oliver, R.; Sloan, P.; Ogden, G.; Shepherd, S. *Cochrane Database Syst. Rev.* **2010**, *11*, CD004150.

(20) Hood, L.; Heath, J. R.; Phelps, M. E.; Lin, B. *Science* **2004**, *306*, 640.

(21) Weston, A. D.; Hood, L. *J. Proteome Res.* **2004**, *3*, 179.

(22) Lea, P.; Ling, M. *Curr. Opin. Mol. Ther.* **2008**, *10*, 251.

(23) Braeckmans, K.; De Smedt, S. C.; Leblans, M.; Pauwels, R.; Demeester, J. *Nat. Rev. Drug Discovery* **2002**, *1*, 447.

(24) Kricka, L. J.; Imai, K.; Fortina, P. *Clin. Chem.* **2010**, *56*, 1797.

(25) Higuchi, R.; Dollinger, G.; Walsh, P. S.; Griffith, R. *Bio/Technology* **1992**, *10*, 413.

(26) Swango, K. L.; Hudlow, W. R.; Timken, M. D.; Buoncristiani, M. R. *Forensic Sci. Int.* **2007**, *170*, 35.

(27) Ng, C. T.; Gilchrist, C. A.; Lane, A.; Roy, S.; Haque, R.; Houpt, E. R. *J. Clin. Microbiol.* **2005**, *43*, 1256.

(28) Zimmermann, T.; Rietdorf, J.; Pepperkok, R. *FEBS Lett.* **2003**, *546*, 87.

(29) Ueberfeld, J.; McKenna, B.; Rubin-Bejerano, I.; Verstrepen, K.; Ehrlich, D. J. *Anal. Chem.* **2008**, *80*, 7430.

(30) Wang, K.; Li, M.; Hakonarson, H. *Nat. Rev. Genet.* **2010**, *11*, 843.

(31) Maskos, U.; Southern, E. M. *Nucleic Acids Res.* **1992**, *20*, 1679.

(32) Khan, J.; Bittner, M. L.; Chen, Y.; Meltzer, P. S.; Trent, J. M. *Biochim. Biophys. Acta* **1999**, *1423*, M17.

(33) Ness, S. A. *Mol. Biotechnol.* **2007**, *36*, 205.

(34) Fu, Y.; Springer, N. M.; Ying, K.; Yeh, C. T.; Iniguez, A. L.; Richmond, T.; Wu, W.; Barbazuk, B.; Nettleton, D.; Jeddeloh, J.; Schnable, P. S. *PLoS One* **2010**, *5*, e14178.

(35) Lin, L.; Liu, S.; Brockway, H.; Seok, J.; Jiang, P.; Wong, W. H.; Xing, Y. *Nucleic Acids Res.* **2009**, *37*, e90.

(36) GeneChip® Technology. http://www.affymetrix.com/_media/images/about-affymetrix-3-large.jpg (accessed 23rd August 2011).

(37) Yu, X.; Schneiderhan-Marra, N.; Joos, T. O. *Clin. Chem.* **2010**, *56*, 376.

(38) Hartmann, M.; Roeraade, J.; Stoll, D.; Templin, M. F.; Joos, T. O. *Anal. Bioanal. Chem.* **2009**, *393*, 1407.

(39) MacBeath, G.; Schreiber, S. L. *Science* **2000**, *289*, 1760.

(40) Harris, J. L.; Winssinger, N. *Chem. Eur. J.* **2005**, *11*, 6792.

(41) Winssinger, N.; Damoiseaux, R.; Tully, D. C.; Geierstanger, B. H.; Burdick, K.; Harris, J. L. *Chem. Biol.* **2004**, *11*, 1351.

(42) Wei, C. W.; Cheng, J. Y.; Huang, C. T.; Yen, M. H.; Young, T. H. *Nucleic Acids Res.* **2005**, *33*, e78.

(43) Russo, G.; Zegar, C.; Giordano, A. *Oncogene* **2003**, *22*, 6497.

(44) Wilson, R.; Cossins, A. R.; Spiller, D. G. *Angew. Chem., Int. Ed.* **2006**, *45*, 6104.

(45) Birtwell, S.; Morgan, H. *Integr. Biol.* **2009**, *1*, 345.

(46) Cederquist, K. B.; Dean, S. L.; Keating, C. D. *Wiley Interdiscip. Rev. Nanomed. Nanobiotechnol.* **2010**, *2*, 578.

(47) Han, M.; Gao, X.; Su, J. Z.; Nie, S. *Nat. Biotechnol.* **2001**, *19*, 631.

(48) Fulton, R. J.; McDade, R. L.; Smith, P. L.; Kienker, L. J.; Kettman, J. R., Jr. *Clin. Chem.* **1997**, *43*, 1749.

(49) Technologies & Science - Luminex Corporation. http://www.luminexcorp.com/TechnologiesScience/index.htm (accessed 23rd August 2011).

(50) FLEXMAP 3D system multiplexes up to 500 assys in one sample - Luminex Corporation. http://www.luminexcorp.com/Products/Instruments/FLEXMAP3D/ (accessed 23rd August 2011).

(51) Smith, P. L.; WalkerPeach, C. R.; Fulton, R. J.; DuBois, D. B. *Clin. Chem.* **1998**, *44*, 2054.

(52) Gordon, R. F.; McDade, R. L. *Clin. Chem.* **1997**, *43*, 1799.

(53) Oliver, K. G.; Kettman, J. R.; Fulton, R. J. *Clin. Chem.* **1998**, *44*, 2057.

(54) Anderson, G. P.; Lamar, J. D.; Charles, P. T. *Environ. Sci. Technol.* **2007**, *41*, 2888.

(55) Oliphant, A.; Barker, D. L.; Stuelpnagel, J. R.; Chee, M. S. *BioTechniques* **2002**, *Suppl*, 56.

(56) Resch-Genger, U.; Grabolle, M.; Cavaliere-Jaricot, S.; Nitschke, R.; Nann, T. *Nat. Meth.* **2008**, *5*, 763.

(57) Rosenthal, S. J. *Nat. Biotechnol.* **2001**, *19*, 621.

(58) Murphy, C. J. *Anal. Chem.* **2002**, *74*, 520A.

(59) Green, M. *Angew. Chem. Int. Ed. Engl.* **2004**, *43*, 4129.

(60) Braeckmans, K.; De Smedt, S. C.; Roelant, C.; Leblans, M.; Pauwels, R.; Demeester, J. *Nat. Mater.* **2003**, *2*, 169.

(61) Derveaux, S.; De Geest, B. G.; Roelant, C.; Braeckmans, K.; Demeester, J.; De Smedt, S. C. *Langmuir* **2007**, *23*, 10272.

(62) Nicewarner-Pena, S. R.; Freeman, R. G.; Reiss, B. D.; He, L.; Pena, D. J.; Walton, I. D.; Cromer, R.; Keating, C. D.; Natan, M. J. *Science* **2001**, *294*, 137.

(63) Evans, M.; Sewter, C.; Hill, E. *Assay Drug Dev. Technol.* **2003**, *1*, 199.

(64) Smith, J.; Onley, D.; Garey, C.; Crowther, S.; Cahir, N.; Johanson, A.; Painter, S.; Harradence, G.; Davis, R.; Swarbrick, P. *Ann. N. Y. Acad. Sci.* **2005**, *1050*, 286.

(65) Pregibon, D. C.; Toner, M.; Doyle, P. S. *Science* **2007**, *315*, 1393.

(66) Lee, W.; Choi, D.; Kim, J. H.; Koh, W. G. *Biomedical Microdevices* **2008**, *10*, 813.

(67) Illumina - Veracode Technology. http://www.illumina.com/technology/veracode_technology.ilmn (accessed 23rd August 2011).

(68) Lin, C. H.; Yeakley, J. M.; McDaniel, T. K.; Shen, R. *Methods Mol. Biol.* **2009**, *496*, 129.

(69) Galitonov, G.; Birtwell, S.; Zheludev, N.; Morgan, H. *Opt. Express* **2006**, *14*, 1382.

(70) Birtwell, S. W.; Galitonov, G. S.; Morgan, H.; Zheludev, N. I. *Opt. Commun.* **2008**, *281*, 1789.

(71) Broder, G. R.; Ranasinghe, R. T.; She, J. K.; Banu, S.; Birtwell, S. W.; Cavalli, G.; Galitonov, G. S.; Holmes, D.; Martins, H. F.; Macdonald, K. F.; Neylon, C.; Zheludev, N.; Roach, P. L.; Morgan, H. *Anal. Chem.* **2008**, *80*, 1902.

(72) Schena, M.; Shalon, D.; Davis, R. W.; Brown, P. O. *Science* **1995**, *270*, 467.

(73) Nelson, J. M.; Griffin, E. G. *J. Am. Chem. Soc.* **1916**, *38*, 1109.

(74) Roach, P.; Farrar, D.; Perry, C. C. *J. Am. Chem. Soc.* **2005**, *127*, 8168.

(75) Cha, T.; Guo, A.; Zhu, X. Y. *Proteomics* **2005**, *5*, 416.

(76) Moirangthem, R. S.; Chang, Y.-C.; Hsu, S.-H.; Wei, P.-K. *Biosens. Bioelectron.* **2010**, *25*, 2633.

(77) Engel, M. F. M.; Visser, A. J. W. G.; van Mierlo, C. P. M. *Proc. Natl. Acad. Sci. U. S. A.* **2004**, *101*, 11316.

(78) Karlsson, M.; Ekeroth, J.; Elwing, H.; Carlsson, U. *J. Biol. Chem.* **2005**, *280*, 25558.

(79) Molin, S. O.; Nygren, H.; Dolonius, L. *J. Histochem. Cytochem.* **1978**, *26*, 412.

(80) Staros, J. V.; Wright, R. W.; Swingle, D. M. *Anal. Biochem.* **1986**, *156*, 220.

(81) Grabarek, Z.; Gergely, J. *Anal. Biochem.* **1990**, *185*, 131.

(82) Kumar, P.; Choithani, J.; Gupta, K. C. *Nucleic Acids Res.* **2004**, *32*, e80.

(83) Schena, M.; Shalon, D.; Davis, R. W.; Brown, P. O. *Science* **1995**, *270*, 467.

(84) Lockhart, D. J.; Winzeler, E. A. *Nature* **2000**, *405*, 827.

(85) Lueking, A.; Cahill, D. J.; Mullner, S. *Drug Discov. Today* **2005**, *10*, 789.

(86) Peramo, A.; Albritton, A.; Matthews, G. *Langmuir* **2006**, *22*, 3228.

(87) Fall, B. I.; Eberlein-Konig, B.; Behrendt, H.; Niessner, R.; Ring, J.; Weller, M. G. *Anal. Chem.* **2003**, *75*, 556.

(88) Halliwell, C. M.; Cass, A. E. G. *Anal. Chem.* **2001**, *73*, 2476.

(89) Nam, Y.; Branch, D. W.; Wheeler, B. C. *Biosens. Bioelectron.* **2006**, *22*, 589.

(90) Szunerits, S.; Das, M. R.; Boukherroub, R. *J. Phys. Chem. C* **2008**, *112*, 8239.

(91) Sui, G. D.; Wang, J. Y.; Lee, C. C.; Lu, W. X.; Lee, S. P.; Leyton, J. V.; Wu, A. M.; Tseng, H. R. *Anal. Chem.* **2006**, *78*, 5543.

(92) Waugh, D. S. *Trends Biotechnol.* **2005**, *23*, 316.

(93) Wegner, G. J.; Lee, N. J.; Marriott, G.; Corn, R. M. *Anal. Chem.* **2003**, *75*, 4740.

(94) Thess, A.; Hutschenreiter, S.; Hofmann, M.; Tampe, R.; Baumeister, W.; Guckenberger, R. *J. Biol. Chem.* **2002**, *277*, 36321.

(95) Hendrickson, W. A.; Pahler, A.; Smith, J. L.; Satow, Y.; Merritt, E. A.; Phizackerley, R. P. *Proc. Natl. Acad. Sci. U. S. A.* **1989**, *86*, 2190.

(96) Eakin, R. E.; Snell, E. E.; Williams, R. J. *J. Biol. Chem.* **1940**, *136*, 801.

(97) Cantor, C. R.; Sano, T.; Smith, C. L. In *Biomarkers and Occupational Health: Progress and Perspectives*; Mendelsohn, M. L., Peeters, J. P., Normandy, M. J., Eds.; John Henry Press: Washington, D.C., 1995, p 257 (ISBN:0-309-05187-8).

(98) Livnah, O.; Bayer, E. A.; Wilchek, M.; Sussman, J. L. *Proc. Natl. Acad. Sci. U. S. A.* **1993**, *90*, 5076.

(99) Hiller, Y.; M., G. J.; Bayer, E. A.; Wilchek, M. *Biochem. J.* **1987**, *248*, 167.

(100) Vermette, P.; Gengenbach, T.; Divisekera, U.; Kambouris, P. A.; Griesser, H. J.; Meagher, L. *J. Colloid Interface Sci.* **2003**, *259*, 13.

(101) Keefe, L. J.; Quirk, S.; Gittis, A.; Sondek, J.; Lattman, E. E. *Protein Sci.* **1994**, *3*, 391.

(102) Lorenz, H.; Despont, M.; Fahrni, N.; Brugger, J.; Vettiger, P.; Renaud, P. *Sens. Actuators, A* **1998**, *64*, 33.

(103) Shaw, J. M.; Gelorme, J. D.; LaBianca, N. C.; Conley, W. E.; Holmes, S. J. *Ibm Journal of Research and Development* **1997**, *41*, 81.

(104) Dellmann, L.; Roth, S.; Beuret, C.; Racine, G. A.; Lorenz, H.; Despont, M.; Renaud, P.; Vettiger, P.; de Rooij, N. F. *Sens. Actuators, A* **1998**, *70*, 42.

(105) Abgrall, P.; Conedera, V.; Camon, H.; Gue, A. M.; Nguyen, N. T. *Electrophoresis* **2007**, *28*, 4539.

(106) Chellis, L. N. Epoxy Composition. U.S. Patent 4,550,128, 1984.

(107) McGall, G.; Labadie, J.; Brock, P.; Wallraff, G.; Nguyen, T.; Hinsberg, W. *Proc. Natl. Acad. Sci. U. S. A.* **1996**, *93*, 13555.

(108) Banu, S.; Birtwell, S.; Galitonov, G.; Chen, Y. F.; Zheludev, N.; Morgan, H. *J. Micromech. Microeng.* **2007**, *17*, S116.

(109) Cavalli, G.; Banu, S.; Ranasinghe, R. T.; Broder, G. R.; Martins, H. F. P.; Neylon, C.; Morgan, H.; Bradley, M.; Roach, P. L. *J. Com. Chem.* **2007**, *9*, 462.

(110) These microparticles were donated by Biocartis S.A., Lausanne, Switzerland.

(111) Mcbride, L. J.; Caruthers, M. H. *Tetrahedron Lett.* **1983**, *24*, 245.

(112) Preininger, C.; Bodrossy, L.; Sauer, U.; Pichler, R.; Weilharter, A. *Anal. Biochem.* **2004**, *330*, 29.

(113) Marie, R.; Schmid, S.; Johansson, A.; Ejsing, L. E.; Nordstrom, M.; Hafliger, D.; Christensen, C. B. V.; Boisen, A.; Dufva, M. *Biosens. Bioelectron.* **2006**, *21*, 1327.

(114) Blagoi, G.; Keller, S.; Johansson, A.; Boisen, A.; Dufva, M. *Appl. Surf. Sci.* **2008**, *255*, 2896.

(115) Tao, S. L.; Popat, K. C.; Norman, J. J.; Desai, T. A. *Langmuir* **2008**, *24*, 2631.

(116) Kay, C.; Lorthioir, O. E.; Parr, N. J.; Congreve, M.; McKeown, S. C.; Scicinski, J. J.; Ley, S. V. *Biotechnol. Bioeng.* **2000**, *71*, 110.

(117) Pivonka, D. E.; Simpson, T. R. *Anal. Chem.* **1997**, *69*, 3851.

(118) Swali, V.; Bradley, M. *Anal. Commun.* **1997**, *34*, H15.

(119) Yan, B. *Curr. Opin. Chem. Biol.* **2002**, *6*, 328.

(120) Kay, C.; Lorthioir, O. E.; Parr, N. J.; Congreve, M.; McKeown, S. C.; Scicinski, J. J.; Ley, S. V. *Biotechnol. Bioeng.* **2000**, *71*, 110.

(121) Kaiser, E.; Colescot.Rl; Bossinge.Cd; Cook, P. I. *Anal. Biochem.* **1970**, *34*, 595.

(122) Sarin, V. K.; Kent, S. B. H.; Tam, J. P.; Merrifield, R. B. *Anal. Biochem.* **1981**, *117*, 147.

(123) Ovechko, V. S.; Dmytruk, A. M.; Fursenko, O. V.; Lepeshkina, T. P. *Vacuum* **2001**, *61*, 123.

(124) Langley, L. A.; Villanueva, D. E.; Fairbrother, D. H. *Chem. Mater.* **2006**, *18*, 169.

(125) Smith, P. K.; Krohn, R. I.; Hermanson, G. T.; Mallia, A. K.; Gartner, F. H.; Provenzano, M. D.; Fujimoto, E. K.; Goeke, N. M.; Olson, B. J.; Klenk, D. C. *Anal. Biochem.* **1985**, *150*, 76.

(126) Scriven, E. F. V.; Turnbull, K. *Chem. Rev.* **1988**, *88*, 297.

(127) Kolb, H. C.; Finn, M. G.; Sharpless, K. B. *Angew. Chem., Int. Ed.* **2001**, *40*, 2004.

(128) Tornoe, C. W.; Christensen, C.; Meldal, M. *J. Org. Chem.* **2002**, *67*, 3057.

(129) Alper, P. B.; Hendrix, M.; Sears, P.; Wong, C. H. *J. Am. Chem. Soc.* **1998**, *120*, 1965.

(130) Nyffeler, P. T.; Liang, C. H.; Koeller, K. M.; Wong, C. H. *J. Am. Chem. Soc.* **2002**, *124*, 10773.

(131) Cavender, C. J.; Shiner, V. J. *J. Org. Chem.* **1972**, *37*, 3567.

(132) Oyelere, A. K.; Chen, P. C.; Yao, L. P.; Boguslavsky, N. *J. Org. Chem.* **2006**, *71*, 9791.

(133) Ruff, J. K. *Inorg. Chem.* **1965**, *4*, 567.

(134) Goddard-Borger, E. D.; Stick, R. V. *Org. Lett.* **2007**, *9*, 3797.

(135) Sikanen, T.; Heikkila, L.; Tuornikoski, S.; Ketola, R. A.; Kostiainen, R.; Franssila, S.; Kotiaho, T. *Anal. Chem.* **2007**, *79*, 6255.

(136) Wang, Y. L.; Pai, J. H.; Lai, H. H.; Sims, C. E.; Bachman, M.; Li, G. P.; Allbritton, N. L. *J. Micromech. Microeng.* **2007**, *17*, 1371.

(137) Zhi, Z. L.; Morita, Y.; Hasan, Q.; Tamiya, E. *Anal. Chem.* **2003**, *75*, 4125.

(138) Maruyama, Y.; Terao, S.; Sawada, K. *Biosens. Bioelectron.* **2009**, *24*, 3108.

(139) Tugulu, S.; Arnold, A.; Sielaff, I.; Johnsson, K.; Klok, H. A. *Biomacromolecules* **2005**, *6*, 1602.

(140) Tugulu, S.; Harms, M.; Fricke, M.; Volkmer, D.; Klok, H. A. *Angew. Chem., Int. Ed.* **2006**, *45*, 7458.

(141) Carrara, S.; Shumyantseva, V. V.; Archakov, A. I.; Samori, B. *Biosens. Bioelectron.* **2008**, *24*, 148.

(142) Ma, H. W.; Hyun, J. H.; Stiller, P.; Chilkoti, A. *Adv. Mater.* **2004**, *16*, 338.

(143) Gotz, H.; Beginn, U.; Bartelink, C. F.; Grunbauer, H. J. M.; Moller, M. *Macromol. Mater. Eng.* **2002**, *287*, 223.

(144) Groll, J.; Fiedler, J.; Engelhard, E.; Ameringer, T.; Tugulu, S.; Klok, H. A.; Brenner, R. E.; Moeller, M. *J. Biomed. Mater. Res., Part A* **2005**, *74A*, 607.

(145) Klok, H. A.; Tugulu, S.; Arnold, A.; Sielaff, I.; Johnsson, K. *Abstr. Pap. Am. Chem. Soc.* **2005**, *230*, U4291.

(146) Klok, H. A.; Vandermeulen, G. W. M.; Rosler, A. *Abstr. Pap. Am. Chem. Soc.* **2002**, *224*, U482.

(147) Wang, J.; Gibson, M. I.; Barbey, R.; Xiao, S. J.; Klok, H. A. *Macromol. Rapid Commun.* **2009**, *30*, 845.

(148) Meldal, M. *Tetrahedron Lett.* **1992**, *33*, 3077.

(149) Basso, A.; De Martin, L.; Gardossi, L.; Margetts, G.; Brazendale, I.; Bosma, A. Y.; Ulijn, R. V.; Flitsch, S. L. *Chem. Commun.* **2003**, 1296.

(150) Renil, M.; Ferreras, M.; Delaisse, J. M.; Foged, N. T.; Meldal, M. *J. Pept. Sci.* **1998**, *4*, 195.

(151) Meldal, M.; Auzanneau, F. I.; Hindsgaul, O.; Palcic, M. M. *J. Chem. Soc., Chem. Commun.* **1994**, 1849.

(152) Iguerb, O.; Bertrand, P. *Surf. Interface Anal.* **2008**, *40*, 386.

(153) Renil, M.; Meldal, M. *Tetrahedron Lett.* **1995**, *36*, 4647.

(154) Won, C. Y. *Polym. Bull. (Berlin)* **2004**, *52*, 109.

(155) Barbey, R.; Lavanant, L.; Paripovic, D.; Schuwer, N.; Sugnaux, C.; Tugulu, S.; Klok, H. A. *Chem. Rev.* **2009**, *109*, 5437.

(156) Broder, G. R.; Roach, P. L., School of Chemistry, University of Southampton, Southampton, U.K. Personal communication, November 2010.

(157) Ellington, A. A.; Kullo, I. J.; Bailey, K. R.; Klee, G. G. *Clin. Chem.* **2010**, *56*, 186.

(158) Laleman, G.; Kambale, M.; Vankerckhoven, I.; Kapila, N.; Konde, M.; Selemani, U.; Piot, P.; Vandergroen, G. *Ann. Soc. Belg. Med. Trop.* **1991**, *71*, 287.

(159) Lok, A. S. F.; Zoulim, F.; Locarnini, S.; Mangia, A.; Niro, G.; Decraemer, H.; Maertens, G.; Hulstaert, F.; De Vreese, K.; Sablon, E. *J. Clin. Microbiol.* **2002**, *40*, 3729.

(160) Howell, W. M.; Carter, V.; Clark, B. *J. Clin. Pathol.* **2010**, *63*, 387.

(161) Baeumner, A. J.; Leonard, B.; McElwee, J.; Montagna, R. A. *Anal. Bioanal. Chem.* **2004**, *380*, 15.

(162) Stampi, S.; Caprioli, A.; De Luca, G.; Quaglio, P.; Sacchetti, R.; Zanetti, F. *Int. J. Food Microbiol.* **2004**, *90*, 257.

(163) Vearrier, D.; Curtis, J. A.; Greenberg, M. I. *EXS* **2010**, *100*, 489.

(164) Drel, V. R.; Lupachyk, S.; Shevalye, H.; Vareniuk, I.; Xu, W.; Zhang, J.; Delamere, N. A.; Shahidullah, M.; Slusher, B.; Obrosova, I. G. *Endocrinology* **2010**, *151*, 2547.

(165) van de Waterbeemd, H. *Curr. Opin. Drug Discovery Dev.* **2002**, *5*, 33.

(166) Kitamura, D. *How the Immune System Recognizes Self and Nonself: Immunoreceptors and Their Signaling*; 1st ed.; Springer: Shinano, 2008 (ISBN: 978-4-431-73883-1).

(167) Ezekowitz, R. A. B.; Hoffmann, J. A. *Innate Immunity*; 1st ed.; Human Press Inc.: Totowa, New Jersey, 2003 (ISBN: 1-58829-046-8).

(168) Reid, B. M.; Sim, R. B. *Molecular Aspects of Innate and Adaptive Immunity*; 1st ed.; Royal Society of Chemistry: Cambridge, 2008 (ISBN: 978-0-85404-698-0).

(169) Harlow, E.; Lane, D. *Antibodies: A Laboratory Manual*; 1st ed.; Cold Spring Harbor Laboratory Press: New York, 1988 (ISBN: 0-87969-314-2).

(170) Shepherd, P.; Dean, C. *Monoclonal Antibodies: A Practical Approach*; 1st ed.; Oxford University Press: Oxford, 2000 (ISBN: 0-19-963722-9).

(171) Harris, L. J.; Larson, S. B.; Hasel, K. W.; McPherson, A. *Biochemistry* **1997**, *36*, 1581.

(172) Kohler, G.; Milstein, C. *Nature* **1975**, *256*, 495.

(173) Yalow, R. S. *Science* **1978**, *200*, 1236.

(174) Yalow, R. S.; Berson, S. A. *J. Clin. Investig.* **1960**, *39*, 1157.

(175) Seitz, W. R. *Clin. Biochem.* **1984**, *17*, 120.

(176) Engvall, E.; Jonsson, K.; Perlmann, P. *Biochim. Biophys. Acta* **1971**, *251*, 427.

(177) Engvall, E.; Perlmann, P. *J. Immunol.* **1972**, *109*, 129.

(178) Voller, A.; Bidwell, D.; Huldt, G.; Engvall, E. *Bull. World Health Organ.* **1974**, *51*, 209.

(179) Plianbangchang, S. Guidelines for HIV Diagnosis and Monitoring of Antiretroviral Therapy; SEA-HLM-382 (Rev. 2); W.H.O.; W.H.O.: New Delhi, 2009.

(180) Burnette, W. N. *Anal. Biochem.* **1981**, *112*, 195.

(181) Renart, J.; Reiser, J.; Stark, G. R. *Proc. Natl. Acad. Sci. U. S. A.* **1979**, *76*, 3116.

(182) Swartzman, E. E.; Miraglia, S. J.; Mellentin-Michelotti, J.; Evangelista, L.; Yuan, P. M. *Anal. Biochem.* **1999**, *271*, 143.

(183) Park, M. K.; Briles, D. E.; Nahm, M. H. *Clin. Diagn. Lab. Immunol.* **2000**, *7*, 486.

(184) Fulton, R. J.; McDade, R. L.; Smith, P. L.; Kienker, L. J.; Kettman, J. R. *Clin. Chem.* **1997**, *43*, 1749.

(185) Nolan, J. P.; Sklar, L. A. *Trends Biotechnol.* **2002**, *20*, 9.

(186) Holmes, D.; She, J. K.; Roach, P. L.; Morgan, H. *Lab Chip* **2007**, *7*, 1048.

(187) Ng, A. H.; Uddayasankar, U.; Wheeler, A. R. *Anal. Bioanal. Chem.* **2010**, *397*, 991.

(188) Bruls, D. M.; Evers, T. H.; Kahlman, J. A. H.; van Lankvelt, P. J. W.; Ovsyanko, M.; Pelssers, E. G. M.; Schleipen, J. J. H. B.; de Theije, F. K.; Verschuren, C. A.; van der Wijk, T.; van Zon, J. B. A.; Dittmer, W. U.; Immink, A. H. J.; Nieuwenhuis, J. H.; Prins, M. W. J. *Lab Chip* **2009**, *9*, 3504.

(189) Richman, D. D.; Cleveland, P. H.; Oxman, M. N.; Johnson, K. M. *J. Immunol.* **1982**, *128*, 2300.

(190) Moks, T.; Abrahmsen, L.; Nilsson, B.; Hellman, U.; Sjoquist, J.; Uhlen, M. *Eur. J. Biochem.* **1986**, *156*, 637.

(191) Zola, H.; Garland, L. G.; Cox, H. C.; Adcock, J. J. *Int. Arch. Allergy Appl. Immunol.* **1978**, *56*, 123.

(192) Miller, T. J.; Stone, H. O. *J. Immunol. Methods* **1978**, *24*, 111.

(193) Hober, S.; Nord, K.; Linhult, M. *J. Chromatogr., B: Anal. Technol. Biomed. Life Sci.* **2007**, *848*, 40.

(194) Dorval, G.; Welsh, K. I.; Wigzell, H. *Scand. J. Immunol.* **1974**, *3*, 405.

(195) Biberfield, P.; Ghetie, V.; Sjoquist, J. *J. Immunol. Methods* **1975**, *6*, 249.

(196) Moran, D. M.; Dupe, B. E.; Gauntlett, S. *J. Immunol. Methods* **1978**, *24*, 183.

(197) Sato, S.; Religa, T. L.; Daggett, V.; Fersht, A. R. *Proc. Natl. Acad. Sci. U. S. A.* **2004**, *101*, 6952.

(198) Wang, X. D.; Chen, Y.; Banu, S.; Morgan, H.; Fu, S. J.; Cui, Z. *Microelectron. Eng.* **2007**, *84*, 872.

(199) Balkwill, F. *Cytokine Molecular Biology*; 3rd ed.; Oxford University Press: Oxford, 2000 (ISBN: 0-19-963857-8).

(200) O'Garra, A. *Immunity* **1998**, *8*, 275.

(201) Balkwill, F. *The Cytokine Network*; 1st ed.; Oxford University Press: Oxford, 2000 (ISBN: 019-963-702-4).

(202) Kragsbjerg, P.; Jones, I.; Vikerfors, T.; Holmberg, H. *Thorax* **1995**, *50*, 1253.

(203) Pène, J.; Rousset, F.; Brière, F.; Chrétien, I.; Wideman, J.; Bonnefoy, J. Y.; De Vries, J. E. *Eur. J. Immunol.* **2005**, *18*, 929.

(204) O'Shea, J. J. *Immunity* **1997**, *7*, 1.

(205) Dinarello, C. A. *Chest* **1997**, *112*, 321S.

(206) Gabay, C.; Lamacchia, C.; Palmer, G. *Nat. Rev. Rheumatol.* **2010**, *6*, 232.

(207) Kaminskyy, V.; Zhivotovsky, B. *J. Intern. Med.* **2010**, *267*, 473.

(208) Chen, G.; Goeddel, D. V. *Science* **2002**, *296*, 1634.

(209) Dinarello, C. A. *Chest* **2000**, *118*, 503.

(210) Dinarello, C. A. *J. Infect. Dis.* **1991**, *163*, 1177.

(211) Moldawer, L. L. *Crit. Care Med.* **1994**, *22*, S3.

(212) Standiford, T. J. *Curr. Pharm. Des.* **2000**, *6*, 633.

(213) Opal, S. M.; DePalo, V. A. *Chest* **2000**, *117*, 1162.

(214) Rama Iniguez, S.; Dea-Ayuela, M. A.; Sanchez-Brunete, J. A.; Torrado, J. J.; Alunda, J. M.; Bolas-Fernandez, F. *Antimicrob. Agents Chemother.* **2006**, *50*, 1195.

(215) Kruse, N.; Pette, M.; Toyka, K.; Rieckmann, P. *J. Immunol. Methods* **1997**, *210*, 195.

(216) Popko, K.; Gorska, E.; Stelmaszczyk-Emmel, A.; Plywaczewski, R.; Stoklosa, A.; Gorecka, D.; Pyrzak, B.; Demkow, U. *Eur. J. Med. Res.* **2010**, *15 Suppl 2*, 120.

(217) EZ-Link Sulfo-NHS-Biotinylation Kit; 1775.2; Thermo Scientific; 2010

(218) EZ-Link Sulfo-NHS-LC-Biotinylation Kit; 1776.2; Thermo Scientific; 2010

(219) de Jager, W.; te Velthuis, H.; Prakken, B. J.; Kuis, W.; Rijkers, G. T. *Clin. Diagn. Lab. Immunol.* **2003**, *10*, 133.

(220) Nguyen, T. H.; Langley, L. A.; Fairbrother, D. H.; Ball, W. P. *Abstr. Pap. Am. Chem. Soc.* **2005**, *230*, U1515.

(221) Pierce Biotin Quantitation Kit; 1423.12; Thermo Scientific; 2011

Appendix A

A1. Buffers

A1.1. MES

100 mM MES, 150 mM NaCl, pH 6

A1.2. MEST

MES supplemented with 0.2% (v/v) Tween-20

A1.3. PBS

150 mM Na_2HPO_4, 1.76 mM KH_2PO_4, 137 mM NaCl, 2.7 mM KCl, pH 7.4

A1.4. PBST

PBS supplemented with 0.2% (v/v) Tween-20

A1.5. Tris-HCl buffer

100 mM Tris-HCl, 150 mM NaCl, pH 8

Appendix B

B1. Determine number of protein A layers on GMA beads

GMA density

$\rho_{GMA} = 1.05\ g \cdot cm^{-3}$

Volume of a single GMA bead

$V_{GMA} = \frac{4}{3}\pi r^3 = \frac{4}{3}\pi(3 \times 10^{-6})^3 = 1.13 \times 10^{-16}\ m^3 = 1.13 \times 10^{-10}\ cm^3$

Mass of a single GMA bead

$m_{GMA} = \rho_{GMA} \times V_{GMA} = 1.05\ g \cdot cm^{-3} \times 1.13 \times 10^{-10} cm^3 = 1.19 \times 10^{-10} g$

Number of GMA beads in 1 g

$N_{GMA\ 1\ g} = \frac{1}{1.19 \times 10^{-10}} = 8.40 \times 10^9\ units$

Surface area of a single GMA bead

$S.A._{GMA} = 4\pi r^2 = 4\pi(3 \times 10^{-6})^2 = 1.13 \times 10^{-10} m^2$

Total surface area of 1 g of GMA beads

$S.A._{Total\ GMA} = 1.13 \times 10^{-10} \times 8.40 \times 10^9 = 0.949\ m^2$

Protein A loading level determined by BCA assay

$loading\ level_{GMA} = 45\ nmol \cdot g^{-1}$

Number of protein A molecules immobilised to 1 g of GMA beads

$$N_{protein\ A} = no.of\ mole \times Avogadro's\ number$$

$$= 45\ \times 10^{-9}\ mol \times 6.02 \times 10^{23}\ mol^{-1} =\ 2.71 \times 10^{16}\ units$$

Cross-sectional radius of a protein A molecule

$$r_{protein\ A} = 2.5 \times 10^{-9}\ m$$

Cross-sectional area of a protein A molecule

$$A_{protein\ A} = \pi r^2 = \pi(2.5 \times 10^{-9})^2 = 1.96 \times 10^{-17}\ m^2$$

Total cross-sectional area of protein A molecules attached to 1 g of GMA beads

$$A_{Total\ protein\ A} = N_{protein\ A} \times A_{protein\ A} = 2.71 \times 10^{16} \times 1.96 \times 10^{-17}\ m^2$$

Number of protein A layers on GMA beads

$$No.of\ protein\ layer_{GMA} = \frac{A_{Total\ protein\ A}}{S.A._{Total\ GMA}} = \frac{0.531\ m^2}{0.949\ m^2} = 0.6\ layers$$

B2. Determine number of protein A layers on SU-8 particles

SU-8 density

$\rho_{SU-8} = 1.24\ g \cdot cm^{-3}$

Volume of a single SU-8 particle

$V_{SU-8} = 30 \times 10^{-6} \times 10 \times 10^{-6} \times 5 \times 10^{-6}\ m^3 = 1.50 \times 10^{-9}\ cm^3$

Mass of a single SU-8 particle

$m_{SU-8} = \rho_{SU-8} \times V_{SU-8} = 1.24\ g \cdot cm^{-3} \times 1.50 \times 10^{-9} cm^3 = 1.86 \times 10^{-9} g$

Number of SU-8 particles in 1 g

$N_{SU-8\ 1\ g} = \dfrac{1}{1.86 \times 10^{-9}} = 5.38 \times 10^8\ units$

Surface area of a single SU-8 particle

$S.A._{SU-8} = 10 \times 10^{-10} m^2$

Total surface area of 1 g of SU-8 particles

$S.A._{Total\ SU-8} = 10 \times 10^{-10} \times 5.38 \times 10^8 = 0.538\ m^2$

Protein A loading level determined by BCA assay

$loading\ level_{SU-8} = 414\ nmol \cdot g^{-1}$

Number of protein A molecules immobilised to 1 g of GMA beads

$N_{protein\ A} = no.of\ mole \times Avogadro's\ number$

$= 414\ \times 10^{-9}\ mol \times 6.02 \times 10^{23}\ mol^{-1} = \ 2.49 \times 10^{17}\ units$

Total cross-sectional area of protein A molecules attached to 1 g of GMA beads

$$A_{Total\ protein\ A} = N_{protein\ A} \times A_{protein\ A} = 2.49 \times 10^{17} \times 1.96 \times 10^{-17}\ m^2 = 4.88\ m^2$$

Number of protein A layers on SU-8 particles

$$No.of\ protein\ layer_{SU-8} = \frac{A_{Total\ protein\ A}}{S.A._{Total\ GMA}} = \frac{4.88\ m^2}{0.538\ m^2} = 9\ layers$$

Appendix C

C1. MALDI-TOF mass spectrum of peptide

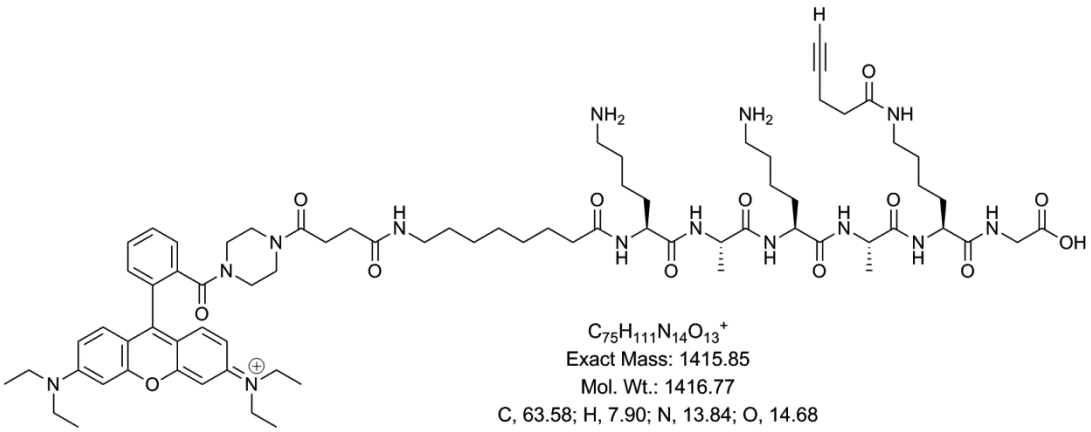

$C_{75}H_{111}N_{14}O_{13}^{+}$
Exact Mass: 1415.85
Mol. Wt.: 1416.77
C, 63.58; H, 7.90; N, 13.84; O, 14.68

Predicted

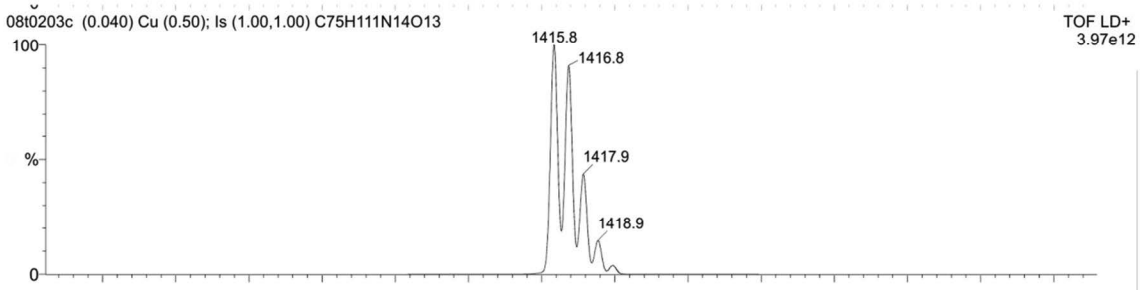

Measured

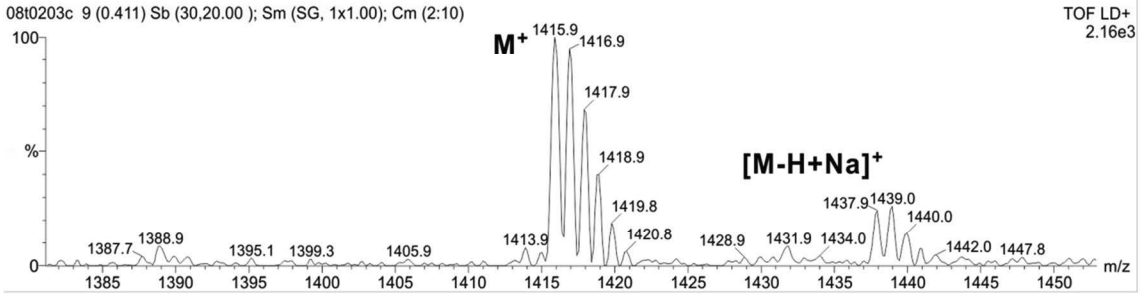

Appendix D

D1. Anti-IL-6 antibody ELISA sensitivity

IL6C-0107

Page 2

EIA test with coating mAb IL6 (Lot #IL6C-0107)

Control date : 03/12/2007

Revealing time		1 h 30
	Control	Normal Range
Non Specific Binding (AU)	0.001	≤ 0.06 AU
Sensitivity (pg/ml)	< 3.9	≤ 10 pg/ml

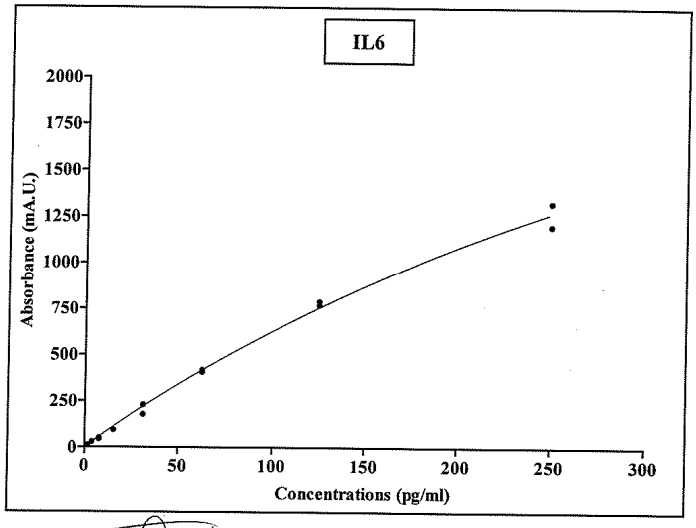

Karine Mouchain
ImmunoAssay Laboratory Engineer

Gwenaëlle EVENO
Head of Sales and Technical Department

SOCIETE DE PHARMACOLOGIE ET D'IMMUNOLOGIE-BIO • bertin
Parc d'Activités du Pas du Lac • 10 bis avenue Ampère - F-78180 Montigny Le Bretonneux
Tel : 33 (0)1 39 30 62 60 • Fax : 33 (0)1 39 30 62 99 • E-Mail : contact@spibio.com
S.A.S. au capital de 72 000 €uros • 380 608 380 RCS Versailles • APE 731Z • ID TVA : FR 31 380 608 380
Web : www.spibio.com

D2. Anti-TNF-α antibody ELISA sensitivity

AcTNFα-0306

EIA test with coating mAb TNFα

Control date : November, 2006

Revealing time	60 min	
	Control	Normal Range
Non Specific Binding (AU)	0.000	≤ 0.060 AU
Sensitivity (pg/ml)	1.00	≤ 10 pg/ml

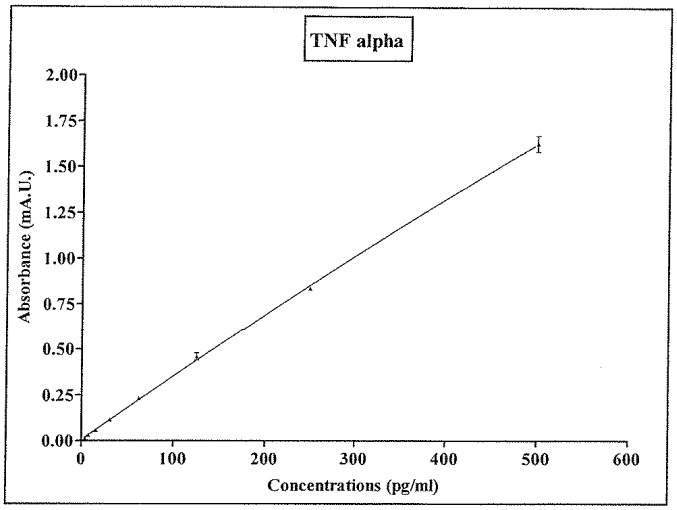

Karine Mouchain
ImmunoAssay Laboratory Engineer

Gwenaëlle EVENO
Head of Sales and Technical Department

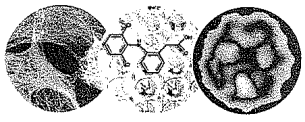

SOCIETE DE PHARMACOLOGIE ET D'IMMUNOLOGIE-BIO · bertin
Parc d'Activités du Pas du Lac · 10 bis avenue Ampère · F-78180 Montigny Le Bretonneux
Tel : 33 (0)1 39 30 62 60 · Fax : 33 (0)1 39 30 62 99 · E-Mail : contact@spibio.com
S.A.S. au capital de 72 000 €uros · 380 608 380 RCS Versailles · APE 731Z · ID TVA : FR 31 380 608 380
Web : www.spibio.com